Universidad Autónoma de Madrid

Doctoral Thesis

FORMATION OF THE ACTIVE SURFACE OF SUPPORTED NANO GOLD CATALYSTS FOR LIQUID-PHASE SELECTIVE OXIDATION OF PRIMARY ALCOHOLS

A thesis submitted to Universidad Autónoma de Madrid in fulfilments of the requirements for the degree of Doctor of Philosophy with International Mention by

Ekaterina Pakrieva

Programa de Doctorado en Química Aplicada,
Universidad Autónoma de Madrid

Instituto de Catálisis y Petroleoquímica (CSIC)

National Research Tomsk Polytechnic University

Director: Prof. Vicente Cortés Corberán (Tutor)
Co-director: Prof. Alexey Pestryakov

Madrid, 2021

SUMMARY

Selective oxidation of alcohols to valuable chemical products, such as carbonyl and carboxyl compounds, plays a significant role in fine organic synthesis and is also of great industrial importance.

In this thesis, for the first time, a comprehensive study of gold catalysts supported on titania has been carried out, including the study of their structural, electronic, acid-base, and catalytic properties for selective oxidation of different types of primary alcohols, both inactivated (alkyl) and activated (containing an aromatic ring), represented by n-octanol and 1-phenylethanol, respectively. Catalytic investigation was done under mild conditions (T = 80 °C, 1 atm, no added bases), and using non-toxic oxidants (tert-butyl hydroperoxide, TBHP or molecular oxygen, O_2) in order to follow «green» chemistry principles.

The combined effects of the gold content, the nature of the support modifier (M_xO_y = CeO_2, Fe_2O_3, La_2O_3 or MgO), and the pretreatment atmosphere (H_2 or O_2) on the formation of the active surface of Au/(M_xO_y)/TiO_2 catalysts and, as a consequence, on their catalytic behaviour for the selective oxidation of n-octanol and 1-phenylethanol, has been investigated. Based on this, the key parameters to purposely influence the activity and selectivity of gold-containing catalysts in the oxidation of these alcohols have been determined.

The cationic nature of the active centers in nano gold catalysts has been experimentally proved, based on the direct correlation found between the catalytic activity in both reactions and the content of Au^+ ions. The concentration, stability, and adsorption strength of Au^+ sites are highly dependent on the nature of the support and the pretreatment atmosphere. The catalysts' deactivation observed in both reactions in parallel to the reduction of Au^+($Au^{\delta+}$) states, as well as Density Functional Theory (DFT) simulations, confirmed the cationic nature of the active sites. In addition, the negative effect of Au^{3+} and Au^0 species for aerobic n-octanol oxidation has also been proved by theoretical calculations.

The effect of tuning (through modifiers) the acid-base properties of the support on the formation of the active surface of Au/M_xO_y/TiO_2 catalysts has been shown for the first time. And, likewise, the functional groups of the support surface (Brønsted acid centers and Brønsted basic centers) also affect the direction of secondary reactions (acid and ester formation) of the oxidation of n-octanol.

In conclusion, this research revealed that catalytic systems based on gold nanoparticles deposited on titanium oxide modified with lanthanum oxide are promising for the selective liquid-phase oxidation of n-octanol and 1-phenylethanol into highly valuable chemicals, as their oxo-derivatives are widely used in cosmetologic, pharmaceutical, agrochemical and other industries.

RESUMEN

La oxidación selectiva de alcoholes a productos químicos valiosos, tales como compuestos carbonílicos y carboxílicos, juega un papel importante en la síntesis orgánica fina y también reviste gran importancia industrial.

En esta tesis, por primera vez, se ha llevado a cabo un estudio comparativo integral de catalizadores de oro soportados en óxido de titanio, incluyendo el estudio de sus propiedades estructurales, electrónicas, ácido-base y catalíticas para oxidación selectiva de diferentes tipos de alcoholes primarios, tanto inactivados (alquilico) como activados (que contienen un anillo aromático), representados por n-octanol y 1-feniletanol, respectivamente. La investigación catalítica se realizó en condiciones suaves (T = 80 °C, 1 atm, sin adición de bases), y usando oxidantes no-tóxicos (hidroperóxido de terc-butilo u oxígeno molecular, O_2) para seguir los principios de la química "verde".

Se ha investigado el efecto combinado del contenido de oro, la naturaleza del modificador de soporte (M_xO_y = CeO_2, Fe_2O_3, La_2O_3 o MgO) y la atmósfera de pretratamiento (H_2 u O_2) sobre la formación de la superficie activa de los catalizadores $Au/(M_xO_y)/TiO_2$ y, en consecuencia, sobre su comportamiento catalítico para la oxidación selectiva de n-octanol y 1-feniletanol. En base a esto se han determinado los parámetros clave para influir deliberadamente en la actividad y selectividad de los catalizadores de oro en la oxidación de estos alcoholes.

Se ha demostrado experimentalmente la naturaleza catiónica de los centros activos de los catalizadores de nano oro sobre la base de la correlación directa encontrada entre la actividad catalítica en ambas reacciones y el contenido de iones Au^+. La concentración, estabilidad y fuerza de de adsorción de los sitios Au^+ dependen en gran medida de la naturaleza del soporte y la atmósfera de pretratamiento. La desactivación de los catalizadores en ambas reacciones en paralelo a la reducción de los estados de $Au^+(Au^{\delta+})$, así como las simulaciones de la Teoría Funcional de la Densidad (DFT), confirmaron la naturaleza catiónica de los sitios activos. Además, mediante cálculos teóricos se ha demostrado también el efecto negativo de las especies Au^{3+} y Au^0 en la oxidación aeróbica del n-octanol.

Se ha demostrado por primera vez el efecto de ajustar las propiedades ácido-base del soporte (mediante modificadores) en la formación de la superficie activa de los catalizadores de $Au/(M_xO_y)/TiO_2$. Asimismo, que los grupos funcionales de la superficie de soporte (centros ácidos Brønsted y centros básicos Brønsted) también afectan la dirección de las reacciones secundarias (formación de ácido y éster) de la oxidación del n-octanol.

En conclusión, esta investigación ha revelado que los sistemas catalíticos basados en nanopartículas de oro depositadas sobre óxido de titanio modificado

con óxido de lantano son muy prometedores para la oxidación selectiva de n-octanol y 1-feniletanol en fase líquida a productos químicos de alto valor, ya que sus oxo-derivados se utilizan ampliamente en las industrias cosmetológica, farmacéutica, agroquímica y otras.

Acknowledgements

First of all, I want to express special thanks to Dr. Ekaterina Kolobova, who initiated my PhD project, supported and taught me throughout my research and career. Your wealth of ideas, unique way to find always the right words of encouragement as well as optimism gave me enormous energy and motivation. Спасибо, Катюшка!

I would like to thank my supervisor Prof. Alexey Pestryakov for giving me the opportunity to work in his laboratory during the past six years, and for providing me with all the necessary means for doing this thesis as well as for the support and encouragement. Благодарю Вас!

I also want to thank my scientific adviser and tutor Prof. Vicente Cortés Corberán for all the discussions, scientific and nonscientific, that benefited me greatly and the time that you invested in me. Thanks to you for helping me take the first steps into research abroad and more importantly, for overcoming fear of English practice. ¡Muchas gracias!

My special acknowledgements to wonderful Prof. Sónia Carabineiro**,** who hosted me at Instituto Superior Técnico (IST, Universidade de Lisboa, Lisbon, Portugal) in spite of the difficulties. Thanks for all knowledge that I learned from you and for all the experiences you have shared with me. Without your help, things would have been very complicated, so you were a very important part of all this. Muito obrigada!

I want also to thank both Prof. Vicente Cortés Corberán and Prof. Sónia Carabineiro for those laborious hours in correcting my grammatical and spelling errors. ¡Muchas gracias y Muito obrigada!

It was a great honor and pleasure to work with Prof. Armando Pombeiro, Director of Centro de Química Estrutural from IST, who made enormous effort to provide financial support for my internship and its successful realization. Muito agradecida!

I am thankful to Dr. Laura Pascual from Instituto de Catálisis y Petroleoquímica (ICP-CSIC, Madrid, Spain) for the great help with all microscopic measurements. It was a great pleasure to meet with scientist as you are. ¡Muchas gracias!

I thank all the people from both ICP and IST for their warm welcome and help with technical assistance, especially to Dr. Susanna Martinez Gonzaléz, Patricia Perez Bailac, Inês Matias and Dr. Marta Andrade, Jiahe Lee and Mohamed Soliman, with whom I have spent great times. Also Dr. Arturo Martinez Arias for teaching me the technique of Infrared spectroscopy and his support during all experiments. Prof. Luísa Martins and Dr. Ana Ribeiro for share of information, help and guidance in the lab. ¡Muchas gracias y Muito obrigada!

I want also to thank my workmate from ICP and subsequently friend Dr. Alba Diaz for encouraging me to keep going, for a cozy atmosphere and the outings, trips and good moments. I thank Diana Pastor from UAM International help service for all her efforts and kind help with my residence and visa matters in Spain. ¡Gracias por todo!

My acknowledgement to Dr. Darya Pichugina from Moscow State University (MSU, Moscow, Russia) for her great job on theoretical calculations, that confirmed our ideas based on experimental results. Also I want to thank Dr. Andrey Kharlanov from MSU for the infrared spectroscopic measurements of the catalysts. Благодарю!

Special thanks to Dr. Nina Bogdanchikova, Dr. Mario Farias and Dr. Yulia Kotolevich from Universidad Nacional Autónoma de México (Ensenada, Mexico) for some characterization of samples and results discussion. Благодарю! ¡Muchas gracias!

My acknowledgement for Centre of Materials (CEMUP) of the University of Porto (Portugal) and its technical staff, notably Dr. Carlos Sá, for the assistance with the XPS analyses performed there. Obrigada!

I am thankful to Dr. Grygory Mamontov from Tomsk State University (TSU, Tomsk, Russia) for some TPR measurements. Спасибо!

Last, but no less important, I want to thank my family for being with me in the ups and downs. Mami, Pasha and Dana, this thesis is specially dedicated to all of you. Вы всегда в моем сердце!

The works here presented were supported by the Tomsk Polytechnic University Competitiveness Enhancement Program, projects VIU-RSCBMT-65/2019 and VIU-RSCBMT-197/2020, Russian Foundation of Basic Research, project 18-29-24037, Tomsk Polytechnic University Task Program "Science" project FSWW-2020-0011, Scholarship of the President of the Russian Federation for training abroad in 2016/17 and 2017/2018 (Russia).

This work was also partially supported by Fundação para a Ciência e a Tecnologia (FCT), Portugal, through project UIDB/00100/2020 of the Centro de Química Estrutural, Investigador FCT IF/01381/2013/CP1160/CT0007 project and Associate Laboratory LSRE-LCM – UID/EQU/50020/2019, UIDB/50006/2020 – funded by national funds through FCT/MCTES (PIDDAC) (Portugal), MINECO project CTQ2017-86170-R (Spain) and CONACYT project 279889 and PAPIIT-UNAM projects IT200114, IN105114 and IN107715 (Mexico).

Finally, I thank the Autonomous University of Madrid for accepting me in their doctorate program.

CONTENT

INTRODUCTION

Global increases in energy consumption, exhaustion of easily accessible fossil fuels and environmental concerns show the urgent need to produce fuels and chemicals based on renewable raw materials. The potential of biomass, as a valuable source of energy, biological and chemical raw materials, is far from being fully utilized. This is due to the fact that the processes developed to date for the chemical processing of biomass are significantly inferior in efficiency to petrochemical processes. In this regard, the development of new ways and methods of processing biomass into fuel and chemical products is important for any sustainable energy and industrial development strategy.

One typical example is the selective oxidation of alcohols, present in large quantities in biomass processing products, into valuable carbonyl and carboxylic compounds that plays an important role in fine organics synthesis and is of great industrial importance [1, 2].

Conventionally, numerous oxidizing reagents (including toxic, expensive, stoichiometric oxidants [3, 4]), have been employed to accomplish this transformation, along with the use of harmful solvents and harsh reaction conditions. Thus, these methods lead to environmental pollution and economic problems [5–8]. This generates an urgent and considerable need for harmless and sustainable technologies that require renewable feedstock, e.g., biomass, as replacement for fossil resources [9]. Therefore, a green process, involving the use of a heterogeneous catalyst (used as a recyclable solid material in biomass processing) and non-toxic and cheap oxidants, such as oxygen or peroxides, in mild conditions (atmospheric pressure, low temperature and absence of bases and radical initiators) would be of utmost interest [10–13]. The implementation of these processes will be impossible without the creation of new, highly efficient catalytic systems with high activity, selectivity and stability.

In this frame, supported nanogold catalysts are characterized by high activity and selectivity, and more stability in liquid-phase oxidation of alcohols, as compared to catalysts based on Pt and Pd [14-17]. At the same time, the purposeful organization of the active surface of gold-containing catalysts implies taking into account a combination of many factors, such as dispersion of gold, preparation method, nature of the support and its interaction with gold, etc. [18-21]. The influence of these factors has been repeatedly discussed in the literature, but up to date there is no consensus on how these factors influence the formation of the active surface. The solution of these issues is a powerful lever on the way of increasing the efficiency and stability of gold-containing catalysts. In this regard, the study of the genesis of the active surface of gold-containing catalysts under the

influence of the above factors is an important and relevant topic of scientific research.

Previous studies on supported gold catalysts in the liquid-phase oxidation of n-octanol [22, 23], have suggested that monovalent gold ions act as the active sites, and the modification of titanium oxide supports with transition metal oxides leads to stabilization of these active states of gold. However, the combined effect of gold load, nature of the modifying additive and pretreatment atmosphere on the formation of the active surface in such catalytic systems was not considered. Moreover, the process of deactivation of the catalysts was not studied and the factors that determine the selectivity of the process were not established.

Notably, n-octanol belongs to the group of low fatty alcohols, whose physical properties impose constraints to the implementation of green chemistry approaches. Oxo derivatives of n-octanol (aldehydes, acids and esters) are widely used in pharmaceutical, cosmetology, agrochemical and other industries [24-28]. Due to its low reactivity, n-octanol is often used for comparative studies of catalytic activity in oxidation of alcohols, as a convenient model of primary alcohols of long chain. However, among these studies, very few are devoted to understanding and improving the efficiency of selective liquid-phase oxidation of n-octanol using supported gold catalysts under mild conditions [29-35].

Indeed, gold catalysts exhibit higher catalytic activity in the oxidation of the more reactive, activated alcohols, such as 1-phenylethanol [36-46]. However, even in the oxidation of such a reactive alcohol, the study of the mechanism of formation of the active surface of gold-containing systems responsible for its excellent catalytic performance is still the subject of numerous discussions. The main oxidation product of this aromatic alcohol is acetophenone (methylphenylketone, $C_6H_5COCH_3$). Acetophenone is used in perfumes, soaps and creams, as well as a flavouring substance in food, soft drinks and tobacco. It is also used as a solvent and has a sleeping effect, important in the manufacture of medicines.

Thus, there is an urgent need to create new methods and approaches to the production of these substances, which would replace existing stoichiometric processes leading to the formation of a large amount of toxic waste, but, at the same time, to ensure a quantitative yield of the target product and a reduction of its cost. The most promising way to solve this problem is to develop new heterogeneous catalytic production methods. The most promising solution is the use of catalytic systems based on gold nanoparticles, since they have high activity and selectivity in the oxidation of alcohols under mild conditions using eco-friendly oxidizing agents.

The overall objective of this thesis is the design and development of new nano gold catalysts for sustainable processes of selective oxidation of alcohols, both activated and non-activated. To reach this goal, a

comprehensive comparative study of the combined effects of gold concentration, support and its modifying additives, as well as redox pretreatments, on the formation of the active surface species of gold-containing catalysts for the liquid-phase oxidation of n-octanol and 1-phenylethanol.

In the frame of this purpose, the following tasks were carried out:

1. Synthesis of catalysts based on gold supported on unmodified and modified titanium oxide, varying the gold content, the modifiers, and the atmosphere of the pretreatment (reducing or oxidizing);
2. Study of the catalytic properties of the obtained systems in the processes of liquid-phase oxidation of n-octanol and 1-phenylethanol;
3. Investigation of the structural, electronic, as well as acid-base properties of the obtained catalytic systems;
4. Evaluation of the combined effect of gold content, nature of the modifying additive and pretreatment atmosphere on the various states of gold, their contribution and stabilization in the systems under study;
5. Identification of the relationships between catalytic performance and structural, electronic and acid-base properties;
6. Investigation of desorption of both alcohol substrates, as well as used solvents on different gold sites with Density functional theory (DFT) simulations to find a theoretical conclusion about the effect of gold sites on alcohol activation;
7. Based on the analysis of the above results, formulation of ideas about the formation and genesis of the active surface species.

This PhD thesis is based on the following published papers:

1. Kolobova, E.; Pakrieva, E.; Pascual, L.; Cortés Corberán, V.; Bogdanchikova, N.; Farias, M.; Pestryakov, A. Selective oxidation of n-octanol on unmodified and La-modified nanogold catalysts: Effect of metal content. *Catal. Today* **2019,** 333C, 127–132, https://doi.org/10.1016/j.cattod.2018.04.046

   Impact factor of Catalysis Today (Elsevier, Netherlands) in 2019 was 5.825. Quartile 1 in Chemical Engineering Category according to Journal Citation Report, JCR.

2. Pakrieva, E.; Kolobova, E.; Mamontov, G.; Bogdanchikova, N.; Farias, M.H.; Pascual, L.; Cortés Corberán, V.; Martinez Gonzalez, S.; Carabineiro, S.A.C.; Pestryakov, A. Green oxidation of n-octanol on supported nanogold catalysts: Formation of gold active sites under combined effect of gold content, additive nature and redox pretreatment. *ChemCatChem* **2019**, *11*, 1615–1624, https://doi.org/10.1002/cctc.201801566.

Impact factor of ChemCatChem (Wiley - VCH Verlag GmbH & CO. KGaA, Germany**)** in 2019 was 4.853. Quartile 1 in Chemical Engineering Category acoording to Journal Citation Report, JCR.
The paper was selected for the issue Front Cover: Green Oxidation of *n*-Octanol on Supported Nanogold Catalysts: Formation of Gold Active Sites under Combined Effect of Gold Content, Additive Nature and Redox Pretreatment (ChemCatChem 6/2019)

3. Pakrieva, E.; Ribeiro, A.P.C.; Kolobova, E.; Martins, L.M.D.R.S.; Carabineiro, S.A.C.; German, D.; Pichugina, D.; Jiang, C.; Pombeiro, A.J.L.; Bogdanchikova, N.; Cortés Corberán, V.; Pestryakov, A. Supported gold nanoparticles as catalysts in peroxidative and aerobic oxidation of 1-phenylethanol under mild conditions. *Nanomaterials* **2020**, *10*, 151, doi:10.3390/nano10010151 (Open Access)

4. Pakrieva, E.; Kolobova, E.; Kotolevich, Y.; Pascual, L.; Carabineiro, S.A.C.; Kharlanov, A.N.; Pichugina, D.; Nikitina, N.; German, D.; Zepeda Partida, T.A.; Tiznado Vazquez, H.J.; Farias, M.H.; Bogdanchikova, N.; Cortés Corberán, V.; Pestryakov, A. Effect of gold electronic state on the catalytic performance of nano gold catalysts in n-octanol oxidation. *Nanomaterials* **2020**, *10*, 880. doi:10.3390/nano10050880 (Open Access)

   Impact factor of Nanomaterials (MDPI Multidisciplinary Digital Publishing Institute, Switzerland) in 2020 was 4,080, Quartile 1 in Chemical Engineering Category according to Journal Citation Report, JCR.

Some results of this work were presented at the following conferences:

IV Encuentro de Jóvenes Investigadores de la SECAT, Cursos de Verano de la Universidad del País Vasco, Bilbao, País Vasco, 21-23 September 2020. Abstract "Selective oxidation of n-octanol over supported nano gold catalysts";

International School of Chemistry "Chemistry for everyday life", School of Pharmacy and School of Science and Technology, University of Camerino, Camerino, Italy, 1-6 September 2020. Abstract "Green oxidation of n-octanol over gold supported catalysts";

XXVI Congresso Ibero-Americano de Catalise – CICAT 2018, Coimbra, Portugal, 9-14 September, 2018. Abstracts "Oxidación selectiva de alcanoles sobre catalizadores de oro soportados: efecto de la carga metálica y pretratamientos" and "Gold supported catalysts in solvent free peroxidative oxidation of 1-phenylethanol under mild conditions".

International Scientific internship: at Instituto Superior Tecnico, Universidade de Lisboa (Lisbon, Portugal) under supervision of Prof. Sonia

Carabineiro. Topic: «Studies on the oxidation of 1-phenylethanol using gold based catalysts» during period: 2nd November 2017 – 9th July 2018.

The personal contribution of the author consisted in the search, analysis and generalization of literature data, the choice of methods and synthesis of the studied catalytic systems, the study of the catalytic activity of samples in liquid-phase oxidation of n-octanol and 1-phenylethanol, chemisorption measurements, participation in setting goals and objectives, interpretation results of physicochemical and catalytic studies, discussion of results and formulation of conclusions.

The scope and outline of this thesis is as follows:

The dissertation contains 117 pages, 20 figures and 18 tables. The work consists of an Introduction, three chapters of Results, Conclusions and 225 References.

Chapter 1 shortly reviews the effect of a number of parameters on catalytic properties of supported gold catalysts in oxidation reactions, then summarizes and discusses in detail the catalytic systems found in the literature for n-octanol and 1-phenylethanol oxidation, under mild conditions. Based on the literature review, the aim of the study is formed, namely the importance of the detailed study of the active surface formation of $Au/M_xO_y/TiO_2$ catalysts under the influence of several factors (gold content, pretreatments, support modifier).

Chapter 2 presents the experimental part of the work: modification of support and gold catalysts preparation, type of treatments for catalyst activation, catalytic experiments procedure and the physicochemical methods of studying the samples are described in detail. Besides that, theoretical calculations are described in this Chapter.

In *Chapter 3*, a detailed study on catalytic properties in oxidation of n-octanol and 1-phenylethanol under comparable mild conditions with study of influence oxidant type (TBHP or O_2) on activity in both reactions was carried out; summarizing general trends and differences in the activity of catalysts in these processes. Then, by using a series of physicochemical methodologies, structural, electronic, and acid-base properties of catalysts were studied in detail. Based on this comprehensive study, the active centers of both reactions were proposed, and the reasons for the deactivation were revealed. Finally, density functional theory (DFT) simulations confirmed the nature of active sites proposed based on experimental results, as well as the sites responsible for inhibiation of an oxidation process.

Finally, the main findings of this PhD thesis, including the general conclusions regarding factors influencing the active surface formation in $Au/M_xO_y/TiO_2$ catalysts, the reasons of deactivation and factors determining the selectivity of the process are summarized.

CHAPTER 1. LITERATURE REVIEW

1.1. Supported Gold Nanoparticles for Catalysis

Dispersed gold particles (clusters, nanoparticles, ionic associates) are currently the object of intensive research because of their extraordinary properties. It was found that dispersed gold has anti-tumor, anti-arthritic and antibacterial properties [47-51].

However, the main interest in gold is due to the discovery of Haruta et al. of the high catalytic activity of dispersed gold deposited on oxides of various metals in low-temperature oxidation of CO [52-54]. Prior to this finding, gold was traditionally considered as catalytically inert. Therefore, it is not surprising that over the last twenty years gold catalysis has become a "hot topic," as it can have applications in several industrially and environmentally important reactions, as supported gold catalysts have the ability to carry out liquid-phase oxidations under mild conditions [55-61].

Usually, the formation of the active surface of the deposited metal systems occurs under the influence of a number of factors - the method of metal deposition on the support, the nature of the support, modifying additives of various compounds, reaction conditions, etc.

However, at the beginning, it is worth to consider the main types of dispersed particles and how they differ from each other.

During the preparation of the supported material, a part of the introduced metal is concentrated on the surface of the support granules with the formation of relatively large metal particles with a size of 1 nm or more - *nanoparticles*, or a relatively compact metal layer. The other part of the metal forms is dispersed as ionic and cluster states. For example, higher ions or M^{+} ions strongly bound to support and clusters of the $M_n^{\sigma+}$ type. Moreover, *ionic states* can be both in the form of isolated cations, which are closely associated with the support, and in the form of oxides, hydroxides or salts. According to a number of electronic properties – stability of the d-orbital, manifestation of the effective charge of monovalent ions – gold is located between silver and copper. Alike silver, gold in supported catalysts has a stable oxidation state of +1, although the highest valence states (Au^{3+}) in gold are more stable and are found in supported systems stabilized by chlorine [62].

Clusters differ from nanoparticles both in size (they are usually less than 1 nm) and in physicochemical properties. Although they contain a M–M bond, the nature of this bond is covalent and not metallic, as in a nanoparticle, due to the size effect [63]. Also, clusters are much more reactive and can have a negative or positive charge, and be closely associated with the support and adsorb molecules, unlike bulk gold. Thus,

clusters occupy an intermediate position between the metal and individual atoms and ions.

Typically, the catalytic activity of a gold catalyst increases with decreasing nanoparticle size. This occurs due to an increase in the free surface area (which increases the contact between reactant molecules and catalytic sites) to volume ratio: the smaller the particle, the highest this ratio. Nevertheless, in most reviews, it is noted that particles with size below 5 nm are more active and selective in the oxidation of alcohol than larger ones, which are almost inactive at low temperatures [64-66]. Moreover, according to some reports, gold clusters less than 2 nm in size are the most active [21, 66-69].

In addition to the size effect, the nature of the support is also an important factor. The most widely used supports are divided into two groups: «active supports» are reducible metal oxide supports (Fe_2O_3, CeO_2, TiO_2, Co_3O_4, etc.) and «inert supports» are non-reducible oxide supports (MgO, Al_2O_3, La_2O_3, etc.). The active supports are transition metal oxides, which activate adsorbed oxygen and show strong metal-support interaction, while the inert ones are characterized by higher specific surface areas than those of active ones, thus decreasing the sintering effect [70-72].

Although non-reducible oxide supports are much less efficient in oxygen activation than reducible ones, and are generally regarded as the "spectator" of the process, the transfer of electrons between gold and these supports is still very important [73]. Another important factor that can affect the properties of gold nanoparticles is the electronic effect. It was reported that CeO_2 can stabilize cationic gold on the surface by attracting electrons from gold [74], while MoOx stabilizes nanoparticles by donating its electrons to gold [75]. Despite the oppositely directed electron transfer, the gold-support interaction increases in both cases.

The dependence of gold dispersion on the preparation method is quite strong. There is a popular simple *impregnation method* for obtaining deposited disperse systems based on noble metals. In this technique, the metal salts are dispersed on the surface or mostly in existing pores of support (depending on the porosity of the support) and then dried and calcined under suitable thermal conditions. However, it is almost impossible to obtain highly dispersed gold due to its melting point (1063 °C), lower than that of Pd (1550 °C) and Pt (1769 °C). Moreover, nanosized gold particles have a melting point even lower than bulk gold [63], easily sintered into large aggregates (up to 400 nm [59]). Meanwhile, the chloride ions of the precursor ($HAuCl_4$), if not completely removed, poison the catalyst at lower temperatures (< 600 °C).

Thus, three extremely useful methods for depositing gold particles with a diameter <5 nm on oxide supports are:

1) Co-precipitation method, widely used for gold catalysts preparation because of its simplicity. A precipitating reagent (Na_2CO_3, urea, etc.) is added to

an aqueous solution of $HAuCl_4$ and metal nitrate to obtain a mixture of precipitates of the active component and support. Then the precursor is washed, dried and calcined at temperatures above 250 °C. Highly dispersed gold with small particle size can be obtained by this technique. However, a significant concentration of Na^+ and Cl^- ions in some cases, can act as a catalyst poison. In addition, impurities such as metal hydroxides or carbonates, can be co-precipitated with $Au(OH)_3$, limiting the applicability of this method.

2) Immobilization method, in which colloidal gold nanoparticles are first synthesized in the presence of an excess of stabilizing (capping) agents/ligands or surfactants and then dispersed on the support. This procedure can be used to prepare gold on carbon or oxide supports and it provides control of the size and shape of the formed nanoparticles, preventing them from agglomerating. However, stabilizing agents might partially block the active metal sites due to bonds formed between agent and support. Thus, the removal of these compounds, by treatment at 300 °C, as an example, is highly important.

3) Deposition–precipitation (DP) technique is the most widely and successfully used method in the preparation of active gold-based catalysts with high dispersion of Au NPs. This method, developed by Haruta [76], consists of the precipitation, using sodium hydroxide (DP NaOH), of the metal salt in the form of hydroxide on the surface of the support by varying the pH (6-10) of the solution. The obtained precipitate $[Au(OH)_nCl_{4-n}]^-$ may be nucleated by the surface functional groups, simultaneously allowing the active phase to attach to the support or to be reduced afterwards. It should be mentioned that DP technique is not very suitable for supports with a point of zero charge (PZC) below 5, activated carbon [77-79] or zeolites [80], due to those high isoelectric point.

In alternative to DP NaOH, Zanella and co-workers used DP with urea (DPU) [81]. They found that instead of gold(III) hydroxide formed in the solution by DP NaOH, the gold is deposited on the TiO_2 surface (PZC ≈ 6) as an amorphous gold(III) precipitate, containing urea hydrolysis products. Thus, the metallic gold particles obtained after calcination exhibit a decreasing size (2–3 nm) when the time of urea decomposition increases (until 16 h for progressive increase of pH), while no sodium poison was introduced. Also, urea has been shown to yield larger quantities of gold deposited on the surface in contrast to NaOH.

It should be emphasized that, according to Haruta, the DP method allows to obtain hemispherical particles that strongly interact with the support by their flat side and are thermally more stable than spherical particles [82].

As can be seen from the described methods, a proper thermal treatment is also crucial for active surface formation since, otherwise, it may lead to sintering of gold Au NPs. As an example, Park and Lee [83] reported that calcination at

300 °C results in more active Au/TiO_2, Au/Fe_2O_3, and Au/Al_2O_3 catalysts for CO oxidation than those calcined at higher temperatures. At the same time, the type of thermal pretreatment also affects the formation of active centers. Thus, Lee and co-workers found [84] that due to a stronger interaction between the metal and the oxidized manganese, catalysts treated under air at 120 °C are more active than those dried in vacuum or hydrogen at 30 °C.

There is no consensus on the optimal gold content in catalysts. In some studies, the activity of gold-based materials is proportional to the gold content [85, 86]; in others, on the contrary, activity decreases with increasing gold content. For example, Abad and co-workers [87] found that the sample with 0.44 wt.% Au was significantly more active than the sample with 1.8 wt.% Au in spite of the same particle size, ≈ 4 nm. In general, it is believed that the gold content should vary from 0.5 to 5% to achieve good activity without the costs related to the catalyst synthesis [88].

Despite the large number of studies, the valence state (Au^0, $Au^{\delta-}$ or $Au^{\delta+}$) of the active site of Au catalysts remains a controversial issue. This can be observed with the example of the simplest model reaction of CO oxidation. Thus, Haruta [89], Campbel [90], Gates et al. [91] suggest that the active centers are small metal particles of gold. At the same time, Guzman and Gates [92] found an increased rate of CO_2 formation with increasing Au^+ concentration. Lee and Schwank [93], Hutchings et al. [94], and Pestryakov et al. [95, 96] also support the idea of cationic nature of gold (Au^+ or Au^{3+}). At a variance, Chen and Goodman [97] highlighted the important role of negatively charged gold particles. The same division in conclusions about electronic gold state responsible for activity is observed in the selective liquid-phase oxidation of alcohols, which will be described in detail in the following sections of the literature review (Sections 1.2 and 1.3). Other parameters, such as an effect of support, preparation method, particle size, etc., will be discussed in these sections as well.

A comprehensive knowledge of the chemical and physical properties of Au NPs as heterogeneous catalysts is necessary to understand the nature of active sites. A deeper understanding of the structure of metal particles, their size, shape and catalytic properties of materials can be obtained through a number of methodologies [98]. In general, a number of characterization methods for the identification and characterization of gold catalysts are:

- Elemental composition: energy-dispersive X-ray (EDX), atomic absorption spectroscopy (AAS), inductively coupled plasma (ICP);
- Morphology: microscopic technique by transmission (TEM) or scanning electron microscopy (STEM);
- Structural properties: X-ray diffraction (XRD), ultraviolet-visible (UV-vis) and vibrational spectroscopies;

- Composition and surface structure: spectroscopic methods (infrared (IR), X-ray photoelectron spectroscopy (XPS), Raman spectroscopy) and temperature-programmed methods, such as temperature-programmed reduction (TPR) and temperature-programmed desorption (TPD).

1.2. Catalytic Oxidation of Fatty Alcohols: n-Octanol

Among the different alcohol reactions, their selective oxidation to valuable carbonylic compounds is one of the most important transformations in industrial organic chemistry and a challenging process in terms of green chemistry [1, 2]. Catalytic oxidations can be classified into two types [99]: complete (or total) oxidation, used for catalytic destruction of various toxic compounds, and selective oxidation, used for organic compounds in fine chemistry, aiming at the synthesis of desired chemical products.

Traditional methods for the latter involve the use of toxic, expensive, stoichiometric metal oxidants and harmful organic solvents and often require harsh reaction conditions [3, 4]. Catalysis research is working towards favourable solutions to these problems through the development of effective heterogeneous catalysts for environment friendly applications. Therefore, performing of alcohol oxidation reaction on heterogeneous catalysts (used as a recyclable solid material in biomass processing) with clean non-toxic oxidants such as air, oxygen or peroxides at mild conditions (atmospheric pressure, low temperatures and absence of bases and radical initiators) would be a great of interest.

Aliphatic primary alcohols with eight or more carbon atoms, also called "fatty alcohols", are the less reactive alkanols, whose physical properties impose constraints to implementation of green chemistry approaches. Namely, the melting and boiling points, as well as the viscosity, gradually increase with the increase of the number of carbon atoms in the chain, and the solubility in water decreases exponentially [2, 100]. Thus, the physical properties of higher alcohols determine the need to carry out the process in the liquid phase using moderate temperatures (60-130 °C) and inert solvents for using oxygen or air as oxidants (aerobic oxidation).

Fatty alcohols are present in forestry wastes (for example, in beech bark or Douglas fir), in tall oil, as by-products in the preparation of cellulose, mainly from coniferous trees processing [101]; they are also present in non-woody plants, such as flax, hemp, sisal and abaca [102]. Selective oxidation of these alcohols from biomass conversion products may allow them to be used as a new resource for the production of corresponding aldehydes, ketones, esters and fatty acids, which are valuable intermediates for the chemical, pharmaceutical [103] and agrochemical industries. For example, behenic acid ($C_{22}H_{44}O_2$) is used in cosmetology, hair conditioners and creams because of its high wettability

[104] and lignoceric acid ($C_{24}H_{48}O_2$) is used in pharmaceuticals [105] and as food additive [106].

n-Octanol is the first representative of fatty alcohols and is a very convenient model for investigating the reactivity of this class of compounds and evaluating the properties of the catalysts for reactions dealing with them.

One of the demanded oxidation products of n-octanol is octanal, a.k.a. caprylic aldehyde, which occurs naturally in citrus oils and could be used commercially as a component in perfumes and in flavor production for the food industry [24]. Compounds of octanoic acid, another n-octanol oxidation product, are found naturally in the milk of various mammals, and as a minor constituent of coconut and palm kernel oils [107]. Octanoic acid, a.k.a. caprylic acid, has broad applications. In addition to commercial production of ester (octyl octanoate) for perfumery, as flavor and fragrance agent, and in the manufacture of dyes, octanoic acid can be used as disinfectant [25] in commercial food handling and health care facilities. In addition, it is currently being investigated as a treatment for voice tremor [26, 27] and taken as a dietary supplement [28].

Since *n*-octanol is a convenient model of primary alcohols of long chain, it is often used for comparative studies of catalytic activity in oxidation of alcohols. The majority of the works on liquid-phase oxidation of n-octanol are devoted to the study of catalytic systems based on noble metals: Ru [108-110], Pt [111-113], Pd [114-117], Au [22, 23, 29-36, 115-117], Ag [118, 119] and also other non-noble metal catalysts [120-125]. However, among them, there are very few studies where mild conditions (atmospheric pressure, moderate temperatures and non-toxic oxidants) have been applied for the efficient and selective liquid phase oxidation of n-octanol; they are briefly summarized in Table 1.

The combined homogeneous catalytic system N-Hydroxyphthalimide (NHPI) with $Co(acac)_3$ (0.05 equiv. to NHPI) was effective for n-octanol aerobic oxidation to octanoic acid. It yielded 86% of acid (C_{OL} = 90%) in 5 h using this system (alcohol:NHPI = 10, alcohol:Co = 400) while 71% yield (C_{OL} = 75%) was achieved in 20 h when NHPI was used alone (alcohol:NHPI = 10) [122]. Other authors [123] combined NHPI with heterogeneous silica based cobalt (II) interphase catalyst, prepared by direct grafting mesoporous silica by a silica precursor–Schiff base Co(II) complex, to allow the recyclability of the homogeneous complex. Aerobic oxidation of n-octanol with this system yields 87% octanal (S_{AL} = 95.6%) and 4% octanoic acid (S_{AC} = 4.4%) (alcohol:NHPI:Co catalyst in 1:0.1:0.0025 ratios, T = 60 °C); however, in a rather long reaction time, 40 h. Recycling tests of this catalyst were conducted only for 1-phenylethanol oxidation under conditions comparable for n-octanol oxidation (T = 60 °C, t = 22 h, 1:0.1:0.0025): there was not considerable loss of activity (yield of acetophenone, Y_{ac} = 100-88%) until 4 cycles.

Kumar et al. [124] found that strontium added $CoAl_2O_4$ nanocatalysts with spinel structure catalyze the oxidation of alcohols selectively to aldehydes using

different oxidants such as H_2O_2, TBHP or NaOCl. Poor activity was observed on Co_2AlO_4 spinels alone. Better conversions were obtained using TBHP as oxidant and acetonirile as solvent. Thus, oxidation of n-octanol with TBHP over $Co_{0.7}Sr_{0.3}AlO_4$ yielded 72% octanal (S_{AL} = 100%, C_{OL}= 72%), but required a rather high catalyst loading (TBHP/alcohol = 1, Alcohol/Catalyst = 2.6 w/w, T = 80 °C, t = 5 h).

Table 1. Catalytic liquid-phase oxidation of n-octanol using gold catalysts under mild conditions (1 atm, 60-83 °C).

Catalyst	T, °C	Oxidant	Solvent	Reaction time, h	R [c]	Conv., %	Selectivity, %			Ref.
							Aldehyde	Acid	Ester	
NHPI [a]	75	O_2	MeCN [b]	20	10 [d]	75		95		122
NHPI + $Co(acac)_3$	75	O_2	MeCN	5	10:400 [e]	90		95		122
NHPI + Co(II)–SiO_2	65	O_2	MeCN	40	10:200 [f]	40	4	87		123
$Co_{0.7}Sr_{0.3}AlO_4$	80	TBHP	MeCN	5	2.6	72	100			124
Zr(n-PrO)$_4$	60	TBHP	Toluene	2	10	90	80	20		125
2.3wt.% Ag/TiO_2	80	O_2	n-heptane	6	100	2.5	90	8	2	118
2.3wt.% Ag/Fe_2O_3/TiO_2	80	O_2	n-heptane	6	100	7.6	100	0	0	118
2.3wt.% Ag/MgO/TiO_2	80	O_2	n-heptane	6	100	9	95	3	2	118
2.3wt.% Ag/CeO_2/TiO_2	80	O_2	n-heptane	6	100	12.3	92	3	5	118
1.4wt.% Ru(OH)$_3$/Al_2O_3+Hq [g]	83	O_2	TFT [h]	4	20	87 [i]	98			109
2.1wt.%Ru–CeO_2	60	O_2	TFT	4	10	30		93		110
2.1wt.%Ru–Co(OH)$_2$–CeO_2	60	O_2	TFT	4	10	100	1	97		110
2.5wt.% Au/SiO_2-pH_2	80	O_2	n-heptane	6	100	2.5	85		15	29
2.5wt.% Au/Fe/SiO_2-i- pH_2 [j]	80	O_2	n-heptane	6	100	4	40		60	29
2.5wt.% Au/Ce/SiO_2-i- pH_2	80	O_2	n-heptane	6	100	5	70		30	29
2.5wt.% Au/La/SiO_2-i- pH_2	80	O_2	n-heptane	6	100	3	50		50	30
2.5wt.% Au/La/SiO_2-s- pH_2	80	O_2	n-heptane	6	100	3	60		40	30
2.5wt.%Au/Mg/SiO_2-s- pH_2	80	O_2	n-heptane	6	100	3	60		40	30
6wt.% Au/SiO_2	80	O_2	toluene	4	8	40	17			31
1wt.% Au/$Ga_3Al_3O_9$	80	O_2	toluene	3	67	23	99			32
0.5wt.% Au/MIL-101 [k]	80	O_2	toluene	3	67	38	99			32
2.5wt.% Au/γ-Ga_2O_3	80	O_2	Mes. [l]	2.5	10	45	99			33
1wt.% Au/$Cu_aMg_bAl_cO_x$	80	O_2	Mes.	3	95	34 [i]	98			34
2wt.% Au-Nb_2O_5-D [m]	80	O_2	n-heptane	6	100	5	58	0	42	35
2wt.% Au-Nb_2O_5-H [m]	80	O_2	n-heptane	6	100	6	45	0	55	35
2wt.% Au-ZnO-D	80	O_2	n-heptane	6	100	45	18	0	82	35
2wt.% Au-ZnO-H	80	O_2	n-heptane	6	100	38	20	0	80	35
2wt.% Au-MgO-D	80	O_2	n-heptane	6	100	65	15	10	75	35
2wt.% Au-MgO-H	80	O_2	n-heptane	6	100	27	35	15	50	35
4wt.% Au/TiO_2_pH_2	80	O_2	n-heptane	6	100	11	81	3	16	22
4wt.% Au/CeO_2/TiO_2_pH_2	80	O_2	n-heptane	6	100	23	66	2	32	22
4wt.% Au/La_2O_3/TiO_2_pH_2	80	O_2	n-heptane	6	100	40	36	0	64	22
4wt.% Au/Fe_2O_3/TiO_2_pH_2	80	O_2	n-heptane	6	100	15	58	0	42	23
4wt.% Au/MgO/TiO_2_pH_2	80	O_2	n-heptane	6	100	20	67	2	31	23

[a] NHPI: N-Hydroxyphthalimide; [b] MeCN: acetonitrile; [c] R: Alcohol/Metal ratio (mol/mol); [d] Alcohol:NHPI = 10 (mol/mol); [e] Alcohol:NHPI:Co = 10:400 (mol/mol); [f] Alcohol:NHPI:Co = 10:200 (mol/mol); [g] Hq: hydroquinone; [h] TFT: Trifluorotoluene; [i] Yield of aldehyde instead of conversion; [j] direct synthesis «s» or impregnation method «i» for support modification with following hydrogen treatment at 300 °C of as-prepared catalyst (pH_2); [k] MIL-10: zeolite-type metal-organic framework; [l] mes.: mesitylene and 90 °C; [m] D, dried, or H, after thermal reductive treatment; Conv. — conversion.

Krohn et al. describes also the application of hydroperoxides, such as TBHP or cumene hydroperoxide (CHP), for catalyzing of non-activated primary and secondary alcohols to their corresponding aldehydes and ketones [125]. Thus, n-octanol was almost totally converted (C_{OL} = 98%) at 60 °C to octanal/octanoic acid mixture in ratio 4:1, while a higher octanal formation was observed (aldehyde:acid = 9:1) at 20 °C (C_{OL} = 96%), but in 20 h. Such good aldehyde yields could be obtained not only by decreasing temperature reaction, but also by lowering the amount of TBHP or replacing it by CHP, and/or exchanging the more active catalyst $Zr(O\text{-}t\text{-}Bu)_4$ by $Zr(O\text{-}n\text{-}Pr)_4$ or silica gel-supported $Zr(OR)_x$.

Moving on to catalysts based on precious and noble metals, starting with the paper of Kolobova et al. [118] on the use of 2.3 wt.% $Ag/M_xO_y/TiO_2$ (M_xO_y = Fe_2O_3, MgO, CeO_2, Ti/M = 40) catalysts in n-octanol and betulin oxidation with O_2 at 1 bar, it was suggested that the active sites of modifiers for the liquid-phase oxidation of n-octanol are monovalent Ag^+ ions. The best promotional effect was observed after introduction of Ce oxide onto the support (C_{OL}=12.3%, S_{AL}= 92%, T = 80 °C, 1 atm, Alcohol/Ag = 100, 6 h), while redox pretreatments are detrimental to catalytic activity due to a decrease in the surface concentration of silver monovalent ions. Strong interaction was found for silver with TiO_2, which gave a uniform distribution of silver on the support surface, but stabilizing it in the form of inactive surface compounds.

Several catalysts based on ruthenium were found to be active catalysts for n-octanol oxidation under mild conditions; however high ruthenium amount was used. As an example, 1.4 wt.% $Ru(OH)_3/\gamma\text{-}Al_2O_3$ could catalyze the oxidation of 2-octanol to 2-octanal in a 91% yield within 2 h (solvent TFT, A/M = 20, T = 83 °C) [109]. Less reactive primary alcohols 1-octanol and 1-decanol were oxidized more slowly to their corresponding aldehydes. Increasing the reaction time did not improve the yield to aldehydes due to their over-oxidation to carboxylic acids. The addition of a small amount of hydroquinone (1 equiv. based on Ru) completely suppressed the over-oxidation, which allowed obtaining only aldehydes with good yields: 87% octanal and 71% decanal, respectively, in just 4 h.

With the same solvent and reaction time (solvent TFT, t = 4 h), but at lower T (60 °C) and higher ruthenium loading (A/M = 10), a three component catalytic system, 6.4 wt.% $Ru–Co(OH)_2–CeO_2$, was highly efficient for the oxidation of n-octanol to octanoic acid yielding 97% acid at full conversion [110]. Authors noted extremely fast aerobic oxidation of octanal to the acid even at room temperature (Y_{AC} = 93% in 30 min) over this catalyst. Also, the order of activity in terms of component amount was as follows: $Co(OH)_2–CeO_2$ < Ru/CeO_2 < $Ru–Co–Al–CO_3$ < $Ru–Co(OH)_2–CeO_2$, evidencing that synergy of the three metals (Ru, Co and Ce) is needed to achieve high acid yield.

In comparison with platinum group metals catalysts, supported nanogold catalysts are highly active even at low temperatures, and selective in obtaining the desired products in the aerobic oxidation of n-octanol.

In the works Kotolevich et al. [29, 30], 1–2 nm Au NPs on nanosized silicon oxide were obtained. The influence of the support modifier (Fe, Ce, Mg or La) and the preparation method (either direct synthesis «s» or impregnation method «i») on the structural, electronic and catalytic properties in the liquid-phase oxidation of octanol was studied under mild conditions (0.1 M n-octanol in n-heptane, no base added; T = 80 °C, R = 100). It was found that Fe, La and Mg modifiers changed electronic properties of supported gold, favoring the formation and stabilization of $Au^{\delta+}$ states, which are probable gold active sites of selective liquid-phase oxidation of alcohols in redox catalytic processes. However, in spite of the low particle size, the catalysts exhibited low octanol oxidation activity. Maximum 5% conversion in 6 h of reaction was achieved on Au NPs supported on the ultra-small SiO_2 modified with cerium oxide by impregnation method, and relative order of activity was: Au/$CeSiO_2$-i > Au/$FeSiO_2$-i ≫ Au/$MgSiO_2$-i ≈ Au$LaSiO_2$-i ≈ Au/$LaSiO_2$-s > Au/SiO_2 > Au/$FeSiO_2$-s ≫ Au/$CeSiO_2$-s. The enchanced catalytic performance on ceria modified catalyst was probably due to the oxygen mobility and storage capacity of ceria, which allows the formation of Ce^{3+} sites and adsorbed oxygen species due to metal-support interactions.

Li et al. [31] studied silica-supported Au–Cu and Au–Ag alloy NPs for the aerobic oxidation of alcohols. For comparison, they also investigated the corresponding monometallic catalysts in octanol oxidation. With a large load (R = 8) of 6 wt.% Au/SiO_2 catalyst, they could achieve 40% conversion of n-octanol in 4 h, with 17% aldehyde selectivity. Unfortunately, no information of other products nor of electronic state of gold was provided.

Su et al. [32] suggested that the high dispersion of Au NPs and the electron donation effects of aryl rings to the Au NPs within the large cages of the MIL-101 support are the main reasons for the observed high activities of the Au/MIL-101 catalyst in aerobic oxidation of alcohols, including n-octanol (C_{OL} = 38%, S_{AL} = 99%) under base-free conditions (T = 80 °C, 1 atm, R = 67, 3 h).

Liu et al. [33] showed that Au/γ-Ga_2O_3 was effective for oxidation of several alcohols. In particular, 45% octanol conversion was obtained after 2.5 h with 99% aldehyde selectivity, using a low alcohol/Au ratio (R = 10). Nevertheless, the high catalytic performance exhibited was attributed to the significantly enhanced dehydrogenation capability, due to a strong interaction between Au NPs and the γ-Ga_2O_3 support, which was attributed to the presence of gold species detected by XPS with binding energy (BE) 83.1–83.4 eV.

Haider et al. [34] described oxidation of various types of alcohols over 1 wt.% Au/$Cu_aMg_bAl_cO_x$ catalysts. In case of n-octanol oxidation, 34% octanal yield was obtained at 90 °C after 3 h (Table 1). Ex-situ XANES of the fresh and spent

catalysts revealed that a significant fraction of the deposited gold existed as charged species (Au^{+}).

In a recent paper [35], MgO, ZnO and Nb_2O_5, representative of three different types of oxides (basic, amphoteric and acidic, respectively), were used as supports for Au NPs. It was found that the catalytic activity is influenced by the electron mobility between the Au NPs and the support, which depends on the intermediate electronegativity of the support. However, besides the predominant $(Au^{0})^{\delta-}$ species in some active dried catalysts (2 wt.% Au-MgO-D and 2 wt.% Au-ZnO-D), also cationic gold (Au^{+}) was present. Selectivity in n-octanol oxidation, preferably towards ester formation (S_{ES} = 75%, C_{OL} = 65%) in the case of the most active catalyst (2 wt.% Au-MgO-D), was influenced by redox properties of the gold species, acid-base properties of the supports and catalyst pretreatment.

Other studies on supported gold catalysts in the liquid-phase oxidation of n-octanol (4 wt.% Au/M_xO_y/TiO_2 catalysts, where M_xO_y = Fe_2O_3, MgO, CeO_2, La_2O_3 modifiers) [22, 23] (Table 1) suggested that the formation of the active surface was strictly dependent on the modifying additives (transition metal oxides) used for better metal-support interaction and as a tool for transforming and stabilizing gold active sites. However, the obtained experimental data turned out to be insufficient to identify the nature of the active site of these catalytic systems. Additionaly, the combined effect of gold loading, nature of the modifying additive and pretreatment atmosphere on the formation of the active surface in such catalytic systems was not considered. Moreover, the process of deactivation of the catalysts was not studied and the factors that determine the selectivity of the process were not established.

1.3. Catalytic Oxidation of Aromatic Alcohols: 1-Phenylethanol

The oxidation of aromatic alcohols is the foundation of several important industrial and fine-chemical processes, such as perfumery, pharmaceutical, dyes and agrochemicals. 1-phenylethanol oxidation is generally treated as a model reaction of alcohol oxidation with higher reactivity than aliphatic primary ones.

1-Phenylethanol can be found naturally as a glycoside in tea flowers (*Camellia sinensis*) [126]. It is also reported to be present in cranberries, grapes, garlic, mint oil, cheeses, cognac, rum, white wine, cocoa, black tea, hazelnuts, cloudberries, beans, mushrooms and endives [127].

The main oxidation product of its oxidation is acetophenone (methylphenylketone, $C_6H_5COCH_3$). Acetophenone is used in perfumes, soaps and creams, as well as a flavouring substance in food, soft drinks and tobacco. It is also used as a solvent and has a sleeping effect, important in the manufacture of medicines. Traditionally, acetophenone is obtained from benzene and acetyl chloride (or acetic anhydride) in the presence of iron or aluminum chlorides by

the Friedel – Crafts reaction (Scheme 1). The disadvantage of this method is the production of a large amount of acidic wastewater after completion of the reaction, which complicates mass production and leads to enviromental problems.

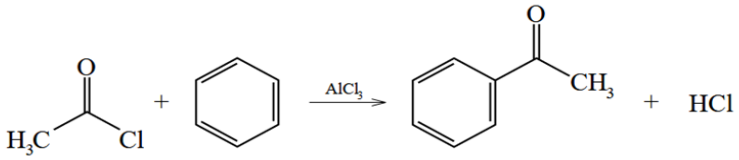

Acetyl chloride Benzene Acetophenone By-product

Scheme 1. Friedel – Crafts acylation of benzene with Lewis acid catalyst ($AlCl_3$).

There are many studies reported for 1-phenylethanol oxidation, using both homogeneous and heterogeneous catalysis (Table 2).

Pombeiro and co-workers [128-132] have proposed a number of effective homogeneous catalysts based on complexes of copper, iron, cobalt for the oxidation of 1-phenylethanol at atmospheric pressure in the absence of a solvent, using TBHP as an oxidizing agent. In most cases, the authors preferred microwave irradiation as a heating method, the use of which, as the researchers note, compared with traditional thermal heating, leads to a shorter reaction time, and increase in yield and selectivity. Thus, when the dimeric copper complex $[Cu_2(R)(CH_3O)(NO_3)]_2(CH_3O)_2$ [128] was used at 80 °C, a 54% yield of acetophenone was achieved within 1 h of reaction. Another copper-based complex under comparable conditions (temperature, using TBHP without solvent) with the previous work, but using traditional heating and a lower catalyst load, provided 12% acetophenone yield in 2 h; however, adding 2% K_2CO_3 resulted in a fivefold increase in ketone yield [129]. With an increase in the reaction temperature to 120 °C and the use of $[Cu(\kappa NOO'HL)Cl(CH_3OH)]$ monomer with a keto ligand in the absence of promoters, the acetophenone yield was 82%, that increased with the introduction of the nitroxyl radical TEMPO up to 92% [130].

In subsequent work, the same group investigated composite catalysts containing 3d metals (Cu, Fe, Co, V) in the peroxidative oxidation of 1-phenylethanol under microwave irradiation. The effect of adding carbon materials to the aforementioned composites [131] was also studied to facilitate the transfer of electrons during redox catalysis due to the transition metal. Thus, the cobalt chloride salt (alcohol/cobalt = 50) with the addition of carbon nanotubes (CNTs) exhibited the best catalytic properties among the studied catalysts; the yield of acetophenone was 82%, while without nanotubes just 28% per hour of reaction at 80 °C. However, when this catalytic system was reused in the oxidation of 1-phenylethanol, a significant loss of activity was observed during the first three cycles, but was more pronounced in the 4th cycle: 17, 19,

and 56% of the initial activity, respectively. The authors attributed the observed deactivation to the leaching of cobalt during the reaction.

Table 2. Catalytic oxidation of 1-phenylethanol using homogeneous and heterogeneous catalysts.

Catalyst	Oxidant	*P*, atm	Solvent	*T*, °C	Reaction time, h	*R* [a]	Y_{ac}, % [b]	Ref.
$[Cu_2(R)(CH_3O)(NO_3)]_2(CH_3O)_2$	TBHP	1	-	80	1 [e]	71	54	128
[Cu(κONN′HL)(NO_3)(*N*,*N*-dimethylformamide(DMF)](NO_3)·H_2 [c]	TBHP	1	-	80	2	1000	12	129
[Cu(κONN′HL)(NO_3)(DMF)](NO_3)·H_2+K_2CO_3 [c]	TBHP	1	-	80	2	1000	62	129
[Cu(1κNOO′,2κO′,3κO″L)]$_n$ [d]	TBHP	1	-	120	1 [e]	250	66	130
[Cu(1κNOO′,2κO′,3κO″L)]$_n$ [d] +2,2,6,6-Tetramethylpiperidin-1-yl)oxyl(TEMPO)	TBHP	1	-	120	1 [e]	250	81	130
[Cu(κNOO′HL)Cl(CH_3OH)] [d]	TBHP	1	-	120	1 [e]	250	82	130
[Cu(κNOO′HL)Cl(CH_3OH)] [d] +TEMPO	TBHP	1	-	120	1 [e]	250	92	130
Carbon nanotubes (CNTs)	TBHP	1	-	80	1 [e]	50	8	131
Graphene oxide (GO)	TBHP	1	-	80	1 [e]	50	14	131
$CoCl_2$	TBHP	1	-	80	1 [e]	50	28	131
$CoCl_2$–5%CNTs	TBHP	1	-	80	1 [e]	50	85	131
$CoCl_2$–5% GO	TBHP	1	-	80	1 [e]	50	72	131
CuO	TBHP	1	-	80	1 [e]	50	16	131
CuO–1%CNTs	TBHP	1	-	80	1 [e]	50	59	131
Fe_2O_3	TBHP	1	-	80	1 [e]	50	10	131
Fe_2O_3–1%CNTs	TBHP	1	-	80	1 [e]	50	32	131
Fe_2O_3–$CoCl_2$–5%CNTs	TBHP	1	-	80	1 [e]	50	73	131
V_2O_5	TBHP	1	-	80	1 [e]	50	45	131
$CoCl_2$–V_2O_5–5%CNTs	TBHP	1	-	80	1 [e]	50	54	131
[$FeCl_2$(L)(2,20bipy)]	TBHP	1	-	150	1 [e]	333	99	132
[$FeCl_2$(L)(2,20bipy)]	TBHP	1	-	150	46	333	99	132
[Fe(bipy)$_3$](CF_3SO_3)$_2$	H_2O_2	1	CH_3CN	100	0.5	100	62	133
[Fe(bipy)$_3$](CF_3SO_3)$_2$)+2-pyridine carboxylic acid	H_2O_2	1	CH_3CN	100	0.5	100	93	133
$VOPO_4$+TEMPO	O_2	4	H_2O	80	6	20	38.5(89) [f]	134
NiO/SiO_2	O_2	1	*p*-xylene	100	6	12	51	135
MnO_2 commercial	TBHP	1	ACN:tol [g]	RT	7	1	84	136
MnO_2 commercial	TBHP	1	ACN:tol [g]	40	7	20	34	136
MnO_2 commercial	H_2O_2	1	ACN:tol [g]	40	5	20	0	136
MnO_2 commercial	TBHP	1	ACN:tol [g]	80	7	10	67	136
MnO_2 commercial	-	1	ACN:tol [g]	80	24	1	30	136
NbP–C	H_2O_2	1	CH_3CN	90	24	11	72 [f]	137
$CeCrO_3$	TBHP	1	DMSO	90	6	10	100 [f]	138
15 wt.% Ag-Octahedral molecular sieve-2	TBHP	1	CH_3CN	75	4	625	71.5 [f]	139
0.9 wt.% Pd/Aerosil380	O_2	10	H_2O	100	6	262	44.9	140
0.9 wt.% Pd/Aerosil380	O_2	10	H_2O	100	12	262	75.1	140
1.0 wt.% Pd/60wt.% Polyketone (PK)–SiO_2	O_2	10	H_2O	100	6	262	62.2	140
1.0 wt.% Pd/60wt.% PK–SiO_2	O_2	10	H_2O	100	12	262	100	140
1.0 wt.% Pd/76wt.% PK–SiO_2	O_2	10	H_2O	100	6	262	58.3	140
1.0 wt.% Pd/76wt.% PK–SiO_2	O_2	10	H_2O	100	12	262	94.8	140
3 wt.% Pd/O-Diamonds(Dia)	O_2	1	*o*-xylene	100	4	1428	27.9 [f]	141
3 wt.% Pd/CeO_2/O-Dia	O_2	1	*o*-xylene	100	4	1428	72.5 [f]	141

Table 2. *Cont.*

Catalyst	Oxidant	*P*, atm	Solvent	*T*, °C	Reaction time, h	*R* [a]	Y_{ac}, % [b]	Ref.
1.57 wt.% Pd/CeO_2	O_2	1	-	120	2	649	91 [f]	142
1.44 wt.% Pd/apatite	O_2	1	-	120	2	649	90 [f]	142
10.10 wt.% Ru/Mg–LaO	O_2	1	toluene	80	4	10	96	143
10.10 wt.% Ru/SiO_2	O_2	1	toluene	80	4	10	45	143
10.10 wt.% Ru/Al_2O_3	O_2	1	toluene	80	4	10	40	143
10.10 wt.% Ru/MgO	O_2	1	toluene	80	4	10	36	143
10.10 wt.% Ru/TiO_2	O_2	1	toluene	80	4	10	36	143
1 wt.% gold nanoparticles (Au NPs)/Ionic liquid (IL)/*N*-hydroxyphthalimide (NHPI)	O_2	4	-	100	24	1356	60(47) [f]	144
1wt.% Au NPs/IL/NHPI	O_2	4	-	160	24	6780	77 (58) [f]	144
1wt.%Au NPs– supported ionic liquid-like phases	H_2O_2	1	H_2O	150	0.25	8	>90	144
1.54 wt.% Au/CeO_2	O_2	1	-	120	2	649	95	36
1 wt.% Au/Active carbon	TBHP	1	-	150	2 [e]	500	55	37
1 wt.% Au/carbon xerogel	TBHP	1	-	150	2 [e]	500	90	37
1 wt.% Au/Graphite	TBHP	1	-	150	2 [e]	500	63	37
1 wt.% Au/Microdiamonds	TBHP	1	-	150	2 [e]	500	100	37
1 wt.% Au/Nanodiamonds for liquid dispersion	TBHP	1	-	150	2 [e]	500	83	37
1 wt.% Au/Silicone carbide	TBHP	1	-	150	2 [e]	500	73	37
0.89 wt.% Au/Hydrotalcite (Ht)	Air	1	toluene	80	0.33	222	99	38
0.89 wt.% Au/Ht	Air	1	toluene	40	3	222	99	38
0.89 wt.% Au/Ht	Air	1	toluene	27	6	222	99	38
0.89 wt.% Au/Al_2O_3	Air	1	toluene	27	3	222	71	38
0.89 wt.% Au/MgO	Air	1	toluene	27	3	222	71	38
0.89 wt.% Au/TiO_2	Air	1	toluene	27	3	222	14	38
0.89 wt.% Au/TiO_2+Na_2CO_3	Air	1	toluene	27	3	222	65	38
0.89 wt.% Au/SiO_2	Air	1	toluene	27	3	222	<1	38
1.8 wt.% Au/Layered double hydroxide	O_2	1	toluene	80	2	200	99	39
1.0 wt.% Au/$Cu_aMg_bAl_cO_x$	O_2	1	mes. [h]	90	1	1181	85.1	40
5 wt.% Au/TiO_2	O_2	1	-	120	6	500	99	41
5 wt.% Au/Carbon black	O_2	1	-	120	4	500	65	41
5 wt.% Au/Single wall carbon nanotubes	O_2	1	-	120	3	500	99	41
5 wt.% Au/MnO_2-R	O_2	4	-	120	8	40000	81	42
Au–Pd(2 wt.%, 1:1)/Sodium titanate nanotubes	Air	1	-	120	10	10000	84(86) [f]	43
7.8 wt.% Au/TiO_2	O_2	10	H_2O	100	8	100	100	44
7.8 wt.% Au/TiO_2+ K_2CO_3	O_2	10	H_2O	100	2	100	93	44
10.83 wt.% Au-dendrimers/ Mesoporous SiO_2SBA-15+ 3 eq. K_3PO_4	O_2	1	CH_2Cl_2/ H_2O	RT	24	33	99.1	45
0.5 wt.% (Au^0–Pd^0)/high surface area-$BaAl_2O_4$	O_2	20	-	140	0.83	50000	[a] 97	46

[a] *R*: Alcohol/Active metal ratio (mol/mol); [b] Y_{ac}: yield of acetophenone; [c] copper complex with Schiff base ligand (HL) of salicylic aldehyde and aminoethylpiperazine [129]; [d] tautomeric forms (*enol* and *keto*) of aroylhydrazone Cu(II) complexes, H_2L = 2-hydroxy(2-hydroxybenzylidene)benzohydrazide [130]; [e] microwave irradiation; [f] Conversion data instead of yield and acetophenone selectivity in brackets; [g] ACN:tol: CH_3CN:toluene (3:1); [h] mes.: mesitylene.

Another work of the same group [132] described the synthesis of three new complexes of iron (III) with low solubility as heterogeneous catalysts for the peroxidative oxidation of 1-phenylethanol in the absence of a solvent. Moreover, using the [$FeCl_2$(L)(2.20bipy)] complex, the authors achieved a quantitative yield of acetophenone (99%) in 1 h of reaction at 150 °C created by microwave irradiation; using traditional heating under the same conditions, 99% yield of acetophenone was reached only after 46 h. Experiments with cheaper and environmentally friendly hydrogen peroxide (30% aqueous solution) as an oxidant turned out to be ineffective, with the likely decomposition of H_2O_2 at 150 °C. In addition, the catalyst proved to be suitable and for reuse since no loss of activity was observed up to at least three consecutive cycles. It is also worth noting that in all these studies, acetophenone was the only oxidation product.

A recent study [133] reported the use of an iron (II) complex as a homogeneous catalyst in the oxidation of 1-phenylethanol with hydrogen peroxide in acetonitrile solution in a microwave reactor. The authors note a less positive effect when using TBHP as an oxidizing agent as compared to H_2O_2. A metal-centered mechanism was proposed for this reaction. Interestingly, the useful role of some heterocyclic amino acids as co-catalysts was noted, the presence of which in solution influenced the activity of the iron complex with hydrogen peroxide. For half an hour of reaction without a co-catalyst at 100 °C, the yield of acetophenone was 62%, while with 5 equiv. 2-pyridinecarboxylic acid (Hpic) the authors achieved the maximum yield in this work, that is, 93%.

Du et al. [134] found a synergistic effect of vanadium and phosphorus in the presence of a nitroxyl radical (2,2,6,6-tetramethylpiperidyl-1-hydroxy) for the oxidation of benzyl alcohols with molecular oxygen in water. The authors suggest that TEMPO acts as an intermediary for the meeting of alcohol and vanadium. Phosphorus plays the role of an inorganic ligand, thereby influencing the form of vanadium. Thus, after 6 h of oxidation at 100 °C under 4 atm oxygen with catalytic mixture of $VOPO_4$ + TEMPO, 1-phenylethanol was partially oxidized to acetophenone (38.5% yield with 89% selectivity).

Returning to heterogeneous catalysts, Sasaki et al. [135] published the first to report on nickel nanoclusters deposited on silicon oxide, that exhibited activity (Y_{AC} = 51% after 6 h at 100 °C) in liquid-phase oxidation of 1-phenylethanol with molecular oxygen at atmospheric pressure and using p-xylene as a solvent. At the same time, the authors emphasized that the effective contribution of the Ni-O-Si interfacial structure is a key factor for this reaction.

Bhaumik et al. [136] reported the selective oxidation of 1-phenylethanol to acetophenone (84% yield) on commercial manganese dioxide using TBHP after 7 h at room temperature using a solvent mixture of acetonitrile and toluene. However, the catalyst loading was equivalent to the molar amount of the substrate, but the authors substantiate this optimal ratio by the low cost of the oxide and the absence pretreatment need. Reuse of the catalyst resulted in a 33% drop in activity. It was also established that MnO_2 catalyzes the decomposition

of hydroperoxides, however, more slowly than the process of alcohol oxidation itself.

Reis et al. reported [137] the catalytic behaviour of mesoporous niobium phosphate in the peroxidative oxidation of 1-phenylethanol using acetonitrile as a solvent at 90 °C, and linked the observed activity (72% conversion of alcohol with 100% selectivity to acetophenone in 24 h) with the low Brønsted acidity of the catalysts.

Nanocrystalline $CeCrO_3$ proved to be effective in the oxidation of many primary and secondary cyclic alcohols, including 1-phenylethanol, using TBHP as oxidant and dimethyl sulfoxide as solvent [138]. Total alcohol conversion was obtained at the same reaction temperature and ratio of alcohol to active metal as in the previous study, but 3.4 times faster.

Yadav and Yadav [139] described the use of octahedral molecular sieves with incorporated silver for the oxidation of 1-phenylethanol under mild conditions. As in most studies on the liquid-phase oxidation of this substrate, TBHP and acetonitrile were found to be the most effective oxidizing agent and solvent. The alcohol/silver ratio was higher than 600. The synergistic effect among the Ag, Mn and K ions contributed to an increase in the catalyst activity. The detailed kinetic study carried out showed that the reaction proceeds according to the model of the Langmuir - Hinshelwood - Hougen - Watson type with weak adsorption of all reagents. It was found that the apparent activation energy is 12.65 kcal/mol for 1-phenylethanol. In addition, the catalyst proved to be more stable to deactivation, and thus recyclable: the initial conversion of 71.5% in 4 h of reaction at 75 °C was retained up to six successive cycles.

When studying supported palladium catalysts, most of the works were devoted to the oxidation of 1-phenylethanol using molecular oxygen as oxidant. Antonetti et al. [140] found a direct relationship between the catalytic activity and the affinity of the support for water in the aerobic oxidation of alcohol with water as a solvent. Thus, the presence of hydrophilic SiO_2 in the hybrid support promoted the activation of the alcohol on the catalyst surface, and the catalyst was also active in recycling: 60% yield of acetophenone was obtained in 5 consecutive cycles without the formation of by-products at 100 °C for 6 h. Yasueda et al. [141] noted an increase in the selectivity and activity in the oxidation of many alcohols, including 1-phenylethanol, with the use of p-xylene as solvent, when cerium oxide was added to a catalytic system consisting of supported palladium on oxidized commercial powder diamond (Pd/O-Dia). The improvement in catalytic performance in the presence of CeO_2 was attributed to the suppression of side reactions by facilitating the removal of hydrogen from palladium. Furthermore, the addition of a small amount of CeO_2 facilitated better dispersion of palladium on the support. The authors also noted that the Pd/O-Dia system was much more efficient than Pd/AC (AC: activated carbon) and Pd/SiO_2 catalysts in the liquid-phase oxidation of alcohols. Abad et al. [36] reported palladium supported on cerium oxide and apatite in the solvent-free oxidation of 1-phenylethanol and secondary aliphatic alcohols. However, the

activity and selectivity of gold supported on the mentioned supports and at a lower reaction temperature (120 °C) turned out to be higher than that of palladium catalysts. It should be noted that in these last two papers [36,141], the formation of a by-product, ethylbenzene, was detected when supported palladium catalysts were used.

Kantam et al. [143] described an efficient method for aerobic oxidation of benzyl and secondary aromatic alcohols to their corresponding aldehydes or ketones using ruthenium supported on mixed oxides of magnesium and lanthanum. This catalyst was successfully reused in the oxidation of 1-phenylethanol dissolved in toluene, while maintaining constant yield and selectivity up to five catalytic cycles. However, a rather high catalyst loading was used (alcohol/ruthenium = 10). The peculiarity of the Mg-LaO support is presumably related to its strong basicity, which stabilizes Ru in the form of ruthenates on the surface of the mixed oxide, which was difficult to achieve on other oxides with weak basic properties, as the authors note.

Concerning Au catalysts, Restrepo et al. [144] described the use of thermally reduced Au NPs dispersed in an ionic liquid (IL) in 1-phenylethanol oxidation under an oxygen pressure of 4 bar. With the introduction of the radical initiator N-hydroxyphthalimide (NHPI) in the reaction mixture, the authors observed 60% and 77% alcohol conversion with acetophenone selectivity of 47% and 58% at 100 °C and 160 °C, respectively, after 24 h of reaction. The by-products were di-(1-phenylethyl) ether and di-(1-phenylethyl) peroxide. The authors explain the low activity of the system without an initiator as follows. Under anaerobic conditions, the ionic liquid stabilizes the Au NPs without the need for the introduction of "ligand coating" to prevent further particle growth. Therefore, in the presence of oxygen, gold nanoparticles begin to aggregate, which leads to their deactivation. In addition, in the absence of a solvent, the ionic liquid can slow down the catalytic reaction due to the limitations of the mass transfer process. The researchers intend to select a support for the deposition of such nanoparticles in the future.

Restrepo et al. [145] also reported for 1-phenylethanol oxidation in water on efficient gold nanoparticles immobilized with a polymer ionic liquid AuNP-SILLPs, using various oxidants and microwave irradiation as a heat source. They evaluated the influence of various parameters and conditions on both the synthesis of nanoparticles and the process. Thus, it was found that the use of hydrogen peroxide as an oxidizing agent, sodium tetraborate as a reducing agent for the formation of AuNPs, and relatively high reaction temperatures (> 120 °C) allow to achieve excellent results (>90% yield) in a short time (15 min). However, when using TBHP, more active than air and H_2O_2, a lower selectivity than in the case of H_2O_2 was observed. Authors found that smaller particles were more active with conventional heating, while larger particles showed better results with microwave irradiation. The effects of hot spots, which depend on the particle diameter, can explain this. The larger the size, the higher the possible temperature gradient between the particle and the

bulk liquid, since the transfer of heat from the nanoparticle to the environment is proportional to the surface area where heat transfer takes place.

Concerning deposited gold catalysts Carabineiro et al. [37] used 1 wt.% Au supported on several carbon materials, namely polymer carbon xerogel, activated carbon, microdiamonds, nanodiamonds, graphite, and silicon carbide, prepared either by colloidal or by double impregnation methods. The resulting materials were tested in microwave oxidation of 1-phenylethanol with TBHP without using a solvent. The catalytic activity was influenced by several factors, such as the nature of the support, reaction time and temperature, amount of catalyst, presence of additives, etc. The highest acetophenone yield (99.9%) was obtained when gold was deposited on microdiamonds by the colloidal method. The authors attribute the increased activity of this catalyst to the presence of Au^{+}, which was not found in the other samples. In comparison with other catalysts, Au/microdiamonds exhibited a much lower loss of activity after each cycle, attributed to an increase in nanoparticle growth, found by TEM for all catalysts. The best results in the oxidation of 1-phenylethanol were achieved on catalysts prepared by the colloidal method, due to the smallest gold nanoparticles with high dispersion on a support. The authors also associate the high oxidation rates under microwave irradiation not only with the thermal effect, but also with the possibility of absorption of electromagnetic waves during rotational transitions of molecules.

Mitsudome et al. [38] reported on a gold catalyst capable of selectively and quantitatively oxidizing alcohols, including 1-phenylethanol under mild conditions (40 °C, in air, toluene solvent, R = 222) without any additives. The catalyst, consisting of 0.89 wt.% Au/Hydrotalcite (Ht), obtained by chemical reduction with KBH_4, did not lose its activity (98% yield of acetophenone) in four successive cycles of 1-phenylethanol oxidation. The authors tested other supported gold catalysts under the aforementioned conditions and reported the following series of activity growth in terms of TOF: Au/Ht > Au/Al_2O_3 = Au/MgO > Au/TiO_2 > Au/SiO_2, thus stating that Au/Ht is the most efficient catalyst in oxidation of highly reactive 1-phenylethanol. Researchers concluded that the Au/HT catalyst with Au NPs with an average size of 2.7 nm and a very narrow size distribution was highly effective in the oxidation of wide range of alcohols, including the less reactive cyclohexanol.

Liang et al. [39] also reported the successful aerobic oxidation of alcohols at room temperature and atmospheric pressure (solvent toluene, R = 200) using a catalytic system consisting of 1.8 wt.% Au deposited on Mg-Al-layered double hydroxide (Au/LDH) by ion exchange and subsequent reduction. Au NPs with a size range of 1-4 nm were homogeneously distributed on the support. In comparison with less active Au/TiO_2 and Au/SiO_2 samples, authors found a larger contribution of negatively charged gold particles to the Au/LDH catalyst due to strong interaction of nanoparticles with the support.

Haider et al. [40] studied a catalytic system consisting of gold (1 wt.%) supported by various methods on mixed oxide of magnesium, aluminum and

copper for oxidation of 1-phenylethanol (R = 1181, T = 90 °C) with molecular oxygen and mesitylene as solvent. The authors also assume that in the $Au/Cu_5Mg_1Al_2O_x$ sample, metallic gold with an average particle size of around 9 nm, obtained by the controlled deposition method, is responsible for the catalytic activity shown for the liquid phase oxidation of 1-phenylethanol (Y_{AC} = 85.1% in 1 h). Particles with a smaller average size (≈ 2 nm) obtained by the colloidal method, were found less active in this process (Y_{AC} = 73.4% in 1 h). Thus, the authors suggest that, in contrast to CO oxidation where the smallest average particle size is responsible for activity, the larger size of gold nanoparticles is fundamental in the effective liquid-phase oxidation of 1-phenylethanol.

Shanahan et al. [41] studied deposited gold (5 wt.%) obtained in-situ on three supports, single-wall carbon nanotubes (SWCNT), black carbon (P90) and titanium oxide (TiO_2), to use these catalysts in green oxidation (in the absence of solvent and bases, oxidizing agent - molecular oxygen, T = 120 °C, R = 500) of cyclic alcohols: 1-phenylethanol, 2-phenylethanol and benzyl alcohol. The most active and selective in all studied reactions were the samples based on carbon nanotubes. The authors linked the activity to the shape and size of the gold particles and the properties of the support. Thus, the quantitative yield of acetophenone (> 99.9%) was obtained in 3 h on Au/SWCNT catalyst (particle size 4-7 nm), in 8 h on Au/TiO_2 (particle size 10-20 nm), and the complete conversion of alcohol was observed after 4 h on Au/P90 (particle size 7-9 nm); however, in this case formation of ethylbenzene as by-product was detected. In addition, the researchers draw a connection between the specific surface area of the catalyst and oxygen adsorption: the larger the area, the more centers for oxygen adsorption and the faster the reaction proceeds. Therefore, on Au/TiO_2 (S_{BET} = 23 m^2/g), the reaction proceeds more slowly than on Au/SWCNT (S_{BET} = 265 m^2/g). Selectivity depended on functional groups and the size distribution of Au NPs. In particular, the formation of a second product, ethylbenzene, up to 35% observed on Au/P90 was due to the surface carbon functional group (H^+), acting as a reducing agent, consumed in the first catalytic cycle. Therefore, in the second cycle, the yield of acetophenone increased and the formation of ethylbenzene was not observed. The rest of the catalysts did not lose their activity during three catalytic cycles.

Wang et al. [42] reported on cationic gold (Au^+) contribution to catalytic activity, along with the optimal metal-support interaction, achieved at 5% gold content on Au/MnO_2-R (reduced manganese oxide nanorods) catalysts for the oxidation of cyclic alcohols in the absence of solvent at 120 °C. The catalysts were prepared by homogeneous controlled precipitation. It should be noted that the loading of gold relative to the substrate was the minimal (R = ca. 40,000) among all the gold catalysts studied in this review; however, oxygen was supplied to the reaction mixture under a pressure of 4 atm. The authors also refer to the article on the role of monovalent gold, which was stabilized by cerium oxide nanoparticles, in the efficient catalytic oxidation of alcohols [145].

Nepak et al. [43] reported, for the first time, the catalytic application of Au-Pd nanoparticles deposited by controlled deposition on sodium titanate nanotubes (NaTNT) for liquid-phase aerobic oxidation of alcohols. The reaction was carried out at 120 °C, 1 atm and under conditions free of solvents and bases. The catalyst was more active and selective (C_{OL} = 84%, S_{AC} = 86%, 10 h reaction time, R = 10,000) than the corresponding monometallic Au and Pd catalysts and Au–Pd/TiO_2, in the oxidation of 1-phenylethanol. The authors believe that the superior activity of the Au-Pd/NaTNT catalyst is due to the higher dispersion, smaller gold particle size and a higher amount of electron density in gold in the presence of palladium, which enhances the activation of molecular oxygen. The formation of by-products is possibly due to the presence of palladium since, despite the low conversion of alcohols, high selectivity was retained on Au/NaTNT.

Yang et al. [44] highlighted the promoting role of water in the aerobic oxidation of benzyl alcohol to benzaldehyde on Au/TiO_2, prepared by deposition-precipitation. The authors also applied these conditions in the oxidation of other alcohols, in particular 1-phenylethanol, and noticed that the addition of a base increased the conversion, but decreased the selectivity for acetophenone, associated with the hydroxyl groups released during the hydrolysis of potassium carbonate. Thus, in 8 h of reaction at 100 °C under 10 atm of oxygen, a 100% yield of acetophenone was obtained using 7.8 wt.% Au/TiO_2 (R = 100) and water as a solvent.

Li et al. [45] could oxidize 1-phenylethanol to acetophenone (Y_{AC} = 99.1%) in 24 h (R = 33) using Au NPs (10.83 wt.%) encapsulated in dendrimer/SBA-15 organic inorganic hybrid composite and 3 eq. K_3PO_4. Without the presence of dendrimers, gold nanoparticles supported on SBA-15 are readily leached, and therefore, catalyst is deactivated during recycling. However, there was no loss of activity, when using gold stabilizing polyamidoamine dendrimers, which also contribute to the production of smaller gold particles (<5 nm) responsible for catalytic activity, as suggested by the authors.

Mertens et al. [46] studied 0.5% (Au_0–Pd_0)/HSA-$BaAl_2O_4$ bimetallic catalyst in the selective oxidation of 1-phenylethanol (R = 50,000, T = 140 °C) without adding bases and solvent, but under 20 atm oxygen. Under these conditions, a 95% yield of acetophenone was obtained in less than 1 h, which was retained in the next five cycles after the catalyst was regenerated. The optimized gold: palladium ratio found (8:2) of in the Au_0-Pd_0 nanocolloidal mixture was proposed as responsible for the demonstrated activity, selectivity and stabilization with the basic support being suitable for reusing.

Therefore, as a summary of these results, it can be concluded that the catalytic oxidation of this alcohol, a representative of cyclic alcohols, can be carried out under mild conditions, say, using green oxidizing agents, such as oxygen, air and peroxides, both with a solvent and in its absence, in moderate temperature ranges: from room temperature to 150 °C and, in most cases, at atmospheric pressure. Also, when using peroxides, a new trend is the reaction

under the influence of microwave heating, which, in comparison with the traditional process, allows obtaining high yields in a short time.

Some disadvantages exist for homogeneous catalysts, namely the inability to reuse them, and the need for addition of bases and radicals, which researchers often apply to increase the yield of acetophenone. However, an exception is the work where catalysts based on iron complexes with low solubility were synthesized and efficiently reused [132].

When heterogeneous base metals catalysts were used, selective oxidation of 1-phenylethanol at room temperature was possible, however, a large catalyst load and a long reaction time up to 24 h were required [136]. Catalysts based on palladium, silver and rutheniums exceeded the activity of previous catalyst systems, as expected, and were not deactivated during the recycling tests [139, 140]. However, the disadvantages in the case of silver and palladium catalysts would include the formation of by-products [36, 139, 141], and the high ratio of ruthenium to alcohol needed when using ruthenium catalysts [143].

Gold-containing systems have been extensively investigated in this process [36-46, 144, 145]. The main feature of these systems is their high activity and selectivity; however, there is a tendency to their gradual deactivation due to an increase in the size of Au NPs during reaction and recycling tests. Also, in most cases, the authors suggest that highly dispersed gold in the metallic state is responsible for the excellent activity in the oxidation of 1-phenylethanol [38, 40, 41, 43, 45]. However, there are also supporters of the cationic nature of gold active centres in this process [37, 42, 145] and Liang et al. [39] even considered negative charged gold as an active site.

Unfortunately, there are very few works in which the mechanism of both aerobic and notably peroxidative oxidation of 1-phenylethanol is proposed. Furthermore, when using TBHP as the oxidizing agent, the role of the catalyst is attributed to the decomposition of this oxidant into radicals responsible for the direct oxidation of alcohol [146, 147].

In general, it can be concluded that supported gold-containing systems are effective catalysts in the oxidation of 1-phenylethanol; however, even in the oxidation of such a reactive alcohol, the study of the mechanism of formation of the active surface of gold-containing systems responsible for excellent catalytic performance is still the subject of numerous discussions.

SUMMARY

Thus, it can be concluded that oxidation of different types of primary alcohols over gold supported catalysts, one inactivated (alkyl) and another activated (bearing an aromatic ring), represented by n-octanol and 1-phenylethanol, respectively, can be carried out under mild conditions (at atmospheric pressure and moderate temperatures, with green oxidants such as

oxygen, air and peroxides, and in the absence of bases). The choice of catalyst is a key factor in determining the activity and selectivity of both reactions.

The results obtained can be used in the processes of utilization and valorization (production of more valuable substances) of by-products of biomass conversion. Almost all oxo-derivatives of alcohols obtained in these processes are widely used in pharmaceutical, cosmetic, agrochemical and other industries.

Moreover, it should be noted there are few studies devoted to the formation of the active surface responsible for the activity and selectivity of catalysts. Knowledge about the nature of the active site will allow the targeted synthesis of highly efficient catalysts with desired properties, select the optimal conditions for the process and thereby achieve the best results.

Therefore, the detailed study of the active surface formation of $Au/M_xO_y/TiO_2$ catalysts under the influence of several factors (nature of the oxidizing agent, modifier nature, redox pretreatments and gold content) for oxidation of alcohols with different reactivity is an important and relevant topic of scientific research.

CHAPTER 2. EXPERIMENTAL

2.1. Catalyst Synthesis

2.1.1. Support preparation

Commercial non-porous TiO_2 P25 Evonik Degussa GmbH, (Essen, Germany, ≥99.5%) was used as the initial support. $Fe(NO_3)_3 \cdot 9H_2O$ or $Mg(NO_3)_2 \cdot 6H_2O$, $La(NO_3)_3 \cdot 6H_2O$ or $Ce(NO_3)_3 \cdot 6H_2O$ (Merck, Darmstadt, Germany, ≥98%) aqueous solutions was used for modification of titania by impregnation method. Nominal molar ratio Ti/M (Ce, La, Fe, Mg) was 40. Impregnated supports were dried at room temperature for 48 h and at 110 °C for 4 h, followed by calcination at 550 °C during 4 h. According to energy dispersive spectroscopy (EDS) results, actual molar ratios Ti/M were close to nominal ones (37-39) for all modified supports and they did not change significantly after gold deposition.

2.1.2. Gold deposition on support

Method of deposition-precipitation with urea was used for gold deposition on the supports with 0.5 and 4 wt.% nominal loadings, using $HAuCl_4 \cdot 3H_2O$ (Merck, Darmstadt, Germany, ≥99%) as precursor. The process of gold deposition was conducted in the absence of light, according to the previously reported procedure [148, 149]. Shortly, the support was added to an aqueous solution (distilled water) containing 4.2×10^{-3} M of the gold precursor and 0.42 M urea (Merck, Darmstadt, Germany, ≥99%). This mixture had initial pH of 2.4. After heating the solution at 80 °C for 16 h, the pH was adjusted to 7.5. The solution was then centrifuged at 11,000 rpm rate for 15 min and washed with water 4 times until complete chloride removal, which was checked by using the silver nitrate test. The final stage was drying of samples under vacuum 2 h at 80 °C. Such samples before any pretreatment (H_2 or O_2 atmosphere) will be denoted herein *as-prepared* samples. To prevent any alteration, the samples were stored in a desiccator at room temperature under vacuum and away from light.

2.1.3. Catalyst pretreatment

Before catalytic experiments, as-prepared samples were either treated in O_2 atmosphere (denoted as *n*% $Au/(M_xO_y)/TiO_2\_pO_2$) or in H_2 atmosphere (denoted as *n*% $Au/(M_xO_y)/TiO_2\_pH_2$) at 300 °C for 1 h (15% of H_2 or O_2 in Ar, 300 ml/min flow rate), where *n* is the gold content in wt.%, M is the metal (La, Mg, Ce or Fe) of the modifier oxide.

2.2. Catalytic Properties Study

2.2.1. Aerobic n-octanol oxidation

The catalytic properties were studied at 80 °C under atmospheric pressure and stirring (800 rpm) for 6 h in a semi-batch reactor, which is a four-necked round bottom flask equipped with reflux, oxygen feed, thermocouple and a septum cap. The appropriate amount of catalyst sample in n-octanol/Au ratio 100 mol/mol was added to a flask with 0.1 M solution of n-octanol (Merck, Darmstadt, Germany, ≥99%, HPLC grade) (25 mL) in n-heptane (Supelco, Darmstadt, Germany, ≥99%, HPLC grade). Oxygen with 30 mL/min rate was bubbled through the reaction mixture. To monitor the reaction progress, small aliquots of the reacting mixture were collected at 0.25, 0.5, 1, 2, 4 and 6 h, with the help of nylon syringe filters (pore 0.45 μm), and then were analyzed in a Varian 450 gas chromatograph (Varian Inc, Palo Alto, USA) with flame ionization detector (FID), using a capillary DB wax column (15 m × 0.548 mm, Varian Inc, Palo Alto, USA), and He as the carrier gas. The identification of compounds was achieved by calibration using reference commercial samples (the absolute calibration method). In the absence of support/catalyst, no activity was observed in oxidation of n-octanol.

n-Octanol conversion (X) and product yields (Y_i) and selectivity (S_i) were calculated in term of moles of C atoms, as follows:

$$Y_i = \frac{n_i C_i}{8 \cdot C_{ROHin}} \times 100 \quad (2.1)$$

Where n_i is the number of carbon atoms in compound i, and C_i is its molar concentration, and $C_{ROH\,in}$ represents initial octanol concentration.

Conversion (X_{ROH}) was calculated as the sum of the yields of carbon containing products, and product selectivity (S_i) as the ratio between product yield and conversion:

$$X_{ROH} = \sum Y_i \quad (2.2)$$

$$S_i = \frac{Y_i}{X_{ROH}} \cdot 100 \quad (2.3)$$

Carbon balances in all reported data were within 100 ± 3% and calculated as follows:

$$C\ balance\ (\%\ mol) = \frac{Final\ carbon\ moles}{Initial\ carbon\ moles} \times 100 \quad (2.4)$$

2.2.2. Peroxidative oxidation of n-octanol

To compare the catalytic results of the peroxidative oxidation of n-octanol with of those of 1-phenylethanol, the conditions selected for the peroxidative oxidation of n-octanol were as follows: R = 5000 mol/mol, T = 80 °C, TBHP (14.6 mmol)/alcohol (6 mmol) = 2.43, stirring 800 rpm, with no solvent or base added. In the absence of support/catalyst in the reaction mixture, no activity was observed in peroxidative oxidation of n-octanol.

2.2.3. Peroxidative oxidation of 1-phenylethanol

The catalytic properties for 1-phenylethanol oxidation were tested in a semi-batch reactor (round bottom flask), equipped with reflux and thermocouple, operated under atmospheric pressure and stirring (800 rpm), at 80 °C for 6 h. The reaction mixture was as follows: 1.27 μmol of Au were introduced in 1-phenylethanol (6 mmol, Merck, Darmstadt, Germany, 98%) as the substrate (R = 5000 mol/mol), TBHP (14.6 mmol, Merck, Darmstadt, Germany, 70% v/v aqueous solution) as the oxidizing agent, in a base- and solvent-free medium.

After the reaction test, the mixture was cooled down to room temperature. Typically, to conduct the product analysis, 10 μL of benzaldehyde as internal standard (Merck, Darmstadt, Germany, ≥99.5%, analytical standard grade) and 1 mL of MeCN (Merck, Darmstadt, Germany, ≥99.9%, HPLC Plus grade) were added to 100 μL of such reaction mixture. The resulting sample was centrifuged for 15 min and analyzed by gas chromatography (GC) using the internal standard method. Blank tests indicated that only traces (4 %) of ketone were generated. Chromatographic analyses were undertaken using a GC 8000 series gas chromatograph (Fisons Instruments, Loughborough, UK) equipped with a BP-20 (WAX) capillary column (SGE Analytical Science Europe Ltd, Milton Keynes, UK) and a flame ionization detector (FID) detector (Fisons Instruments, Loughborough, UK).

Molar yield (%) of acetophenone in both peroxidative and aerobic oxidation of 1-phenylethanol was defined based on substrate, i.e., moles of product per 100 mol of substrate, as determined by GC. Attribution of peaks was made by comparison with chromatograms of genuine samples and, in some cases, by gas chromatography mass-spectrometry (GC–MS) analyses with He as the carrier gas using a Clarus 600C instrument (Perkin Elmer, Waltham, MA, USA), equipped with a 30 m × 0.22 mm × 25 μm BPX5 (SGE Analytical Science Europe Ltd, Milton Keynes, UK) capillary column. According to the GC-MS, acetophenone was the only product in both aerobic and peroxidative oxidation of 1-phenylethanol.

2.2.4. Aerobic oxidation of 1-phenylethanol

To adequately compare the catalytic results of aerobic oxidation of 1-phenylethanol with those of n-octanol, the conditions selected for the oxidation of 1-phenylethanol with molecular oxygen were as follows: alcohol/gold ratio *R* = 100 mol/mol, 25 mL 0.1 M solution of 1-phenylethanol in mesitylene (Merck, Darmstadt, Germany, 98%), O_2 flow = 30 mL/min, stirring 800 rpm.

2.2.5. Recycling tests

To perform the recycling experiments in peroxidative oxidation of 1-phenylethanol, the used sample was separated from the reaction mixture by centrifugation (5000 rpm, 15 min) and decantation, washed 4 times with 5 mL of acetonitrile and dried at 50 °C to constant weight. Then it was reused for the oxidation test as described above.

To study the stability of catalysts in aerobic oxidation of n-octanol (recycling tests), the used sample was separated from the reaction mixture by centrifugation (5000 rpm, 15 min) and decantation, washed 4 times with 5 mL of n-heptane and dried at 50 °C to constant weight. Then it was reused for the oxidation test as described above.

2.3. Characterization Methods

1) Nitrogen adsorption-desorption isotherms at -196 °C were used to study the textural properties of catalysts and supports. A Micromeritics TriStar 3000 apparatus (Norcross, GA, USA) was applied at Instituto de Catálisis y Petroleoquímica ICP, Consejo Superior de Investigaciones Científicas, CSIC, (Madrid, Spain). Degassing of samples under vacuum at 300 °C for 5 h took place before each measurement. Normalization to standard temperature and pressure of adsorbed N_2 volume was carried out. The BET method to the nitrogen adsorption data (P/P_0 range 0.05–0.25) was applied for calculation of the specific surface area (S_{BET}) of the samples.

2) XRD patterns were obtained at Instituto de Catálisis y Petroleoquímica, CSIC (Madrid, Spain) by using a Philips XPert PR diffractometer (Amsterdam, Netherlands) using Ni-filtered CuKα (λ = 0.15406 nm) radiation. Step-scanning procedure included the following parameters (step size 0.02°; 0.5 sec).

3) STEM-HAADF measurements were conducted at Instituto de Catálisis y Petroleoquímica, CSIC (Madrid, Spain) using a microscope (JEOL JEM-2100F, JEOL Ltd., Tokyo, Japan) operated at 200 kV. Prior to the study, samples were grounded to a fine powder state and then, a drop of the suspension was deposited on a lacey carbon coated copper grid. For each sample, at least ten representative microscope images were acquired and at least 150 particles

counted for particle size distribution determination. Gold contents were measured EDS in the same microscope equipped with an Oxford INCA X-sight system detector.

4) XPS was obtained with a SPECS GmbH custom made system using a PHOIBOS 150 WAL hemispherical analyzer and a non-monochromated X-ray source (Al Kα X-rays 1486.6 eV, 200 W) for the study of gold electronic states on the catalyst surface. The measurements were done at Instituto de Catálisis y Petroleoquímica, CSIC, (Madrid, Spain) and partially at Centro de Nanociencias y Nanotecnología, Universidad Nacional Autónoma de México (Ensenada, Mexico). A pass-energy of 50 eV, a stepsize of 0.1 eV per step and a high-intensity lens mode were selected. The diameter of the analyzed area was 3 mm. Charging shifts were referenced against the Ti $2p_{3/2}$peak of TiO_2 at 458.8 eV. The pressure in the analysis chamber was kept lower than 1×10^{-8} mbar. The accuracy of the BE values was about ±0.1 eV. Peak areas were estimated by calculating the integral of each peak after subtracting a Shirley type background, fitting the experimental peak to a combination of Lorentzian/Gaussian lines with a 30/70 proportion and keeping the same width on all lines. Deconvolution of spectra and data analysis were performed with the CASA XPS software (version 2.3.15, CASA Software Ltd, Teignmouth, UK).

The used catalyst samples (i.e., after the reaction test) were characterized by X-ray photoelectron spectroscopy at Centre of Materials (CEMUP) of the University of Porto, Portugal. Surface composition and the chemical state of gold were determined by XPS analysis, performed on an ESCALAB 200A spectrometer (VG Scientific, Waltham, MA, USA) using Al Kα radiation (1486.6 eV). A pass-energy of 40 eV and a step size of 0.1 eV/step were selected. The charge effect was corrected using the C1s peak as a reference (binding energy of 285 eV). The CASA XPS software (version 2.3.15, CASA Software Ltd, Teignmouth, UK) was used for data analysis.

5) DRIFTS measurements were performed at Department of Chemistry of Lomonosov Moscow State University, (Moscow, Russia) on a Bruker EQUINOX 55/S FTIR (Bruker Optik GmbH, Ettlingen, Germany) spectrometer with a resolution of 4 cm^{-1}, equipped with a homemade chamber accessory. All DRIFTS CO spectra on the catalyst samples were recorded at 20 Torr pressure and in some cases at 5, 20 and 50 Torr, for studying of stability and strength of the complexes of Au^{+}-CO ions (5% accuracy measurement), at room temperature. Typically, powdered sample was loaded in a quartz ampoule with a window of CaF_2. Prior to measurements, samples were calcined at 100 °C under vacuum (10^{-4} Torr) for 1 h. Then each catalyst was studied in three states: as-prepared, after pretreatments either in H_2 or in O_2 at 300 °C for 1 h at 100 Torr, and then cooled down to room temperature. After that, hydrogen or oxygen was evacuated and CO adsorption (>99%) was carried out. The obtained DRIFTS data were presented in the form of Kubelka–Munk units (KMU). DRIFT CO spectra were obtained by subtracting the CO gas phase spectrum and the baseline was

corrected. Pure supports did not exhibit bands of adsorbed CO in this region of the spectrum under mentioned conditions.

6) Temperature programmed reduction with hydrogen (H_2-TPR) experiments were carried out at Laboratory of Catalytic Research, Tomsk State University (Tomsk, Russia) using chemisorptions analyzer ChemiSorb 2750 (Micromeritics, US) with TCD-detector. A gas mixture of 10% H_2 in Ar with flow rate of 20 ml/min was flown through samples (50–80 mg). The heating rate was 10 °C/min. To prevent influence of water vapor on TCD-signal, a cold trap with a mixture of liquid nitrogen and isopropanol was used (T ≈ -90°C). The hydrogen consumption was calculated using TPR profiles for Ag_2O standard (Micromeritics, US).

7) Temperature programmed desorption of ammonia (NH_3-TPD) and of CO_2 (CO_2-TPD) methods were applied for studying acidic and basic properties of the catalysts and their corresponding supports at Research School of Chemistry & Applied Biomedical Sciences of Tomsk Polytechnic University, (Tomsk, Russia) on a "Chemosorb" chemisorption analyzer (Neosib, Novosibirsk, Russia) equipped with a thermal conductivity detector (TCD), which was calibrated with NH_3 or CO_2 prior to analysis. Desorption starting temperature was 25 °C in the case of CO_2, and 100 °C for TPD of ammonia. Carrier gas in NH_3-TPD was helium; in CO_2-TPD was argon. Except for the differences listed in these methods, the experimental procedure was the same in both cases. Prior to the measurements, the samples were treated at 300 °C under an inert atmosphere (He or Ar) for 1 h to remove the impurities adsorbed on the surface. Then, temperature was decreased to 100 °C or 25 °C, followed by saturation with NH_3 or CO_2 for 1 h and flushing with He or Ar for 1 h to remove physisorbed ammonia or carbon dioxide. After that, the temperature was increased to 600 °C with a heating rate of 10 °C min^{-1} under inert atmosphere. For comparative analysis, NH_3 and CO_2 desorption profiles of catalysts are demarcated into temperature ranges: 100 (25)–200 °C, 200–400 °C and 400–600 °C, and are denoted as weak, medium and strong acid or basic sites, respectively.

8) Temperature-programmed oxygen desorption (O_2-TPD) was used to assess the nature of the interaction of oxygen with the surface of the catalyst and the support. All experiments were performed on a "Chemosorb" chemisorption analyzer (Neosib, Novosibirsk, Russia) equipped with a thermal conductivity detector (TCD), which was calibrated with O_2 prior analysis. A sample (0.2 g) pretreated at 300 °C in helium flow (60 mL/min) was saturated with oxygen at 40 °C for 1 h. Oxygen desorption was carried out in a helium stream from 40 to 650 °C with a heating rate of 20 °C/min.

2.4. Theoretical Calculations

The adsorption of n-octanol or 1-phenylethanol on gold nanoparticles was simulated in a scalar-relativistic approach using the density functional (DFT)

method PBE [150]. Tetrahedral Au_{20} and Au_{20}^{+} clusters were considered as models of gold nanoparticles. The Au_{20} cluster has been obtained experimentally [151] and is a popular model for studying structural effects in catalysis [152, 153]. Because the cluster has atoms located either at the top, on the facet and on the edge and with different coordination numbers, this model can be effectively applied to study the structural effects in the adsorption of phenylethanol. The cationic gold cluster was obtained by removing one electron from Au_{20} with subsequent optimization of the structure. As a first approximation, the effect of the support was ignored.

To reveal the role of different gold sites in adsorption of solvent molecules, heptane adsorption on simple $(Au^{0}O)^{2-}$, $(Au^{+}O)^{-}$, and $(Au^{3+}O)^{+}$ models containing Au^{0}, Au^{+}, and Au^{3+} were also studied at atomic level using density functional theory calculation with PBE functional [150]. The structures of all molecules were fully optimized, and the total energies of the reagents and products were calculated considering the energy of zero vibrations. Adsorption energies were calculated as the difference in total energies of adsorbed complex and the reagents (heptane and $(Au^{0}O)^{2-}$/$(Au^{+}O)^{-}$/$(Au^{3+}O)^{+}$).

All DFT calculations were performed in the PRIRODA program (version 17, Russia) [154] using the Lomonosov supercomputer [155] at Department of Chemistry of Lomonosov Moscow State University, (Moscow, Russia).

CHAPTER 3. RESULTS AND DISCUSSION

The following results on oxidation of n-octanol with molecular oxygen have been published in papers [156-158], while research on peroxidative oxidation of n-octanol as well as oxidation of 1-phenylethanol with either O_2 or TBHP have been presented in another publication [159].

3.1. Catalytic Results

3.1.1. Aerobic oxidation of n-octanol

Au NPs catalysts supported on pure titania and on titania modified with iron, cerium, magnesium or lanthanum oxides, with different gold contents (0.5 or 4 wt.%), and thermal pretreatment conditions (H_2 or O_2), were investigated in the oxidation of n-octanol with molecular oxygen under mild conditions, i.e., 80 °C, atmospheric pressure and absence of base. The results (Figures 1 and 2) showed that the gold content, modifier nature and the pretreatment atmosphere significantly affect catalytic properties of gold catalysts in the liquid-phase oxidation of n-octanol.

The activity of catalysts in the as-prepared state was insignificant and practically independent on the nature of the support and gold content. The reason is that gold in as-prepared samples was found on the support surface in the form of a trivalent gold complex with urea hydrolysis products, which is catalytically inactive, according to previous results [160]. It should be also noted that in the absence of support/catalyst in the reaction mixture, no activity was observed in aerobic oxidation of n-octanol.

For most of the studied catalysts, the activity increased several times after either the reduction or oxidative treatment. But notably, the effect of gold content on activity was different depending on the pretreatment atmosphere (Figure 1).

After H_2 treatment, the activity increased with the increase of gold content in all cases, except for the lanthanum-modified samples, where the activity did not change with increasing gold amount (n-octanol conversion was about 40% after 6 h for both gold concentrations).

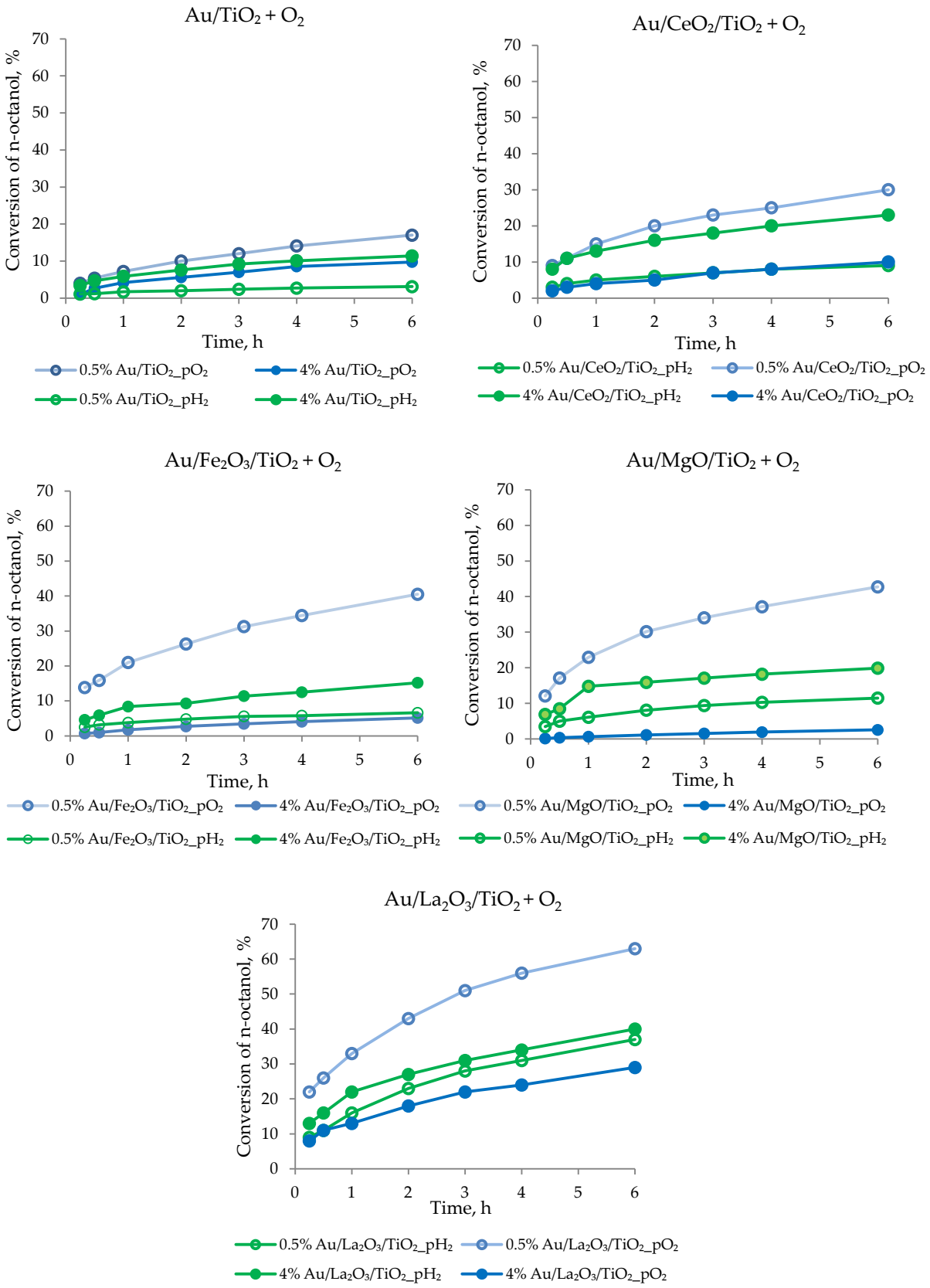

Figure 1. Effect of gold loading and pretreatments on the aerobic oxidation of n-octanol on $Au/M_xO_y/TiO_2$ (M_xO_y = CeO_2, Fe_2O_3, MgO and La_2O_3) catalysts: evolution of conversion with run time. Reaction conditions: T = 80 °C, 0.1 M n-octanol (n-heptane), O_2 = 30 mL/min, R = 100, stirring.

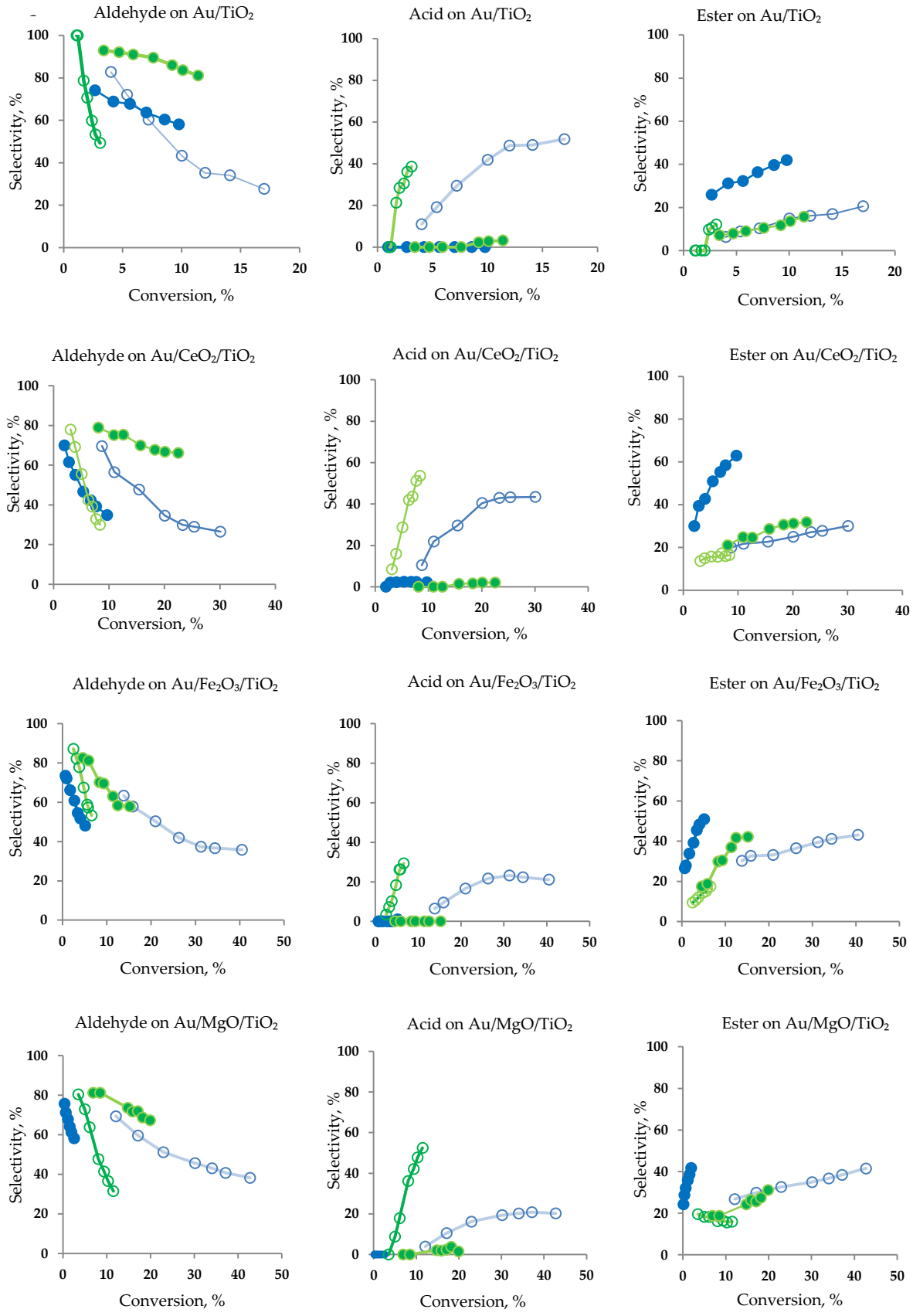

Figure 2. *Cont.*

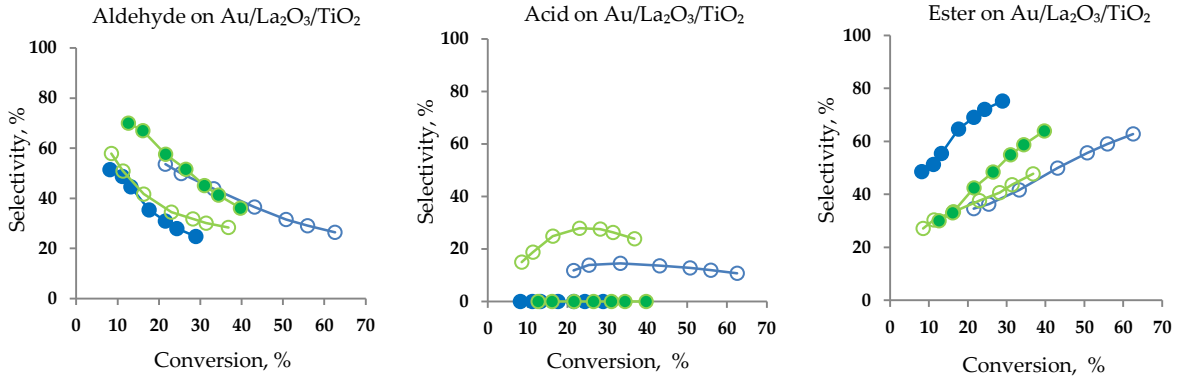

Figure 2. Effect of Au loading and pretreatments on the aerobic oxidation of n-octanol: products selectivity evolution with conversion for Au/(M_xO_y)/TiO_2 (M_xO_y = CeO_2, Fe_2O_3, MgO and La_2O_3) catalysts with 0.5% Au (hollow symbols) or 4% Au (full symbols). Green lines: results after hydrogen pretreatment; blue lines, after oxygen pretreatment. Reaction conditions: T = 80 °C, 0.1 M n-octanol in n-heptane, O_2 = 30 mL/min, R = 100, stirring.

Analysis of the products distribution (Figure 2) for 0.5% Au/TiO_2_pH_2, 0.5% Au/Fe_2O_3/TiO_2_pH_2, 0.5% Au/CeO_2/TiO_2_pH_2, 0.5% Au/MgO/TiO_2_pH_2 samples showed that selectivity to acid formation (39%, 30%, 53% and 53%, respectively) increased, while selectivity to aldehyde sharply decreased from 100% at the reaction start down to 50% for 0.5% Au/TiO_2_pH_2, 53% for 0.5% Au/Fe_2O_3/TiO_2_pH_2, 30% for 0.5% Au/MgO/TiO_2_pH_2 and 20% for 0.5% Au/CeO_2/TiO_2_pH_2. Ester formation was at 12 and 17-20% levels for unmodified sample and samples modified with magnesium, iron and cerium oxides, respectively. For 0.5% Au/La_2O_3/TiO_2_pH_2 sample, octanoic acid was detected as well, having a tendency to decrease after 2 h (24%), with preferable ester formation (48%) by the end of the run time.

The selectivity trends were totally different from their 4 wt.% Au analogues after hydrogen pretreatment. The main product was octanal, except for 4% Au/La_2O_3/TiO_2_pH_2 (62% selectivity to ester after 6 h of reaction). Octanoic acid formation was practically negligible; only some traces of acid were detected at longer run times for 4% Au/TiO_2_pH_2, 4% Au/CeO_2/TiO_2_pH_2 and 4% Au/MgO/TiO_2_pH_2. It was noteworthy that selectivity towards octyl octanoate increased for 4% Au/Fe_2O_3/TiO_2_pH_2 and 4% Au/La_2O_3/TiO_2_pH_2 at the expense of octanal formation with no acid formation.

Such changes in the reaction products distribution with the increase in Au content should be caused by alteration in the acid-base properties of support. Aldehyde formation requires only the first step of the reaction mechanism, that occurs on the gold active centres, while formation of octanoic acid and octyl octanoate requires a second mechanistic step [22, 23, 161] through intermediates

formed by acid-base catalyzed reactions, proceeding mainly on the support surface. In the scheme proposed by Ishida et al. [161], the formation of ester or acid can occur by two routes: hydration to a geminal diol (Scheme 2, A) that can be further oxidized to octanoic acid, or an acetalization to form the hemiacetal, that can be oxidized to octyl octanoate. The ester could be also formed by esterification of the acid with the alcohol (Scheme 2, B).

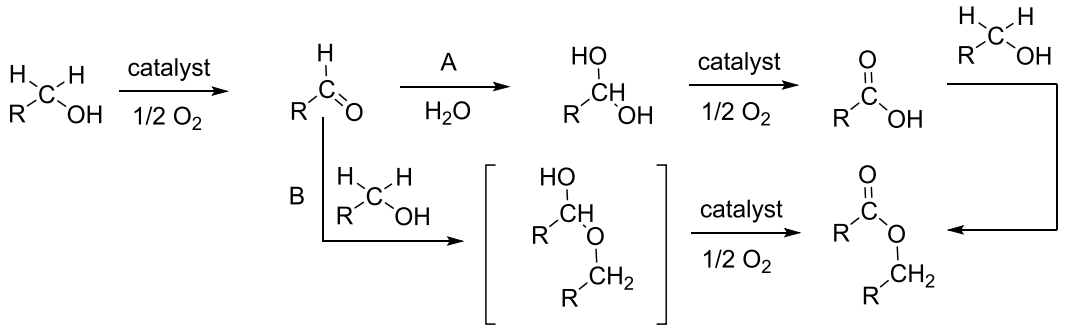

Scheme 2. Possible reaction pathways for the oxidation of n-octanol on supported gold catalysts (adapted from [22, 23, 161]).

In contrast, after pretreatment of samples in an oxygen atmosphere, the opposite dependence on the activity of the gold content was observed, i.e., the catalytic activity decreased with the increase of gold content for all supports.

The tendency to acid formation for 0.5% Au/TiO_2 and 0.5% Au/CeO_2/TiO_2 (43 and 52% selectivity, respectively) was preserved even after pretreatment of the samples in O_2. In case of modified samples with iron and magnesium oxides, acid formation decreased after 3 h of reaction and was 20% after 6 h for both catalysts. n-Octanol oxidation over La-modified sample was less selective to octanoic acid (11 % after 6 h) with higher formation of ester (63% after 6 h).

Similar good results were achieved using modified samples with the lower Au content after oxidative pretreatment at 300 °C for 1 h, namely, 0.5% Au/MgO/TiO_2 and 0.5% Au/Fe_2O_3/TiO_2: the conversion of n-octanol after 6 h reached 43% and 41%, respectively, with increasing ester selectivity in both cases (Figures 1 and 2).

For catalysts with the higher gold loading after oxygen and hydrogen treatment, similar trends were observed in selectivity with almost complete absence of acid formation (only 1 and 2% acid selectivity for 4% Au/Fe_2O_3/TiO_2_pO_2 and 4% Au/CeO_2/TiO_2_pO_2, respectively). However, the difference is a larger selectivity to ester: from 20% on unmodified 4% Au/TiO_2_pO_2, it increased to 40, 42, 63 and 75% on modified catalysts 4% Au/MgO/TiO_2_pO_2, 4% Au/Fe_2O_3/TiO_2_pO_2, 4% Au/CeO_2/TiO_2_pO_2 and 4% Au/La_2O_3/TiO_2_pO_2, respectively. Nevertheless, it is worth noting that the activity of catalysts with 4% Au after O_2 treatment was the lowest among all catalysts (except for 4% Au/TiO_2_pO_2: 9% conversion after 6 h), and especially

for samples modified with iron and magnesium oxides, for which final conversion did not exceed 3 and 7%, respectively (Figure 1).

A common feature of catalysts with 0.5% of Au, independently of the pretreatment, was the preferential formation of acid, but a larger propensity for ester formation was found for catalysts with oxygen pretreatment.

It can be seen that the highest activity in aerobic oxidation of n-octanol under mild conditions (80 °C, 1 atm) was achieved using modified samples with the lower gold content after oxidizing pretreatment at 300 °C for 1 h. The order of activity, in this case, was as follows: $Au/La_2O_3/TiO_2$ > $Au/MgO/TiO_2$ > $Au/Fe_2O_3/TiO_2$ > $Au/CeO_2/TiO_2$ > Au/TiO_2. It should be noted that La-modified samples demonstrated the highest catalytic performance for each combination of the two preparation parameters studied (Au content and pretreatment).

Thus, the best catalytic results were found on 0.5% $Au/La_2O_3/TiO_2$ catalyst after oxidative pretreatment: 63% n-octanol conversion in 6 h with 63% selectivity to ester.

3.1.2. Peroxidative oxidation of n-octanol

Aiming at studying the effect of the oxidizing agent in the oxidation of n-octanol, the same reaction conditions as for 1-phenylethanol oxidation were applied, to perform a comparative analysis of both reactions. Thus, all catalytic experiments in peroxidative oxidation of n-octanol were carried out with enviromentaly friendly tert-butyl hydroperoxide (TBHP) at 80 °C with alcohol/Au ratio R = 5000 in a base- and solvent-free medium. It should be noted that, in the absence of support/catalyst in the reaction mixture, no activity was observed under these conditions.

The results showed similar trends of catalytic behaviour in the aerobic (Figure 1) and peroxidative oxidation (Figure 3) of n-octanol in terms of activity. The most active catalysts were those with low Au loading, after oxidative pretreatment. The order of activity, in this case, was as follows: $Au/La_2O_3/TiO_2$ > $Au/MgO/TiO_2$ > $Au/Fe_2O_3/TiO_2$ > $Au/CeO_2/TiO_2$ > Au/TiO_2. Thus, the highest acivity, namely 60% conversion with selectivity towards acid formation (81%) in 6 h was achieved on 0.5% $Au/La_2O_3/TiO_2\_pO_2$.

Regarding selectivity, it is important to note that when using molecular oxygen as an oxidizing agent, a different behaviour is observed in the distribution of oxidation products, depending on the pretreatment, the nature of the support and the gold content. However, when TBHP was used as oxidizing agent, in the absence of a solvent, the main product, in all cases, was acid with a small amount of ester (up to 20%). This is probably due to the peroxide used as oxidizing agent which decomposed producing water [146], that is needed for octanoic acid formation, according to Scheme 2 (route A) [22, 23, 161].

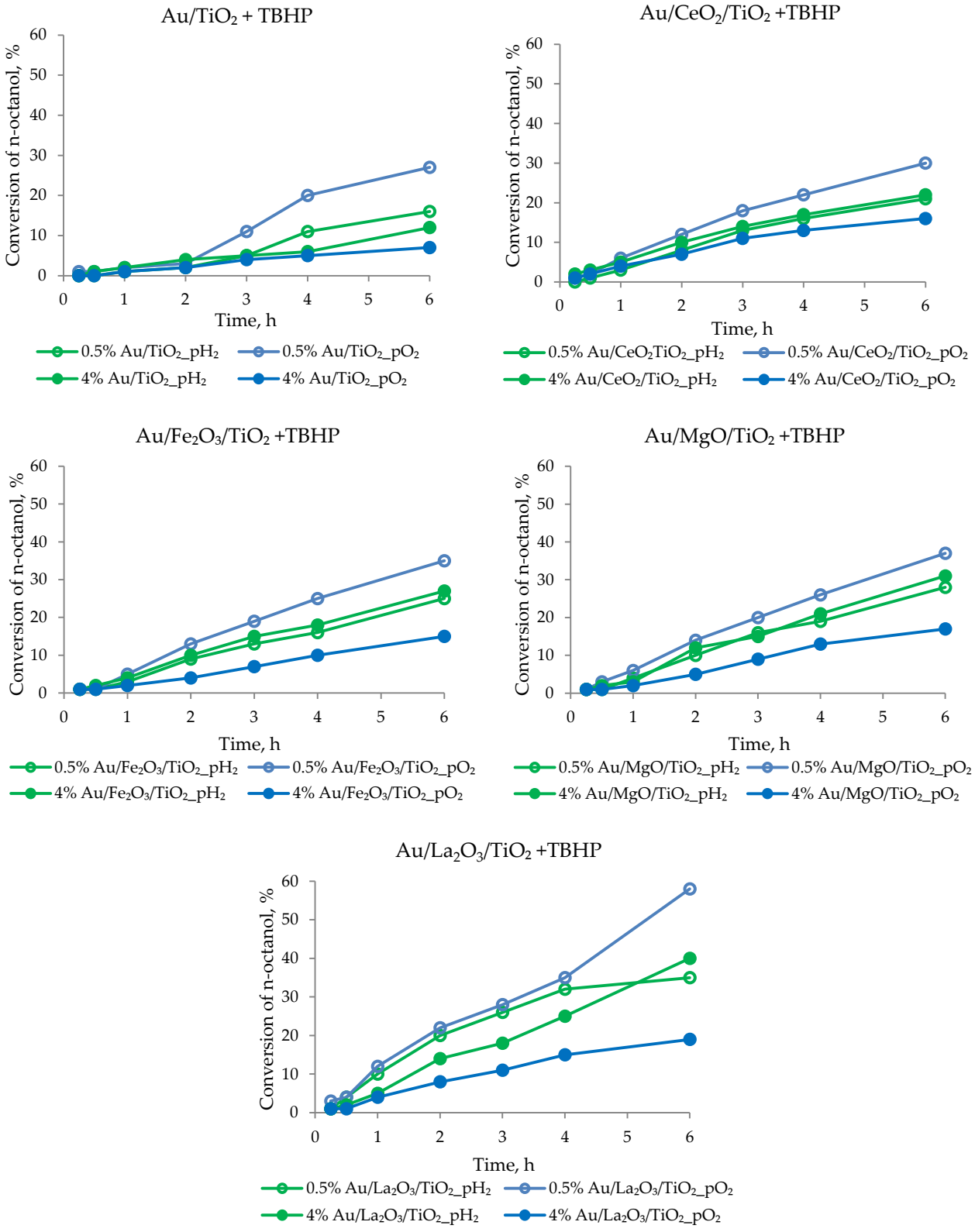

Figure 3. Time evolution of catalytic peroxidative oxidation of n-octanol. Reaction conditions: R = 5000, TBHP: n-octanol = 2.43; T = 80 °C, stirring.

Also, it becomes obvious that the best results in the oxidation of n-octanol were achieved using TBHP, since the gold loading was in 50 times less (R = 5000) than in our tests of n-octanol oxidation with molecular oxygen (R = 100). It

should be noted also that, comparing our results on n-octanol oxidation with other gold supported catalysts under mild conditions (Table 1), Au/(M_xO_y)/TiO_2 system are one of the most effective, when both TBHP and O_2 were used as an oxidizing agents without bases or solvents.

3.1.3. Peroxidative oxidation of 1-phenylethanol

As in the case of n-octanol oxidation, all experiments on both peroxidative and aerobic oxidation of 1-phenylethanol (Scheme 3) were carried out at 80 °C and atmospheric pressure.

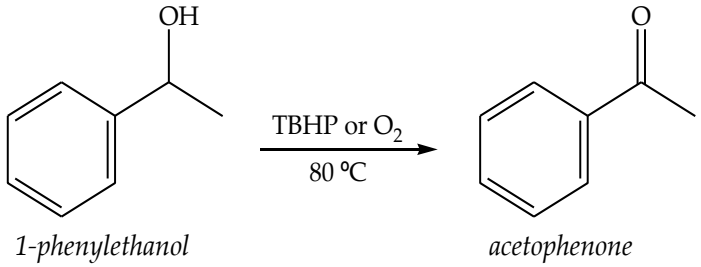

Scheme 3. Oxidation of 1-phenylethanol over Au/(M_xO_y)/TiO_2 catalysts.

The catalytic tests with TBHP as oxidizing agent were conducted with a very low catalyst loading (1-phenylethanol/Au = 5000) in no-solvent conditions. The results are presented in Table 3. As expected, both unmodified and modified catalysts proved to be much more active in the oxidation of 1-phenylethanol than of n-octanol. Taking into account the high alcohol/gold ratio, the catalysts, even in the as-prepared state, reached more than 50% of acetophenone yield after 6 h of reaction, despite the low activity in the first hours.

As in the oxidation of n-octanol, the sample modified with lanthanum oxide 4% Au/La_2O_3/TiO_2 pretreated in H_2 demonstrated the best catalytic performance (Table 3, Entry 34): 98% yield of acetophenone was achieved already in 1 h.

It should also be noted that the activity of the studied catalysts increased with increasing gold content, and the most active samples were those pretreated with hydrogen. Thus, the order of activity in the 4% Au catalysts with hydrogen treatment was as follows: Au/La_2O_3/TiO_2 > Au/MgO/TiO_2 > Au/Fe_2O_3/TiO_2 > Au/CeO_2/TiO_2 > Au/TiO_2.

However, it should be emphasized that the supports also showed some activity under these conditions, as the acetophenone yield increased with time and depended on the support nature (Entries 2–6, Table 3). In the absence of a catalyst or support, the formation of a small amount of acetophenone was also observed (Entry 1, Table 3).

For the oxidation of 1-phenylethanol with molecular oxygen, no activity was observed when using supports only or in the absence of a support/catalyst, as will be discussed below. This shows the very good activity of TBHP, which, when decomposed by heating or by reaction with a metal (see Introduction),

forms radicals (t-BuO·, t-BuOO·), responsible for the direct oxidation of alcohols [146]. Therefore, in the referred work, 97% acetophenone was obtained using 6 equivalents of TBHP at 100 °C in 24 h, without addition of any catalysts or bases [147].

Table 3. Catalytic results of peroxidative oxidation of 1-phenylethanol [1].

Entry	Sample	Yield of acetophenone (mol%) at time (h)						
		0.25	**0.5**	**1**	**2**	**3**	**4**	**6**
1	-	0	0	1	2	3	3	4
2	TiO_2	2	2	2	2	2	4	6
3	CeO_2/TiO_2	3	3	3	4	6	8	14
4	Fe_2O_3/TiO_2	2	2	3	5	8	10	16
5	MgO/TiO_2	2	2	3	3	5	5	7
6	La_2O_3/TiO_2	3	3	3	6	8	10	17
7	0.5% $Au/TiO_2\_pH_2$	25	40	55	80	100	100	100
8	0.5% $Au/TiO_2\_pO_2$	18	30	43	69	81	98	100
9	0.5% Au/TiO_2_as	1	1	3	9	16	28	51
10	4% $Au/TiO_2\_pH_2$	33	46	75	100	100	100	100
11	4% $Au/TiO_2\_pO_2$	30	49	65	99	100	100	100
12	4% Au/TiO_2_as	1	2	6	19	28	45	82
13	0.5% $Au/CeO_2/TiO_2\_pH_2$	27	37	60	85	100	100	100
14	0.5% $Au/CeO_2/TiO_2\_pO_2$	28	36	72	90	100	100	100
15	0.5% $Au/CeO_2/TiO_2$_as	2	3	3	7	14	28	61
16	4% $Au/CeO_2/TiO_2\_pH_2$	36	49	85	100	100	100	100
17	4% $Au/CeO_2/TiO_2\_pO_2$	22	41	75	100	100	100	100
18	4% $Au/CeO_2/TiO_2$_as	3	4	10	25	46	67	100
19	0.5% $Au/Fe_2O_3/TiO_2\_pH_2$	19	41	69	100	100	100	100
20	0.5% $Au/Fe_2O_3/TiO_2\_pO_2$	23	30	58	87	100	100	100
21	0.5% $Au/Fe_2O_3/TiO_2$_as	2	3	5	7	14	30	63
22	4% $Au/Fe_2O_3/TiO_2\_pH_2$	21	39	87	100	100	100	100
23	4% $Au/Fe_2O_3/TiO_2\_pO_2$	24	45	65	100	100	100	100
24	4% $Au/Fe_2O_3/TiO_2$_as	1	4	6	16	30	39	65
25	0.5% $Au/MgO/TiO_2\_pH_2$	31	52	73	100	100	100	100
26	0.5% $Au/MgO/TiO_2\_pO_2$	25	29	78	100	100	100	100
27	0.5% $Au/MgO/TiO_2$_as	1	4	7	9	17	31	70
28	4% $Au/MgO/TiO_2\_pH_2$	28	43	90	100	100	100	100
29	4% $Au/MgO/TiO_2\_pO_2$	20	33	60	100	100	100	100
30	4% $Au/MgO/TiO_2$_as	1	3	8	24	49	98	100
31	0.5% $Au/La_2O_3/TiO_2\_pH_2$	31	45	55	88	100	100	100
32	0.5% $Au/La_2O_3/TiO_2\_pO_2$	38	49	61	96	100	100	100
33	0.5% $Au/La_2O_3/TiO_2$_as	1	1	2	8	18	42	84
34	4% $Au/La_2O_3/TiO_2\_pH_2$	41	55	98	100	100	100	100
35	4% $Au/La_2O_3/TiO_2\_pO_2$	22	40	67	100	100	100	100
36	4% $Au/La_2O_3/TiO_2$_as	1	2	6	29	54	100	100

[1] Reaction conditions: TBHP: 1-phenylethanol = 2.43; T = 80 °C, no solvent, stirring, R= 5000.

In order to more clearly trace the dependence of the acetophenone yield on the catalyst loading, the 4% $Au/La_2O_3/TiO_2\_pO_2$ sample, with a medium activity in 1-phenylethanol peroxidative oxidation among the La-modified samples, was selected. According to the obtained results, direct dependence of the yield of acetophenone on catalyst loading was observed (Table 4). Thus, 100% acetophenone was obtained already after 15 min of reaction when the total gold amount was increased from 1.27 to 10 μmol.

Table 4. Effect of the total gold amount on the peroxidative oxidation of 1-phenylethanol [1] using 4% Au/La_2O_3/TiO_2_pO_2.

Au amount (μmol)	Yield of acetophenone (mol%) at time (min)					
	5	**15**	**30**	**60**	**120**	**180**
1.27	15	22	40	67	100	100
5	33	40	50	81	100	100
10	80	100	100	100	100	100
20	100	100	100	100	100	100

[1] 1-phenylethanol (6 mmol), TBHP (70% aqueous solution, 14.6 mmol), T = 80 °C.

It should be noted that experiments using hydrogen peroxide (30% aqueous solution) as oxidant were not effective. For instance, under the same conditions used with TBHP (T = 80 °C, 6 mmol 1-phenylethanol, 14.6 mmol H_2O_2, 1.27 μmol of Au) only 11% acetophenone yield was achieved after 6 h of reaction using 4% Au/La_2O_3/TiO_2_pH_2 catalyst, compared to 98% yield of acetophenone after 1 h using TBHP (Entry 34, Table 3).

3.1.4. Aerobic oxidation of 1-phenylethanol

After replacing TBHP with molecular oxygen, keeping the same alcohol/gold ratio (R = 5000), no conversion was observed, even after 6 h of reaction (Table 5).

Table 5. Effect of alcohol/Au ratio (R) on aerobic oxidation of 1-phenylethanol [1] with 4% Au/La_2O_3/TiO_2_pH_2 catalyst.

Catalyst	R	Run time, h	Yield of acetophenone, %
4% Au/La_2O_3/TiO_2_pH_2	5000	6	0
	500	6	50
	100	0.5	98

[1] Reaction conditions: 0.1 M 1-phenylethanol in mesitylene, T = 80 °C, 30 mL/min O_2.

The next step was to investigate the effect of the alcohol/gold ratio. With a ten-fold increase in catalyst loading (R = 500), 50% conversion was reached after 6 h. The complete conversion of 1-phenylethanol could be achieved only using a R = 100, that produced 98% acetophenone yield after just 30 min.

Such a different behaviour in the catalytic activity probably lies in the different oxidative capacity of oxygen and TBHP. Therefore, the catalytic activity in the aerobic oxidation of 1-phenylethanol of the remaining catalysts was studied with R = 100.

As it can be seen in Table 6, catalysts with the low gold content with an oxidative pretreatment were the most active and the order of activity was as follows: Au/La_2O_3/TiO_2 > Au/MgO/TiO_2 > Au/Fe_2O_3/TiO_2 > Au/CeO_2/TiO_2 > Au/TiO_2, as in the case of n-octanol (Figure 1).

Table 6. Catalytic results of aerobic oxidation of 1-phenylethanol [1].

Entry	Catalyst	Yield of acetophenone (mol%) at time (h)						
		0.25	**0.5**	**1**	**2**	**3**	**4**	**6**
1	0.5% $Au/TiO_2\_pH_2$	21	25	31	40	45	47	50
2	0.5% $Au/TiO_2\_pO_2$	26	32	38	44	49	52	58
3	4% $Au/TiO_2\_pH_2$	24	30	35	41	42	43	44
4	4% $Au/TiO_2\_pO_2$	19	21	25	30	35	38	40
5	0.5% $Au/CeO_2/TiO_2\_pH_2$	45	50	60	65	68	70	72
6	0.5% $Au/CeO_2/TiO_2\_pO_2$	70	86	96	99	100	100	100
7	4% $Au/CeO_2/TiO_2\_pH_2$	53	59	65	69	71	73	78
8	4% $Au/CeO_2/TiO_2\_pO_2$	40	44	50	55	59	65	70
9	0.5% $Au/Fe_2O_3/TiO_2\_pH_2$	42	57	68	74	79	82	85
10	0.5% $Au/Fe_2O_3/TiO_2\_pO_2$	67	88	97	99	100	100	100
11	4% $Au/Fe_2O_3/TiO_2\_pH_2$	52	57	68	71	75	79	84
12	4% $Au/Fe_2O_3/TiO_2\_pO_2$	40	45	54	58	64	70	75
13	0.5% $Au/MgO/TiO_2\_pH_2$	50	54	65	71	76	79	87
14	0.5% $Au/MgO/TiO_2\_pO_2$	76	90	98	99	100	100	100
15	4% $Au/MgO/TiO_2\_pH_2$	56	64	72	80	83	85	88
16	4% $Au/MgO/TiO_2\_pO_2$	47	50	54	58	64	67	75
17	0.5% $Au/La_2O_3/TiO_2\_pH_2$	90	95	97	100	100	100	100
18	0.5% $Au/La_2O_3/TiO_2\_pO_2$	95	98	100	100	100	100	100
19	4% $Au/La_2O_3/TiO_2\_pH_2$	88	96	99	100	100	100	100
20	4% $Au/La_2O_3/TiO_2\_pO_2$	79	88	93	97	98	99	100

[1] Reaction conditions: R = 100, 0.1 M 1-phenylethanol in mesitylene; T = 80 °C, 30 mL/min O_2, stirring.

From these results, it could be concluded that $Au/(M_xO_y)/TiO_2$ systems were highly effective in the oxidation of 1-phenylethanol, and the catalysts modified with lanthana were the most active, as in the oxidation of n-octanol. Furthermore, comparing our results on 1-phenylethanol oxidation with other gold supported catalysts (Table 2), it could be concluded that the $Au/(M_xO_y)/TiO_2$ systems are one of the most effective in peroxidative selective oxidation of 1-phenylethanol with TBHP in base- and solvent- free conditions, given the high alcohol/gold ratio (R = 5000), and low temperature (T = 80 °C) used.

SUMMARY

Therefore, according to all catalytic results, under comparable reaction conditions, 1-phenylethanol can be much more efficiently and selectively oxidized over $Au/M_xO_y/TiO_2$ catalysts than n-octanol. Moreover, the best results in the oxidation of both alcohols were achieved using TBHP.

In all cases, the best catalytic characteristics were shown by catalysts modified with lanthanum oxide, regardless of the alcohol and the type of oxidizing agent. Also, when a solvent was used and molecular oxygen was present as an oxidizing agent, the catalysts with the lowest gold content after oxidative pretreatment showed the highest activity in both 1-phenylethanol and n-octanol oxidation.

The only difference was that under no-solvent peroxidative conditions, the most active catalysts in 1-phenylethanol oxidation were those with a high gold content and hydrogen treatment, while under the same reaction conditions, low gold content and oxygen treatment were the most beneficial for n-octanol oxidation. The reason for this difference will be discussed in the Summary after Sections 3.1 and 3.2.

3.2. Catalysts Characterization Results

To understand the differences observed in the catalytic behaviour of the samples, a series of physicochemical studies were carried out.

3.2.1. Study of structural, textural properties and morphology of catalysts

XRD method was used to study the phase composition of the catalysts.The diffractograms (Figure 4) showed the almost absence of diffraction lines related to gold and modifiers, indicating either small sizes of Au particles and modifying metal oxides (lower than the XRD sensitivity threshold of 3–4 nm) [162] or their amorphous structures. Thus, the peaks found were mostly those corresponding to crystalline planes of anatase/rutile TiO_2 phases in all samples [22, 23, 163, 164]. For $Au/CeO_2/TiO_2$ samples, CeO_2 phase was present, which may indicate that cerium oxide was not homogeneously distributed on the surface of TiO_2 but was rather concentrated in the form of nanoparticles [22, 165].

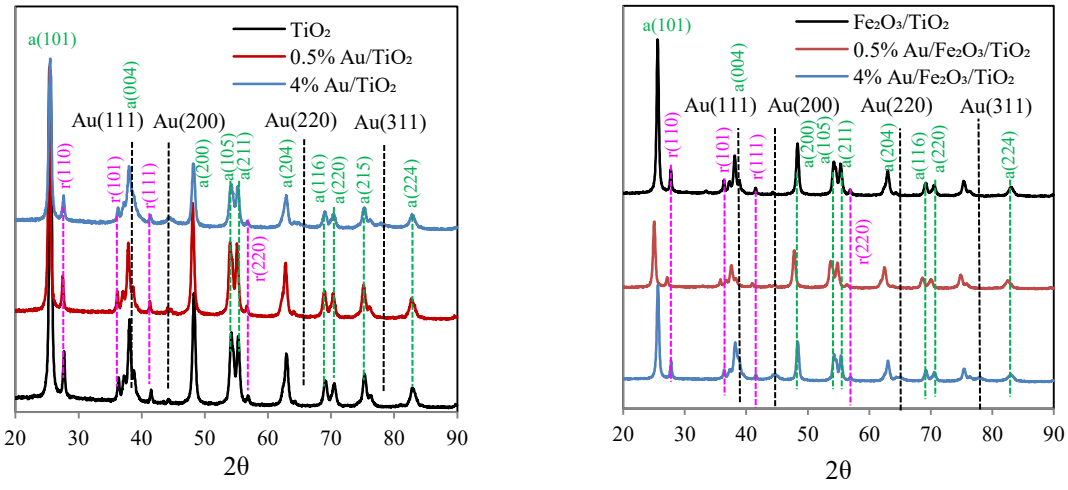

Figure 4. *Cont.*

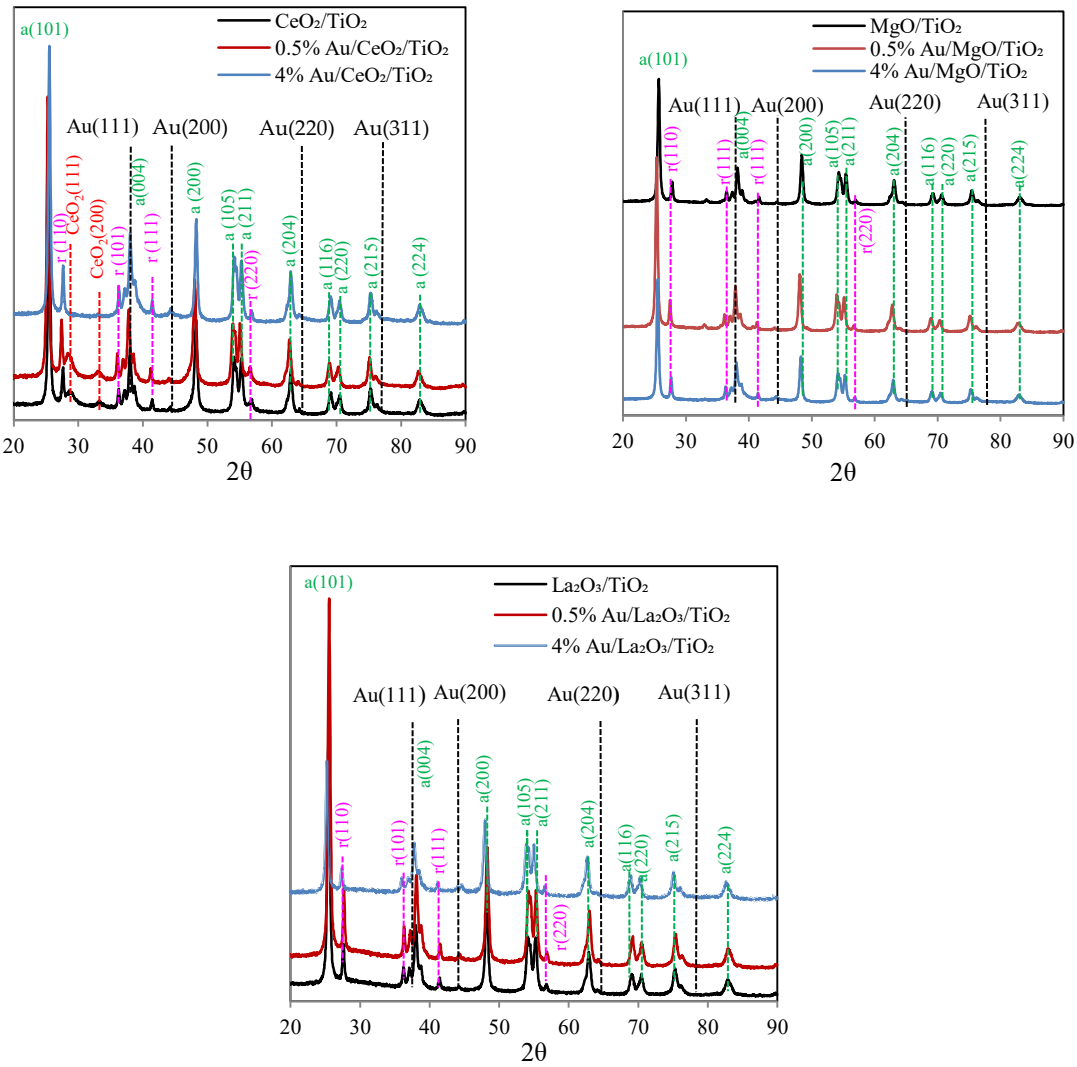

Figure 4. XRD patterns for catalysts Au/TiO_2, Au/Fe_2O_3/TiO_2, Au/CeO_2/TiO_2, Au/MgO/TiO_2 and Au/La_2O_3/TiO_2, treated in H_2 flow (300 °C, 1 h) and their corresponding supports. Diffraction lines labels: "a", TiO_2 anatase; "r", TiO_2 rutile; "Au", metallic gold; "CeO_2", cubic CeO_2.

Table 7 summarizes the specific surface area (S_{BET}), and gold content of the catalysts and their corresponding supports. Because of modification, S_{BET} of the initial TiO_2 support was reduced by 13% (48-49 m^2/g). Further gold deposition did not change significantly the supports S_{BET}, except for catalysts with 4% Au, where S_{BET} had a 10% decrease. Elemental analysis showed that the actual gold loadings obtained were close to their nominal value.

Table 7 also depicts the average Au particle size obtained from STEM-HAADF images shown in Figure 5. The distribution of gold nanoparticles for all the studied catalysts is in the range of 1-10 nm, except for 0.5% Au/TiO_2_pH_2, for which larger particles were observed, up to 15 nm (Figure 5 a). The average size of Au NPs was within the 2.4-5.2 nm interval for the studied materials (Table 7).

Table 7. Textural properties of supports and catalysts, analytical content and particle size of Au.

Entry	Sample	S_{BET}, m^2/g		EDS Au content, wt. %	Au average Particle Size, nm
		Support	Catalyst		
1	0.5% Au/TiO_2_pH_2	55	54	0.4	4.4
2	0.5% Au/TiO_2_pO_2	55	54	0.4	4.2
3	4% Au/TiO_2_pH_2	55	50	4.0	3.0
4	4% Au/TiO_2_pO_2	55	50	4.0	3.3
5	0.5%Au/CeO_2/TiO_2_pH_2	48	47	0.3	3.4
6	0.5%Au/CeO_2/TiO_2_pO_2	48	47	0.3	3.8
7	4%Au/CeO_2/TiO_2_pH_2	48	46	4.1	2.8
8	4%Au/CeO_2/TiO_2_pO_2	48	46	4.1	2.4
9	0.5% Au/Fe_2O_3/TiO_2_pH_2	49	49	0.5	3.4
10	0.5% Au/Fe_2O_3/TiO_2_pO_2	49	49	0.5	3.1
11	4% Au/Fe_2O_3/TiO_2_pH_2	49	44	3.2	5.2
12	4% Au/Fe_2O_3/TiO_2_pO_2	49	44	3.2	3.2
13	0.5% Au/MgO/TiO_2_pH_2	48	47	0.3	2.6
14	0.5% Au/MgO/TiO_2_pO_2	48	47	0.3	3.2
15	4% Au/MgO/TiO_2_pH_2	48	43	4.0	5.1
16	4% Au/MgO/TiO_2_pO_2	48	43	4.0	2.9
17	0.5% Au/La_2O_3/TiO_2_pH_2	48	47	0.5	2.8
18	0.5% Au/La_2O_3/TiO_2_pO_2	48	47	0.5	2.4
19	4% Au/La_2O_3/TiO_2_pH_2	48	43	3.3	2.6
20	4% Au/La_2O_3/TiO_2_pO_2	48	43	3.3	2.7

It can be seen clearly from STEM results that the most active La-modified samples in both reactions have the smallest average particle size range: 2.4-2.8 nm. Also, the most active in n-octanol oxidation (with both O_2 and TBHP) and aerobic oxidation of 1-phenylethanol, 0.5% Au/La_2O_3/TiO_2_pO_2, has the smallest average particle size of gold and the narrowest range of their distribution among the studied samples (Figure 5 r). At the same time, the least active 0.5% Au/TiO_2_pH_2 (Figure 5 a) has one of the largest average particle size and the widest range of their distribution. At the same time, both 4% Au/MgO/TiO_2_pH_2 and 4% Au/Fe_2O_3/TiO_2_pH_2 samples, with the largest average particle size (5.1-5.2 nm), showed medium activity in n-octanol oxidation with O_2 (15-20% conversion).

Catalysts 0.5% Au/Fe_2O_3/TiO_2_pO_2 and 0.5% Au/MgO/TiO_2_pO_2, showing almost equal conversion (41 and 43%) in n-octanol oxidation with O_2, had similar mean particle size (3.4 and 3.2 nm, respectively). However, catalysts with smaller particles size, like 0.5% Au/MgO/TiO_2_pH_2 (2.6 nm) and 4% Au/MgO/TiO_2_pO_2 (2.9 nm) demonstrated low activity in aerobic n-octanol oxidation (12 and 3%, respectively).

Therefore, taking into account the data from catalytic studies, no direct correlation between Au NPs average size and catalytic performance can be found.

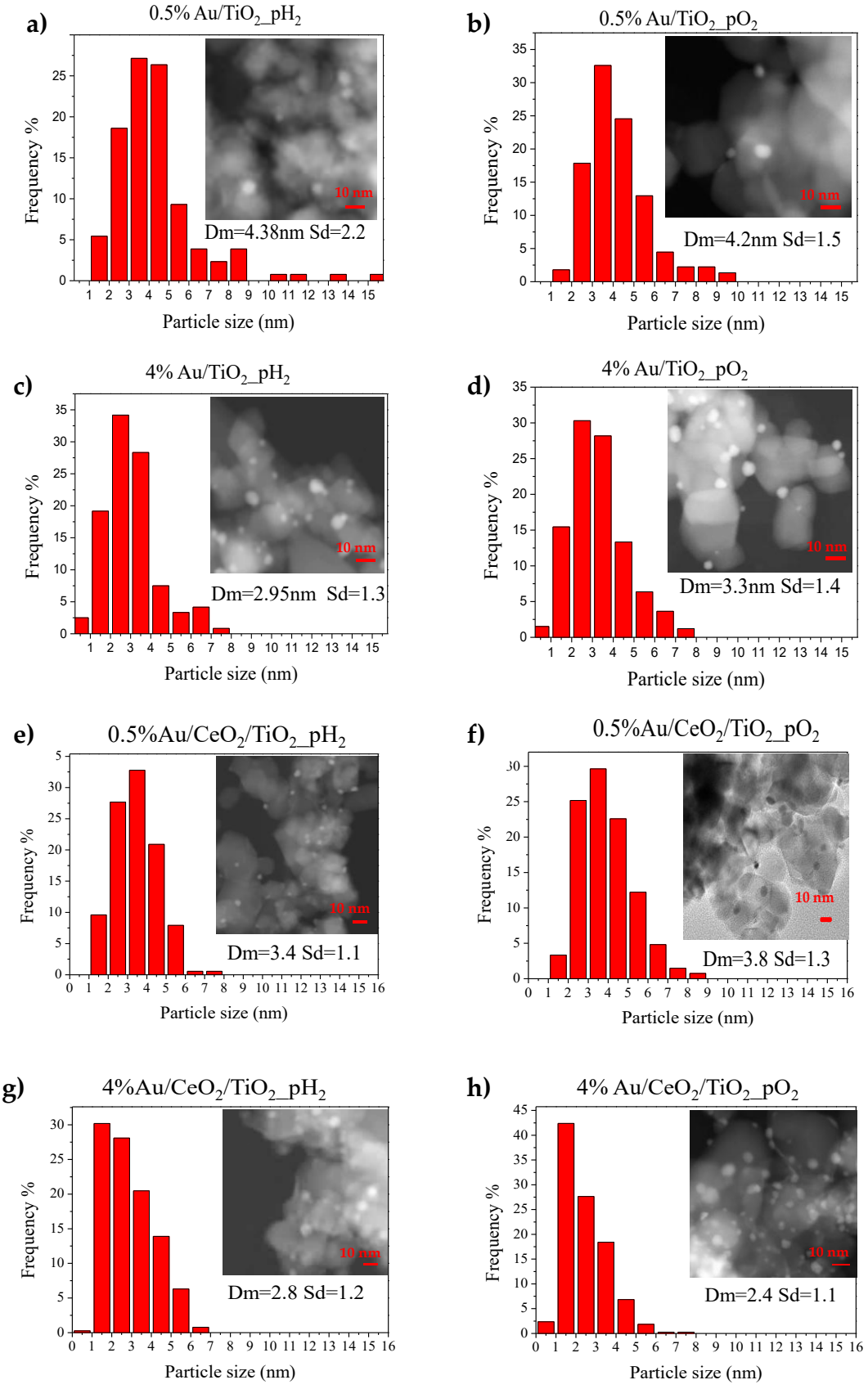

Figure 5. *Cont.*

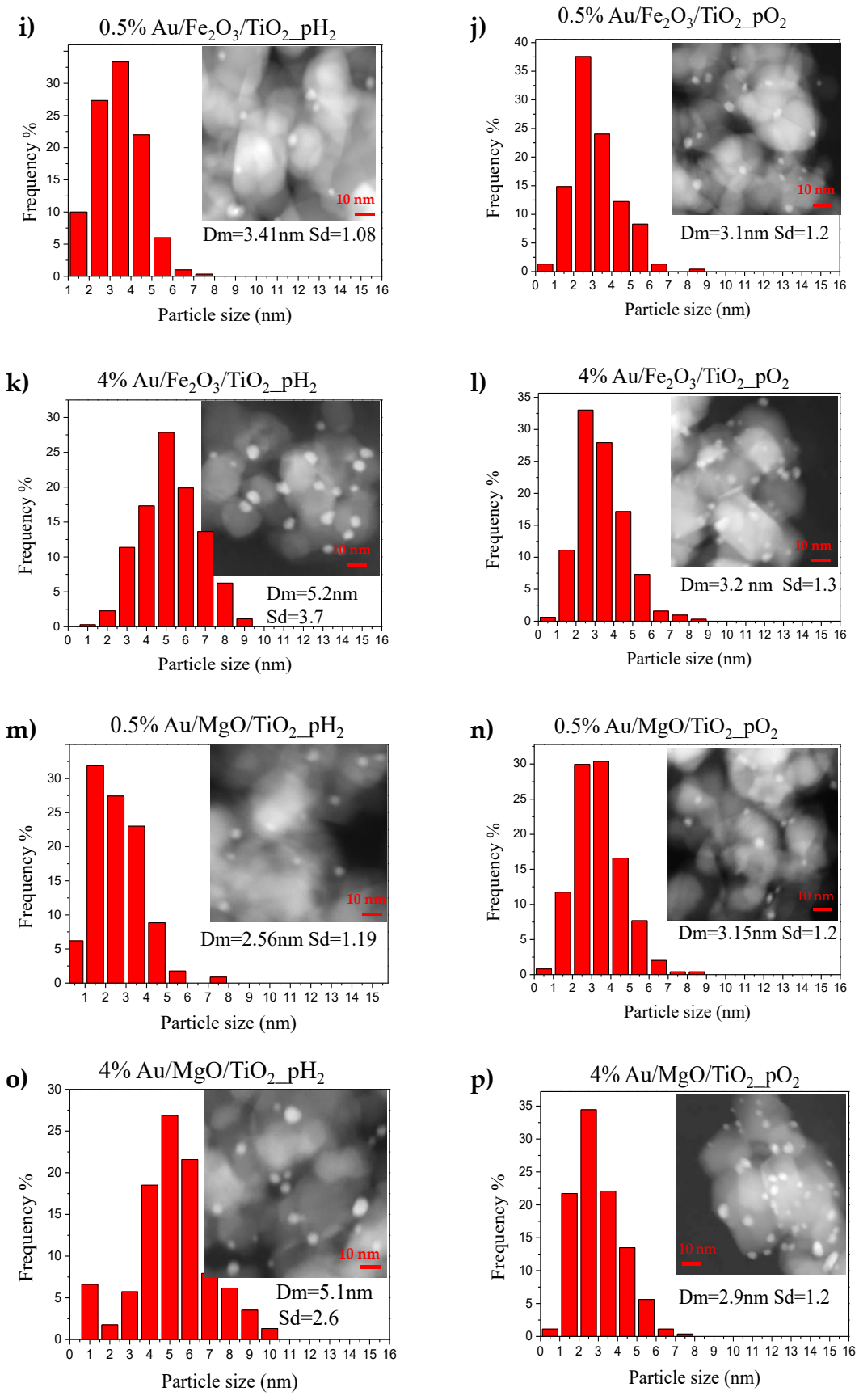

Figure 5. *Cont.*

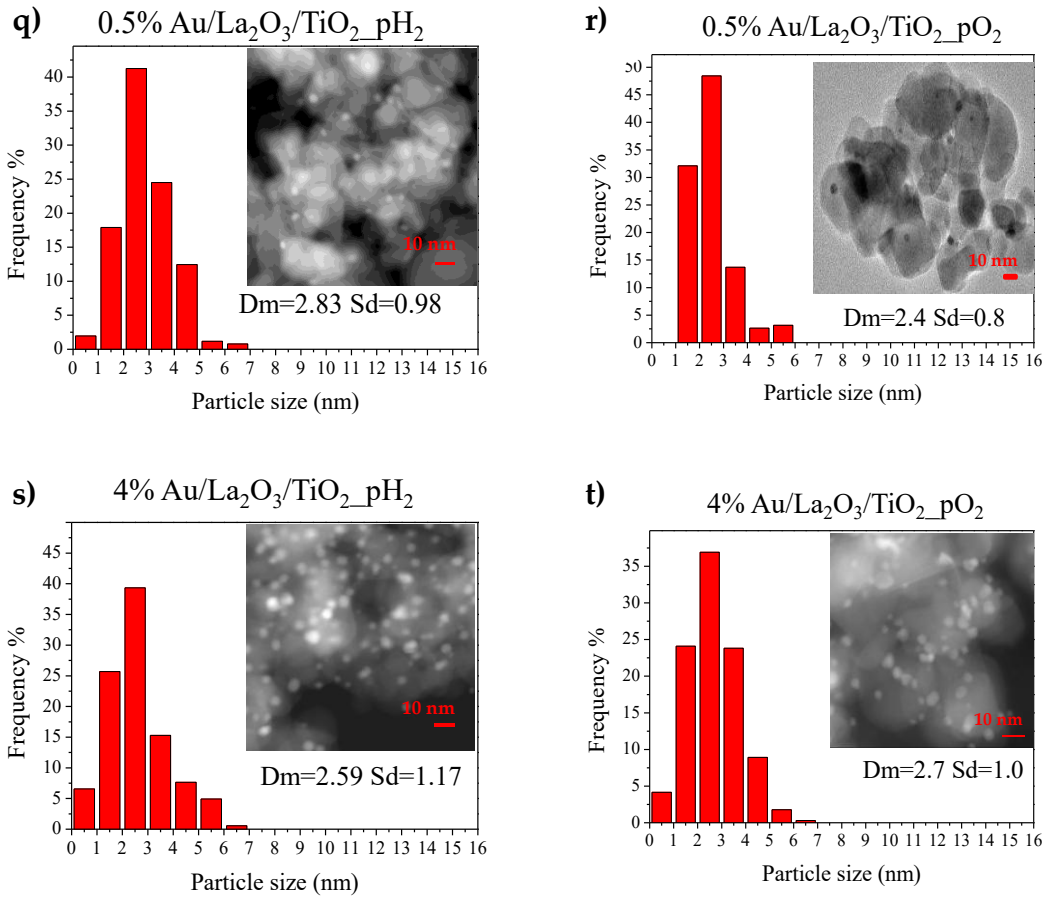

Figure 5. Au particle size distribution and representative TEM/STEM HAADF micrographs of catalysts Au/TiO_2 (**a–d**), $Au/CeO_2/TiO_2$ (**e–h**), $Au/Fe_2O_3/TiO_2$ (**i–l**), $Au/MgO/TiO_2$ (**m–p**) and $Au/La_2O_3/TiO_2$ (**q–t**), for different gold amounts (0.5 or 4 wt.%) and pretreatment atmospheres (H_2 or O_2).

Nevertheless, one should note that according to TPR, DRIFT CO studies and XPS presented below (Table 8, Figures 6, 7, 8 and 10), there is a fraction of gold in ionic state (Au^+ or Au^{3+}), which cannot be detected by TEM. The amount of these gold species depends on the support, pretreatment and gold content. In some samples, this ionic fraction of gold reaches almost half of the total Au content, which may be the reason for the observed discrepancy between particle size and catalytic activity.

Moreover, as suggested by some authors for such types of reaction, not all metal particles visible on the micrographs are active participants in the catalytic process; only particles with size of 1 nm and less, below the threshold of the technique, are active [22, 23, 67-69].

3.2.2. Study of the reduction of gold and supports

Temperature-programmed reduction with hydrogen (H_2-TPR) was used to study the reduction of supports and as-prepared $Au/M_xO_y/TiO_2$ catalysts. (Figure 6).

TiO_2 support (Figure 6 a) is characterized by a small peak of H_2 consumption from 450 to 750 °C, attributed to an insignificant reduction of titania surface [166]. The peaks of H_2 consumption for CeO_2/TiO_2 support correspond to reduction of ceria (Figure 6 b). The peak at 440 °C may be attributed to the reduction of CeO_2 surface oxygen, while peaks at 590 and 750 °C correspond to the reduction of bulk CeO_2 oxygen [167-169].

For Fe_2O_3/TiO_2 support (Figure 6 c), consumption at 336–457 °C is related to the transformation of FeOOH to Fe_2O_3 [170], reduction of Fe_2O_3 to Fe_3O_4, and those at 553 °C and 836 °C with reduction of Fe_3O_4 to FeO and FeO to Fe, respectively [171].

The TPR profiles for MgO/TiO_2 and La_2O_3/TiO_2 supports (Figures 6 d, e) are characterized by a small peak of hydrogen consumption at 380-800 °C, attributed to the reduction of titania. The shift of this peak, in comparison with pure TiO_2 support may indicate the increased reducibility of titania in the presence of modifiers, like La and Mg oxides. Also, for La_2O_3/TiO_2 this broad consumption peak can probably be associated with decomposition of surface lanthanum hydroxocarbonates $La_2(OH)_4(CO_3)$ [172].

For all catalyst samples in as-prepared state, the most intense hydrogen consumption is observed in the range 110–180 °C. According to a previous work [160], this low-temperature consumption is related to the reduction of gold precursor (Au^{3+} complex), weakly interacting with the support, that explains the relatively low activity of the catalysts with modified supports in as-prepared state, because highly charged gold ions Au^{3+} are catalytically inactive.

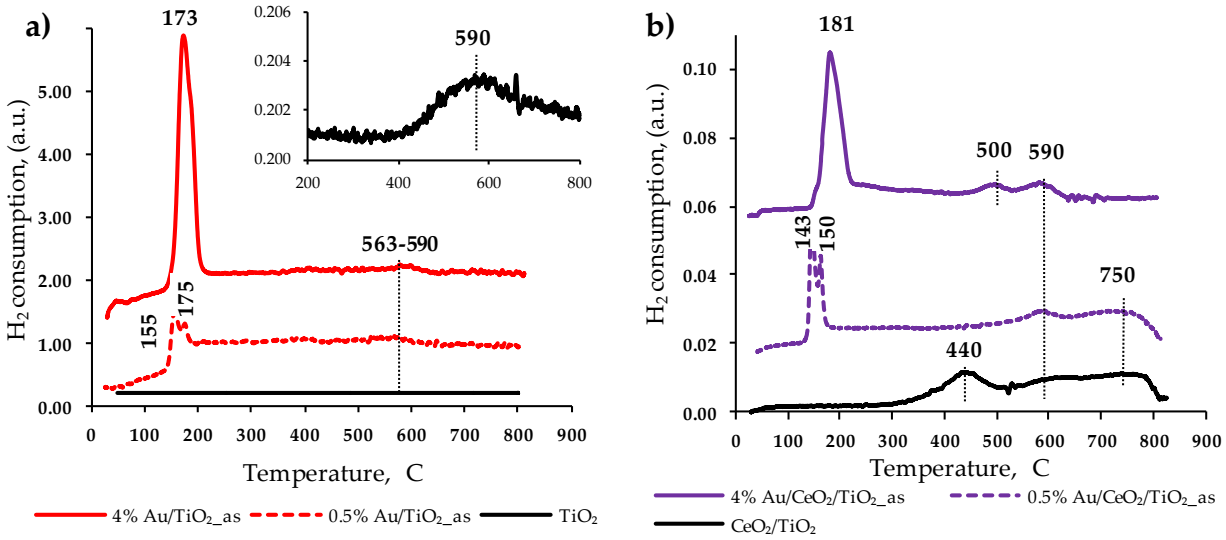

Figure 6. *Cont.*

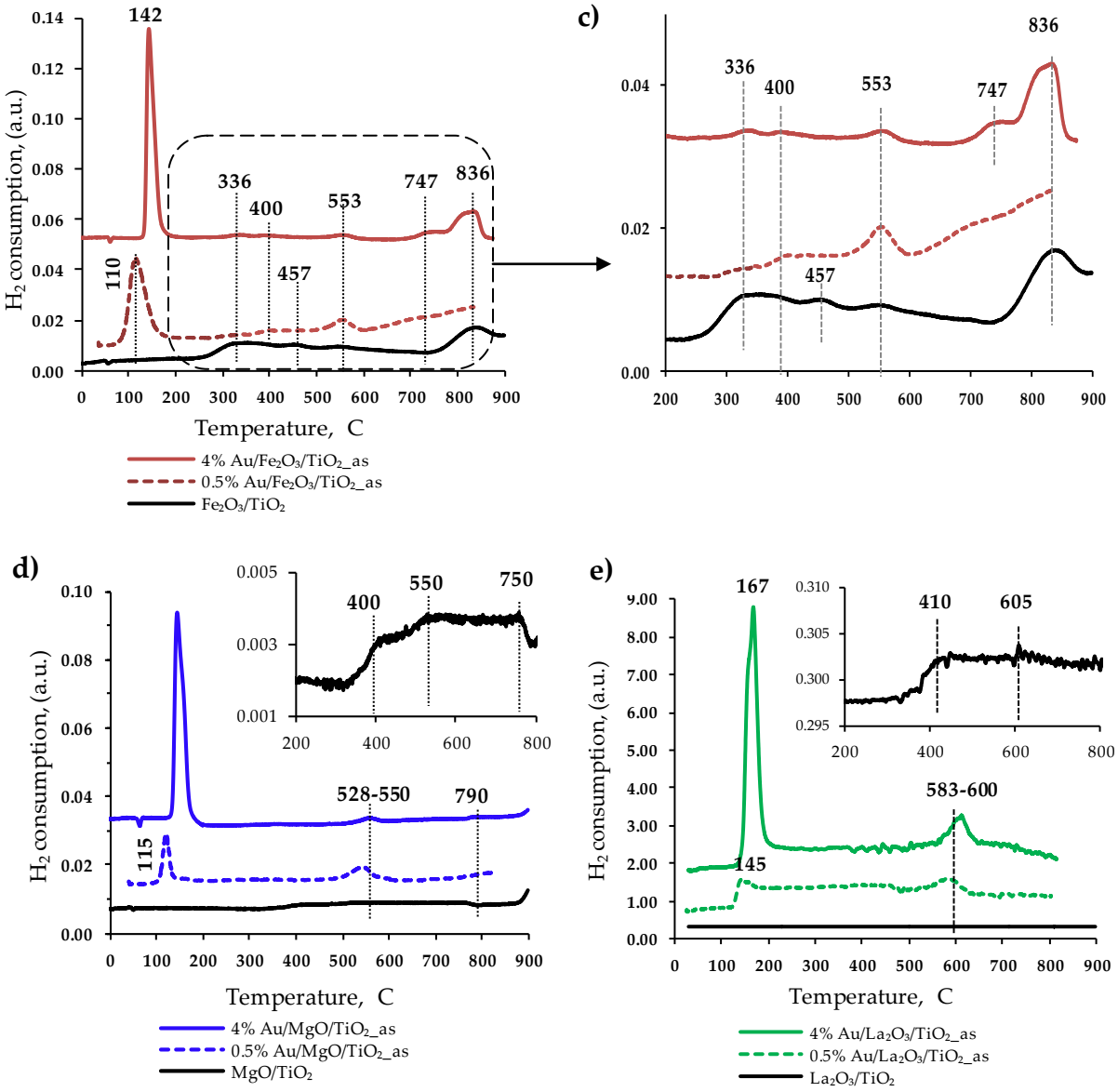

Figure 6. TPR profiles of as-prepared Au/TiO_2 **(a),** $Au/CeO_2/TiO_2$ **(b),** $Au/Fe_2O_3/TiO_2$ **(c),** $Au/MgO/TiO_2$ **(d)** and $Au/La_2O_3/TiO_2$ **(e)** catalysts with different Au loading and their corresponding supports. Some results were previously presented in [160].

In addition, for all samples without exception, high-temperature consumption is observed in the range of 550–590 °C. It relates to the reduction of strongly bound ionic gold, stabilized on the support surface by hydroxyl groups, through the formation of centers as M-O-Au, or reduction of the modifier oxide, or joint reduction of modifier and gold, in case of reducible CeO_2 and Fe_2O_3.

It is important to note the area of the consumption peak for all catalysts in the range 550–590 °C is significantly lower than at 110 to 180 °C, which indicates a limited quantity of functional groups on the support surface stabilizing gold, due to strong bond formation.

Both lanthanum-modified catalysts, 0.5% $Au/La_2O_3/TiO_2$ and 4% $Au/La_2O_3/TiO_2$, have the most intense H_2 consumption at 583 and 600 °C, respectively (Figure 6 e), among all studied samples in as-prepared state. This directly indicates that the gold ions being reduced are stabilized by functional groups of support, due to strong metal-support interaction, since La_2O_3 is a non-reducible oxide.

In the case of Mg-modified samples (Figure 6 d), one should take into account that MgO can be transformed into $Mg(OH)_2$ by reaction with water, during catalyst preparation [173-175]. Carabineiro et al. [175] showed that despite no H_2 consumption was observed on TPR profiles of Au/MgO, a large negative peak was in sight on the TPR profile between approximately 300 and 600 °C, which was due to the interaction of hydrogen with magnesium hydroxide with the formation of magnesium oxide and water. The latter was detected by a mass-spectroscopy detector.

For Fe-modified catalysts (Figure 6 c), the H_2 consumptions at 347, 400, 553 and 836 °C of the support TPR profile, related to the reduction steps $FeOOH \rightarrow Fe_2O_3 \rightarrow Fe_3O_4 \rightarrow FeO \rightarrow Fe$, respectively, were retained in TPR catalysts' profiles. The exception was the disapperance of the peak at 457 °C in both catalysts, indicating that the transformation of Fe_2O_3 to Fe_3O_4 took place at lower temperature, 400 °C. Also, a new peak of consumption at 747 °C was found for 4% $Au/Fe_2O_3/TiO_2$, which could be associated with the beginning of reduction of FeO to Fe, which is completely transformed at 836 °C.

When comparing TPR profiles for ceria-modified catalysts and CeO_2/TiO_2 support (Figure 6 b), the disappearance of the peak at 440 °C observed for CeO_2/TiO_2, confirms the reduction of the surface of ceria at low temperature. Besides, the area of the peak at 120–200 °C, attributed to reduction of the gold precursor, shows a hydrogen consumption higher than the stoichiometric for reduction of Au^{3+} to Au°. This indicates reduction of the ceria surface at this temperature range, like other catalysts based on noble metals supported on ceria [175, 177]. Thus, an increased reducibility is observed for the CeO_2/TiO_2 support, being attributed to reduction of CeO_2. The strong interaction of gold with ceria provides reduction of both surface and bulk ceria at lower temperatures. This may provide the increased activity in oxidation reactions, due to additional amount of oxidative species from ceria.

3.2.3. Study of electronic states of gold on supports

XPS method was applied to investigate gold electronic states on the support surface. The binding energies of Au 4f spectra, according to XPS measurements, show various states of gold: Au^+, Au^{3+} and neutral gold nanoparticles. Their proportion was affected by the support composition, pretreatment atmosphere and Au content (Figure 7 and Table 8).

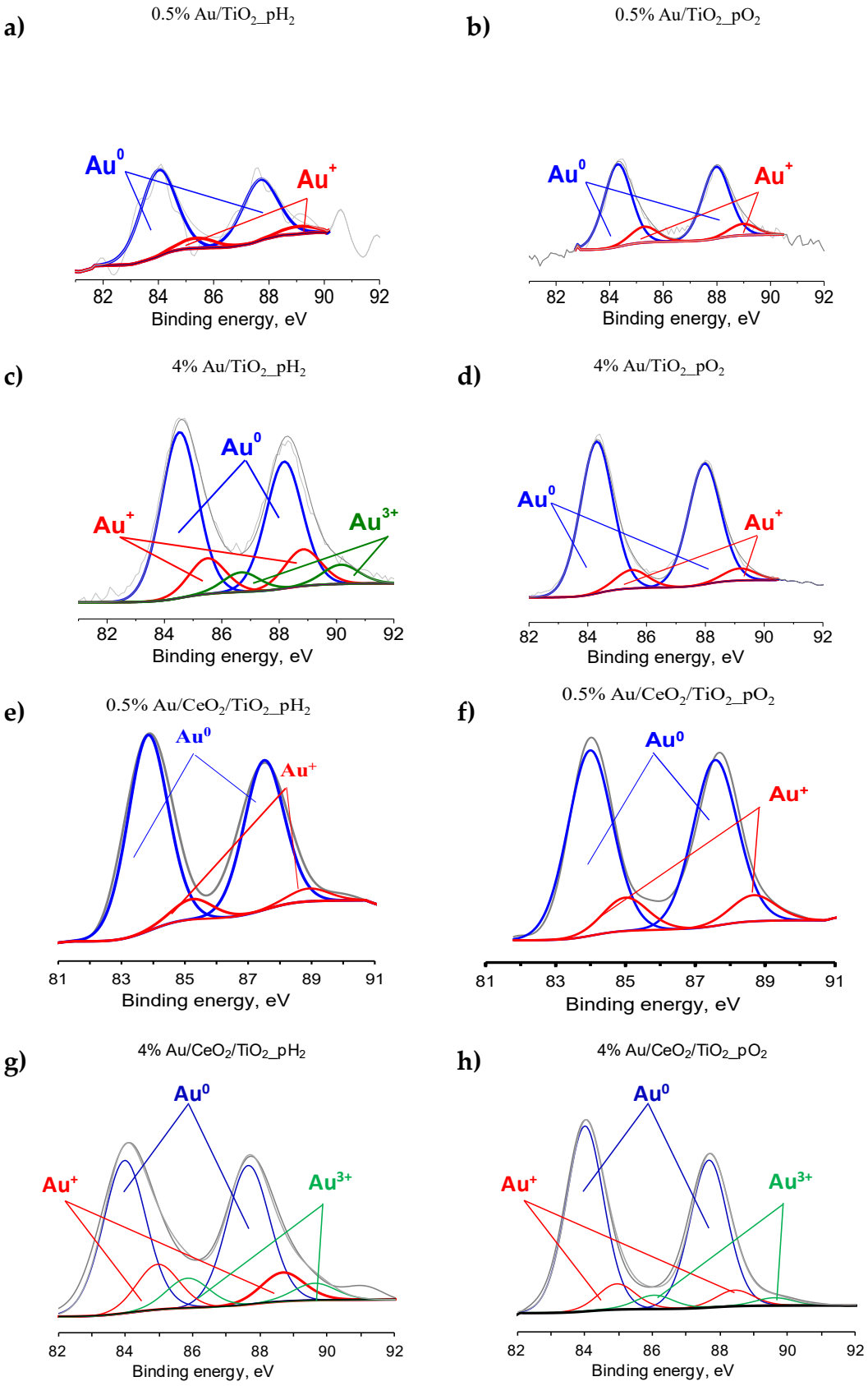

Figure 7. *Cont.*

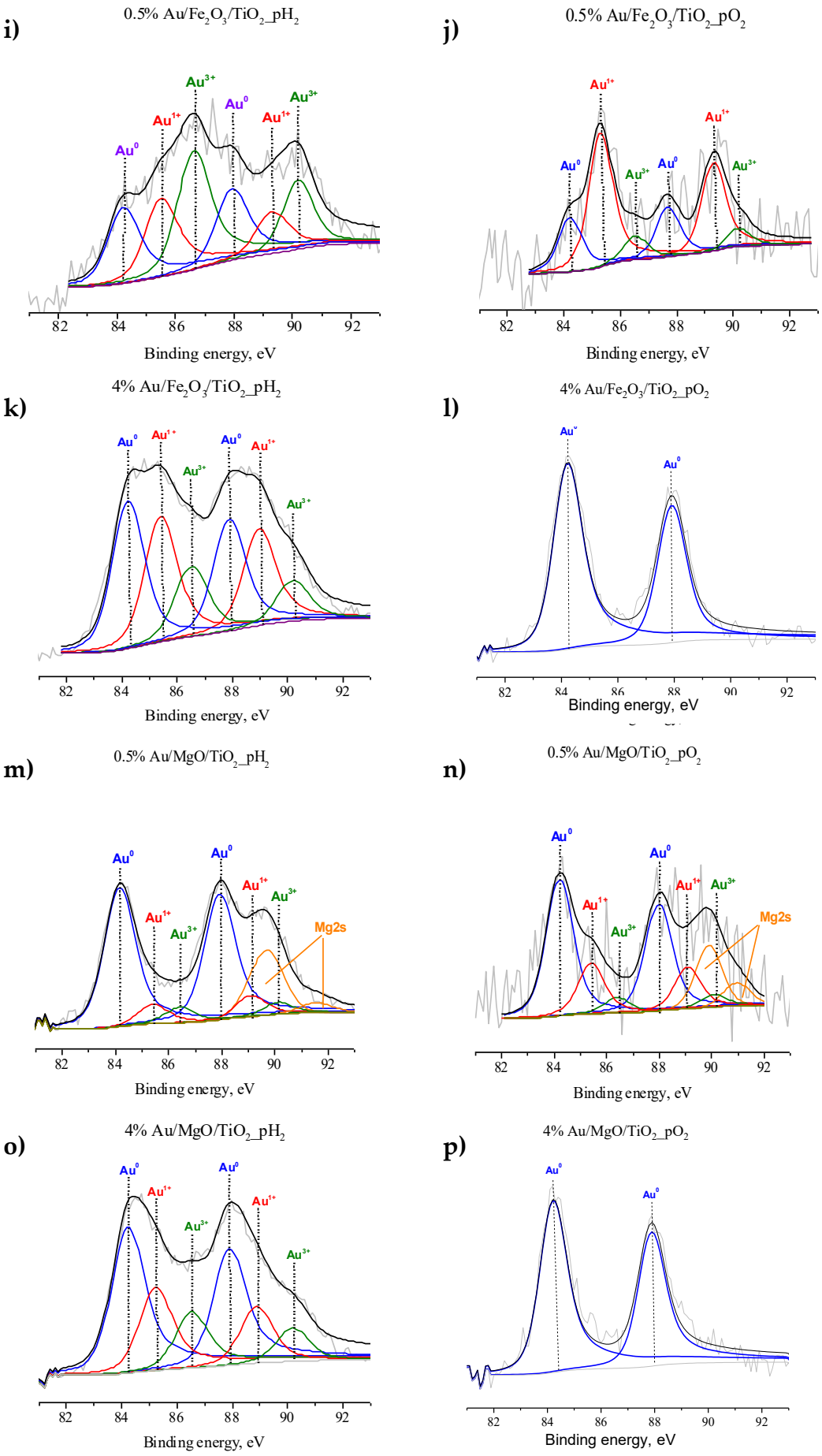

Figure 7. *Cont.*

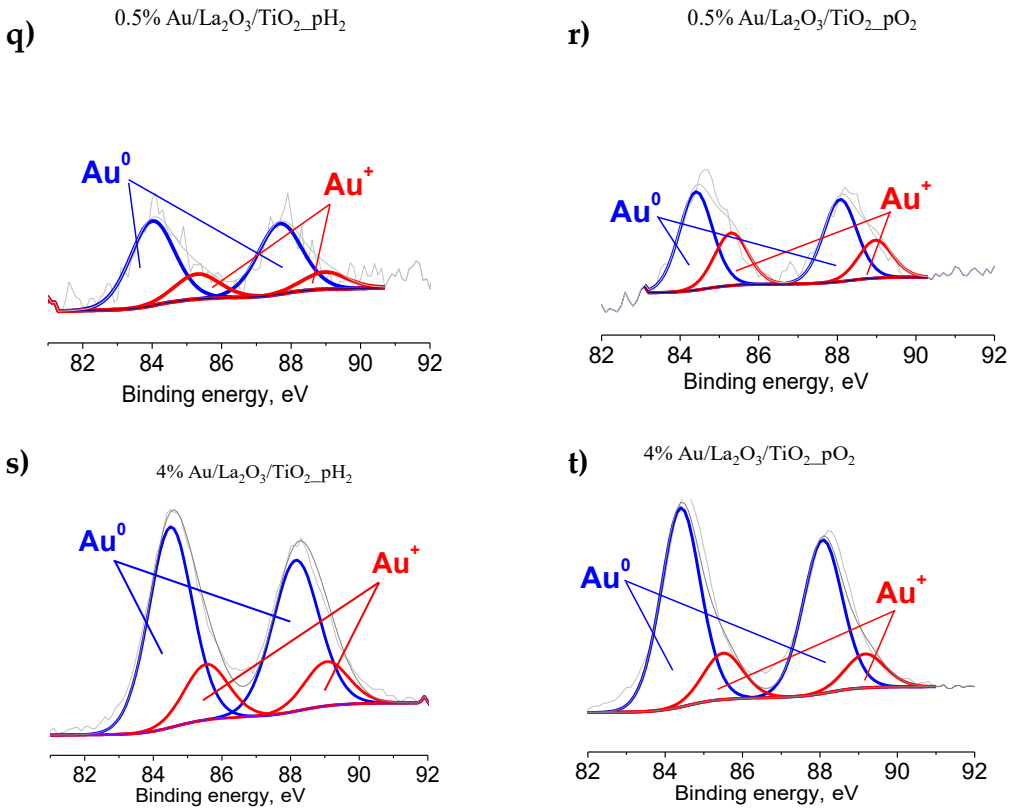

Figure 7. Au4f XP spectra of samples with different gold contents (0.5 or 4 wt.%), pretreated in H_2 or O_2 flow, at 300 °C, for 1 h: Au/TiO_2 (**a–d**), $Au/CeO_2/TiO_2$ (**e–h**), $Au/Fe_2O_3/TiO_2$ (**i–l**), $Au/MgO/TiO_2$ (**m–p**) and $Au/La_2O_3/TiO_2$ (**q–t**).

Table 8. Effect of gold content (0.5 or 4 wt.%) and redox treatment (H_2 or O_2) on the contribution of the different electronic states of Au, determined by XPS, for $Au/(M_xO_y)/TiO_2$ catalysts.

Entry	Catalyst	Au (⁰, ¹⁺, ³⁺) relative content, %		
		Au^0	Au^{1+}	Au^{3+}
1	0.5% Au/TiO_2_pH_2	91	9	0
2	0.5% Au/TiO_2_pO_2	84	16	0
3	4% Au/TiO_2_pH_2	74	15	11
4	4% Au/TiO_2_pO_2	89	11	0
5	0.5% $Au/CeO_2/TiO_2$_pH_2	91	9	0
6	0.5% $Au/CeO_2/TiO_2$_pO_2	85	15	0
7	4% $Au/CeO_2/TiO_2$_pH_2	68	20	12
8	4% $Au/CeO_2/TiO_2$_pO_2	83	11	6
9	0.5% $Au/Fe_2O_3/TiO_2$_pH_2	28	29	43
10	0.5% $Au/Fe_2O_3/TiO_2$_pO_2	26	64	10
11	4% $Au/Fe_2O_3/TiO_2$_pH_2	42	37	21
12	4% $Au/Fe_2O_3/TiO_2$_pO_2	100	0	0
13	0.5% $Au/MgO/TiO_2$_pH_2	81	11	8
14	0.5% $Au/MgO/TiO_2$_pO_2	67	25	8
15	4% $Au/MgO/TiO_2$_pH_2	51	29	20
16	4% $Au/MgO/TiO_2$_pO_2	100	0	0
17	0.5% $Au/La_2O_3/TiO_2$_pH_2	80	20	0
18	0.5% $Au/La_2O_3/TiO_2$_pO_2	65	35	0
19	4% $Au/La_2O_3/TiO_2$_pH_2	81	19	0
20	4% $Au/La_2O_3/TiO_2$_pO_2	83	17	0

All samples showed BE (Au $4f_{7/2}$) 84.2 eV (26–100% relative content), attributed to Au^0 states [178-182], excepting for 4% Au/MgO/TiO_2_pO_2 and 4% Au/Fe_2O_3/TiO_2_pO_2, where only gold in metallic state was found.

Apart from the peak due to the metallic gold, another (Au$4f_{7/2}$) peak in the BE range of 85.2-85.5 eV, attributed to single charged ions (Au^+) [179-182], was detected in the remaining catalysts, with 9-64% relative content. The highest amount of Au^+ was found in the modified samples with 0.5% Au after oxygen treatment and 4% Au after hydrogen treatment (Table 8, Entries 6, 7, 10, 11, 14, 15, 18, 19). The 0.5% Au/Fe_2O_3/TiO_2_pO_2 sample showed the maximum contribution of single charged ions (64%), compared with other catalysts.

Moreover, another oxidized state of gold, three-charged gold (Au^{3+}) with BE (Au$4f_{7/2}$) in the range of 86.4-86.6 eV [183-185], was found with different contents (11-21%) for all the catalysts with 4% Au after reductive treatment (Table 8, Entries 3, 7, 11 and 15). The only exception were La-modified samples, where gold was found only in metallic and monovalent states (Table 8, Entries 17-20). Also, Au^{3+} state was observed only in magnesium and iron modified 0.5% Au catalysts after both treatments, the highest portion of Au^{3+} (43%) being found for 0.5% Au/Fe_2O_3/TiO_2_pH_2.

It should be noted that for both 0.5% Au/MgO/TiO_2_pH_2 and 0.5% Au/MgO/TiO_2_pO_2 catalysts, there was an overlapping of Au$4f_{7/2}$ line with the Mg2s line (Figure 7 m, n), leading to difficulties in the interpretation of these peaks and subsequent uncertainty. However, since the Au$4f_{7/2}$ line is clearly visible, the states were identified correctly.

In order to obtain more information on the gold electronic states of the catalysts, DRIFT spectroscopy of adsorbed CO was used. As can be seen from Figure 8, an absorption band with the maximum in the range of 2090–2130 cm^{-1}, corresponding to the surface carbonyl groups of gold atoms Au^0–CO [186], was observed for all catalysts. The different intensities of the absorption bands, corresponding to Au^0-CO, can be explained by carbon monoxide being very weakly adsorbed on metallic gold, due to some features of the σ-π bond in M^0-CO for Au, compared to other noble metals [187]. Therefore, only the highly dispersed clusters or gold atoms can be sites for the adsorption of CO.

Comparing the data on the band intensity related to Au^0–CO with the STEM results, it can be seen that the average particle size for samples with low frequency absorption bands is larger than for samples with high intensity, and the differences in signal position are due to the adsorption of CO on metal clusters of different sizes. In fact, considering the DRIFT CO results for samples with the same support and Au content, but different pretreatment, e.g., 4% Au/MgO/TiO_2_pO_2 (Figure 8 p) and 4% Au/MgO/TiO_2_pH_2 (Figure 8 o), a higher intensity of the Au^0–CO band is observed for the latter, meaning that this catalyst should have smaller particles than the former. This is confirmed by STEM results shown in Table 7: Entry 15 (4% Au/MgO/TiO_2_pO_2) – 5.1 nm and Entry 16 (4% Au/MgO/TiO_2_pH_2) – 2.9 nm. The same correlation between the average particle size and the intensity of the absorption band of metal particles was observed for

the rest of catalysts, with the exception of 4% Au/CeO_2/TiO_2_pO_2 (Figure 8 h), and especially 4% Au/La_2O_3/TiO_2_pO_2 (Figure 8 t) catalysts. Consequently, it can be assumed that there are larger particles in these samples, which were not taken into account when analyzing TEM images because of their relatively low abundance.

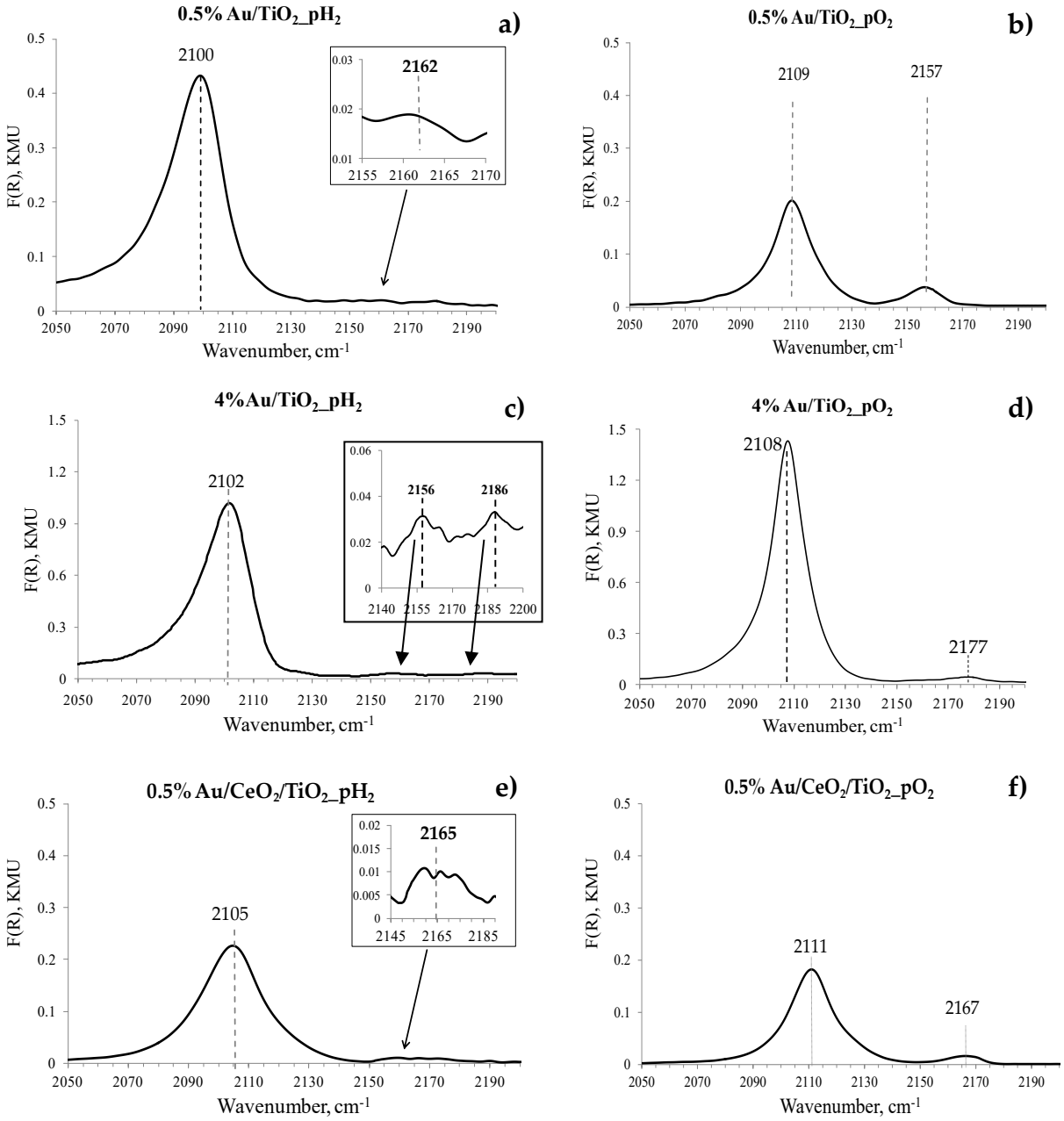

Figure 8. *Cont.*

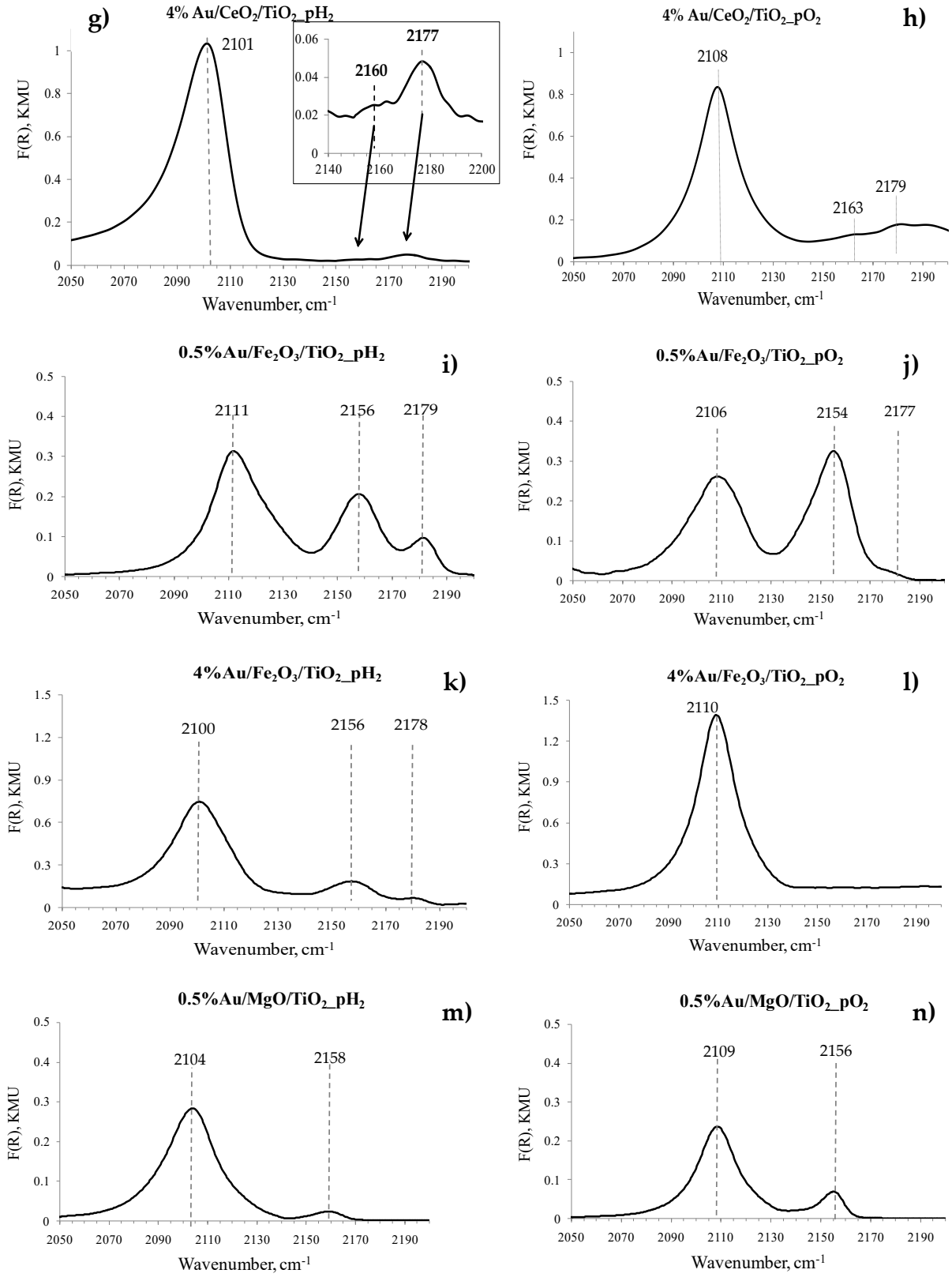

Figure 8. *Cont.*

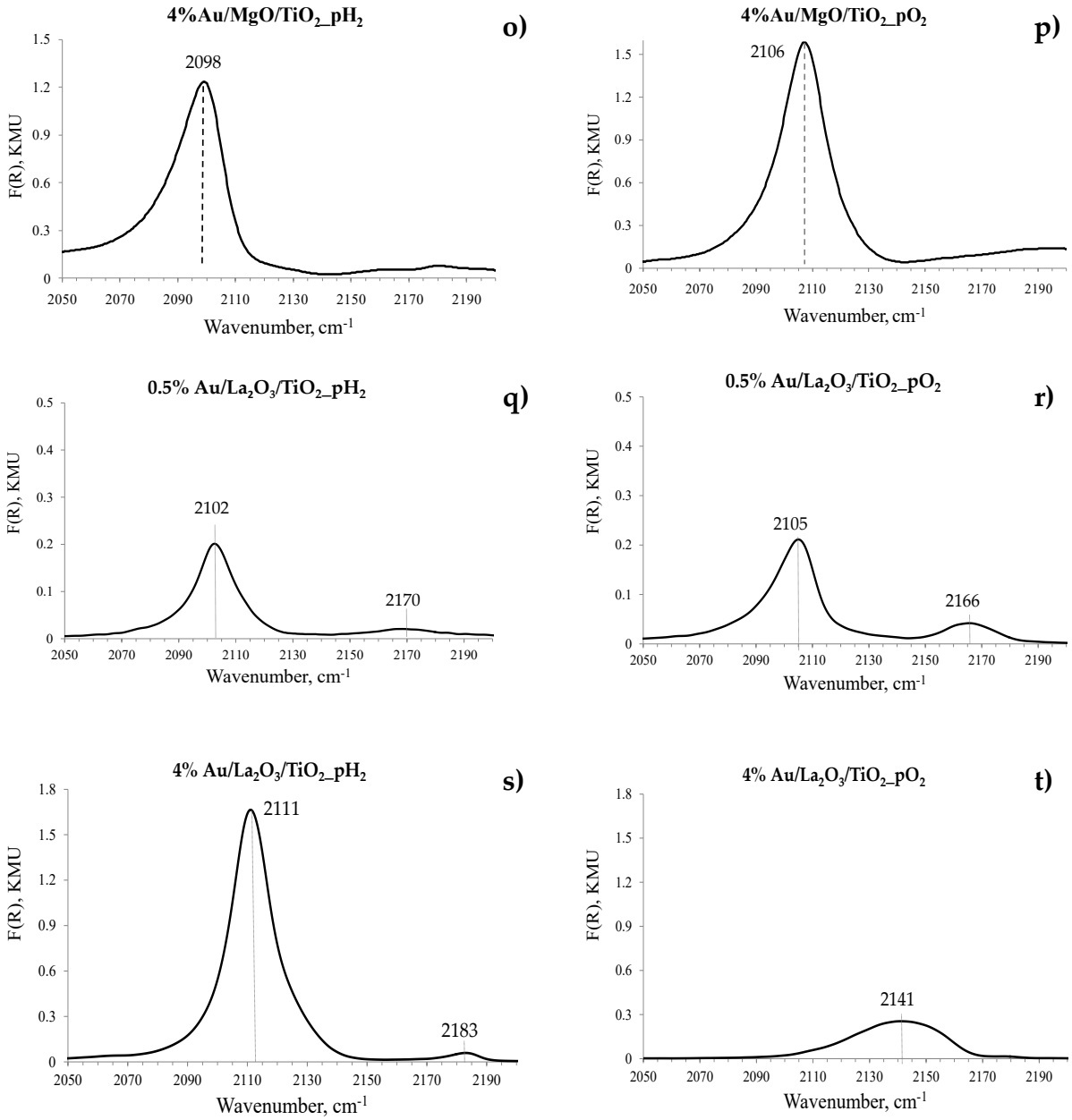

Figure 8. DRIFT spectra of CO adsorbed at 20 Torr on catalysts with different gold contents (0.5 or 4 wt.%), pretreated at 300 °C for 1 h under a H_2 or O_2 atmosphere: Au/TiO_2 (**a–d**), $Au/CeO_2/TiO_2$ (**e–h**), $Au/Fe_2O_3/TiO_2$ (**i–l**), $Au/MgO/TiO_2$ (**m–p**) and $Au/La_2O_3/TiO_2$ (**q–t**).

Another absorption band with the maximum in the range 2150–2170 cm^{-1}, related to the complexes of Au^+–CO ions [95,188], was observed in all cases, except for 4% $Au/Fe_2O_3/TiO_2\_pO_2$ and 4% $Au/MgO/TiO_2\_pO_2$ (Figure 8 l, p). Results for 4% $Au/Fe_2O_3/TiO_2\_pO_2$ and 4% $Au/MgO/TiO_2\_pO_2$ are in a good agreement with XPS data, as no Au^+ was detected in these catalysts (Figure 7 l, p). It should be noted, that this absorption band, related to the complexes of Au^+–CO ions, is less intense than the one attributed to Au^0–CO, except for 0.5% $Au/Fe_2O_3/TiO_2\_pO_2$ (Figure 8 j), which is also well correlated with the

predominant content of Au^{+} (64%) found in this catalyst by XPS (Table 8, Entry 10).

Along with absorption bands at 2090–2130 cm^{-1} and 2150–2170 cm^{-1}, ascribed to carbonyls of metallic and singly charged gold, respectively, a third band appears within 2170-2190 cm^{-1} interval for 4% $Au/TiO_2\_pH_2$, 4% $Au/CeO_2/TiO_2\_pH_2$, 4% $Au/CeO_2/TiO_2\_pO_2$, 4% $Au/Fe_2O_3/TiO_2\_pH_2$, 4% $Au/MgO/TiO_2\_pH_2$, 0.5% $Au/Fe_2O_3/TiO_2\_pH_2$ and 0.5% $Au/Fe_2O_3/TiO_2\_pO_2$, catalysts, its interpretation being ambiguous. In most studies, this absorption band is assigned to the adsorption of CO on monovalent gold ions, as it is believed that a higher-charged gold cation (Au^{3+}) is very unstable, or even does not form carbonyl species. That could be caused by the following reasons: 1) Au^{3+} ions are very easily reduced with CO [189-191]; 2) since Au^{3+} ions are strongly charged, probably, trivalent ions on a support surface are usually saturated by coordination, and evacuation at elevated temperatures will easily lead to the reduction of Au^{3+} [192].

At the same time, according to XPS (Table 8 and Figure 7), Au^{3+} was found for 4% $Au/TiO_2\_pH_2$, 4% $Au/CeO_2/TiO_2\_pH_2$, 4% $Au/Fe_2O_3/TiO_2\_pH_2$, and 4% $Au/MgO/TiO_2\_pH_2$ samples, even after the reduction treatment at 300 °C. Moreover, Au^{3+} relative content in these samples is much higher than in the oxidized ones. Luengnaruemitchai et al. [185] observed that Au^{3+} remains in $Au/Fe_2O_3/TiO_2$ catalytic systems even after calcination at 400 °C. Such trivalent cations could be stabilized by oxygen vacancies, formed under the action of high temperature reduction treatment during the preparation of the catalyst [193-196]. It is also worth noting that the reducibility of supports, such as titania, increases after the gold deposition due to metal-support interactions. A similar mechanism for the stabilization of gold ions was proposed elsewhere [197]. In addition, it was also suggested that modifying the titania surface lead to an increase in the number of oxygen defects, which in turn increases the number of stabilized gold ions. A similar trend was observed in our study.

Mihaylov et al. [194] carried out IR CO experiments for characterization of supported gold catalysts in conditions comparable to our study, and they proved that absorption band with a maximum in the range of 2170-2190 cm^{-1} corresponds to trivalent gold in non-exchange positions. Thus, one can also assume that the absorption band within 2176-2186 cm^{-1} interval belongs to the trivalent gold ion. Again, this is in good agreement with the XPS data.

For 4% $Au/TiO_2\_pO_2$ and 4% $Au/La_2O_3/TiO_2\_pH_2$, the second absorption band is also shifted towards longer wavelengths, with maxima at 2177 and 2183 cm^{-1}, respectively. Despite this fact, by comparing these results with the XPS data, one can assume that these bands can be assigned to the adsorption of CO on monovalent gold ions, in this particular case.

Because no direct correlation was found between the average particle size of gold and the catalytic activity of samples, and neither significant differences in the texture and structural properties of the studied catalysts, it can be assumed that these parameters are not determining for the observed catalytic behavior of

the studied systems. However, another parameter capable of influencing the catalytic behavior of gold catalysts is its electronic state. Based on the analysis performed on the surface of the studied catalysts by the above methods (XPS, DRIFT CO), three electronic states of gold were found with different relative concentrations and ratios.

Table 9 shows the relative contents of the electronic states of gold found in the samples and n-octanol conversion reached on them after 6 h. There is no relationship between the conversion and the content of gold in cationic states (Au^{+} and Au^{3+}), if each state is considered separately. However, if the combined concentration of Au^{+} and Au^{3+} is considered, one tendency can be seen: for samples with a higher concentration of Au^{+}, but with a lower contribution of Au^{3+}, the conversion of octanol is higher. For example, for 0.5% Au/MgO/TiO_2_pH_2 and 0.5% Au/MgO/TiO_2_pO_2 (Table 9, Entries 13 and 14 respectively), the Au^{3+} content is the same (8%). However, the sample after oxygen pretreatment has a larger contribution of monovalent gold (25%) than the reduced sample (11%); similarly, the conversion for Au/MgO/TiO_2_pO_2 (43%) sample is much higher than for 0.5% Au/MgO/TiO_2_pH_2 (12%). And for the same content of monovalent ions (29%), in 0.5% Au/Fe_2O_3/TiO_2_pH_2 and 4% Au/MgO/TiO_2_pH_2 catalysts (Table 9, Entries 9 and 15), octanol conversion is higher in the latter sample, where the content of trivalent gold is 23% lower than in the former. It is worth noting that for samples with a high content of metallic gold (Table 9, Entries 12 and 16), the conversion of n-octanol is very low, 5 and 3%, respectively.

Table 9. Effect of gold content (0.5 or 4 wt.%) and redox treatment (H_2 or O_2) on the proportion of different electronic states of Au calculated by XPS and their activity for aerobic n-octanol oxidation[1] for Au/M_xO_y/TiO_2 catalysts.

Entry	Catalyst	Au (^{0}, $^{1+}$, $^{3+}$) relative content, %			Conversion of n-octanol, %
		Au^0	Au^{1+}	Au^{3+}	
1	0.5% Au/TiO_2_pH_2	91	9	0	3
2	0.5% Au/TiO_2_pO_2	84	16	0	17
3	4% Au/TiO_2_pH_2	74	15	11	11
4	4% Au/TiO_2_pO_2	89	11	0	6
5	0.5% Au/CeO_2/TiO_2_pH_2	91	9	0	10
6	0.5% Au/CeO_2/TiO_2_pO_2	85	15	0	30
7	4% Au/CeO_2/TiO_2_pH_2	68	20	12	23
8	4% Au/CeO_2/TiO_2_pO_2	83	11	6	10
9	0.5% Au/Fe_2O_3/TiO_2_pH_2	28	29	43	7
10	0.5% Au/Fe_2O_3/TiO_2_pO_2	26	64	10	41
11	4% Au/Fe_2O_3/TiO_2_pH_2	42	37	21	15
12	4% Au/Fe_2O_3/TiO_2_pO_2	100	0	0	5
13	0.5% Au/MgO/TiO_2_pH_2	81	11	8	12
14	0.5% Au/MgO/TiO_2_pO_2	67	25	8	43
15	4% Au/MgO/TiO_2_pH_2	51	29	20	20
16	4% Au/MgO/TiO_2_pO_2	100	0	0	3
17	0.5% Au/La_2O_3/TiO_2_pH_2	80	20	0	37
18	0.5% Au/La_2O_3/TiO_2_pO_2	65	35	0	63
19	4% Au/La_2O_3/TiO_2_pH_2	81	19	0	40
20	4% Au/La_2O_3/TiO_2_pO_2	83	17	0	30

[1] Reaction conditions: T = 80 °C, 0.1 M n-octanol (n-heptane), O_2 = 30 mL/min, R = 100, stirring.

Besides, considering only the samples with no trivalent gold, a direct correlation can be found between surface concentration of monovalent gold ions, as well as metallic gold, and catalytic activity in n-octanol oxidation (Figure 9). Thus, the most active catalyst (0.5% $Au/La_2O_3/TiO_2$ pretreated in O_2) has the highest surface concentration of Au^+ and lowest surface concentration of Au^0; that is, an increase in the surface concentration of monovalent gold, with a simultaneous decrease in the surface concentration of metallic gold, leads to an increase in the catalytic activity of the samples in n-octanol oxidation (Figure 9). Moreover, it should be noted that, for samples with close catalytic performance, in particular H_2-pretreated 0.5% $Au/La_2O_3/TiO_2$ and H_2-pretreated 4% $Au/La_2O_3/TiO_2$, the contribution of Au^+ was practically the same.

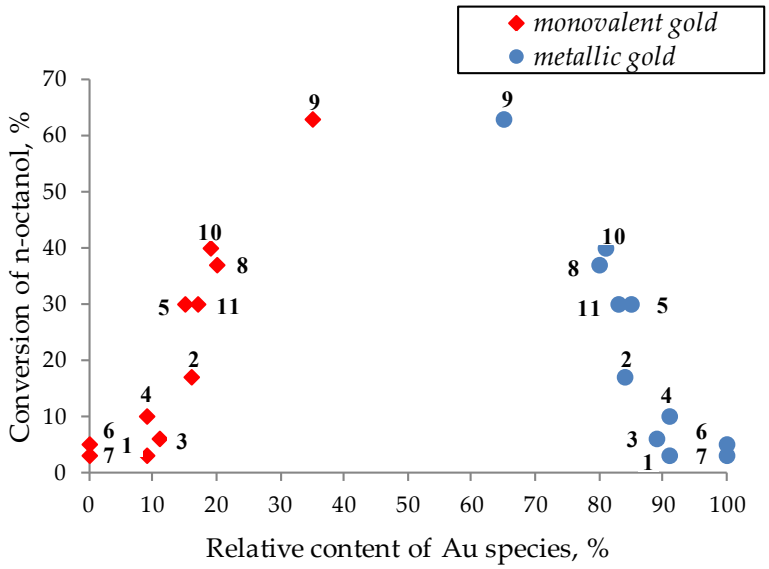

Figure 9. Aerobic oxidation of n-octanol. Influence of the content of Au^0 and Au^+ species on n-octanol conversion. Samples: *1* – 0.5% $Au/TiO_2\_pH_2$, *2* – 0.5% $Au/TiO_2\_pO_2$, *3* – 4% $Au/TiO_2\_pO_2$, *4* – 0.5% $Au/CeO_2/TiO_2\_pH_2$, *5* – 0.5% $Au/CeO_2/TiO_2\_pO_2$, *6* – 4% $Au/Fe_2O_3/TiO_2\_pO_2$, *7* – 4% $Au/MgO/TiO_2\_pO_2$, *8* – 0.5% $Au/La_2O_3/TiO_2\_pH_2$, *9* – 0.5% $Au/La_2O_3/TiO_2\_pO_2$, *10* – 4% $Au/La_2O_3/TiO_2\_pH_2$, *11* – 4% $Au/La_2O_3/TiO_2\_pO_2$). Reaction conditions: T = 80 °C, 0.1 M n-octanol (n-heptane), O_2 = 30 mL/min, R = 100, t = 6 h, stirring.

Therefore, by comparing the spectroscopic and catalytic results, it can be assumed that monovalent gold ions (Au^+) are probably responsible for the enhanced catalytic activity, while metallic gold (Au^0) and three-charged gold (Au^{3+}) have a negative effect on the catalytic activity. The following DFT calculations of n-octanol adsorption on tetrahedral gold clusters, presented in Section 3.3.1., proved that monovalent gold ions play an important role in n-octanol oxidation.

The negative effect of metallic and trivalent gold on catalytic activity probably occurs due to the strong adsorption of the solvent (n-heptane) on both Au^0 and Au^{3+} or to water generated by the dehydrogenation reaction of n-octanol on Au^{3+} (Scheme 2). The calculations of the adsorption energy in Section 3.3.2 confirmed this assumption.

When comparing the XPS and the catalytic results of the catalysts in both peroxidative and aerobic oxidation of 1-phenylethanol after 15 min (Tables 3 and 6), there is no apparent correlation with the electronic gold states as found in n-octanol aerobic oxidation, due to the much greater reactivity of 1-phenylethanol (Table 10). However, the cationic nature of gold as the active site in the case of 1-phenylethanol oxidation is confirmed by the recycling experiments (see Table 12 below) and calculations of the phenylethanol adsorption energy performed in Section 3.3.3.

Table 10. Catalytic results of the most active catalysts in the peroxidative oxidation of 1-phenylethanol and aerobic oxidation of n-octanol and contribution of gold electronic states in these catalysts, calculated by XPS.

Entry	Sample	Yield of acetophenone [1] in 0.25 h, mol %	Converison of n-octanol [2] in 0.25 h, mol %	Relative Au content, %	
				Au^0	Au^+
1	4% $Au/La_2O_3/TiO_2$_pH_2	88	13	81	19
2	0.5% $Au/La_2O_3/TiO_2$_pO_2	95	22	65	35

[1] R = 5000, TBHP:1-phenylethanol = 2.43, T = 80 °C, stirring. [2] R = 100, 0.1 M 1-phenylethanol in mesitylene, T = 80 °C, O_2 = 30 mL/min, stirring.

3.2.4. Study of catalyst stability

In order to evaluate the stability of gold ionic states during redox treatments and reaction media, TPR measurements were carried out for the most and least active catalysts in terms of support, i.e., Au supported on unmodified and La-modified titania, respectively, with optimal gold content and treatment found for the studied reactions (Figure 10). Low gold loading and oxygen treatment (Figure 10 a) were found beneficial for both aerobic and peroxidative oxidation of n-octanol, as well as for the oxidation of 1-phenylethanol with O_2, while samples with 4wt.% of Au after hydrogen treatment (Figure 10 b) were the most active in peroxidative oxidation of 1-phenylethanol.

Both reductive and oxidative pre-treatments lead to disappearance of the peak at 155-175 °C, observed for all catalysts in as-prepared state, that indicates the decomposition of the gold precursor in such conditions. A new low-temperature peak at 77-100 °C is observed for 0.5% Au/TiO_2 and 0.5% $Au/La_2O_3/TiO_2$ catalysts (Figure 10 a). This peak may be attributed to the reduction of Au^+ to Au^0. The high temperature peak at 500-650 °C, present in the spectra of all catalysts after treatments, is attributed to the high stability of $Au^{\delta+}$ species strongly bonded with the support. The highest portion of such gold states was observed in $Au/La_2O_3/TiO_2$ samples, while in the unmodified

samples they were present in much smaller amounts. Thus, modifying additives of La oxides favored formation of very stable ionic species $Au^{\delta+}$ ($0 < \delta < 1$), resistant to reduction treatment up to 550-600 °C. The presence of Au^{+} ions in the catalysts was observed by XPS and DRIFT CO (Section 3.2.3, Figures 7 and 8) for catalysts after both reductive and oxidative pretreatments.

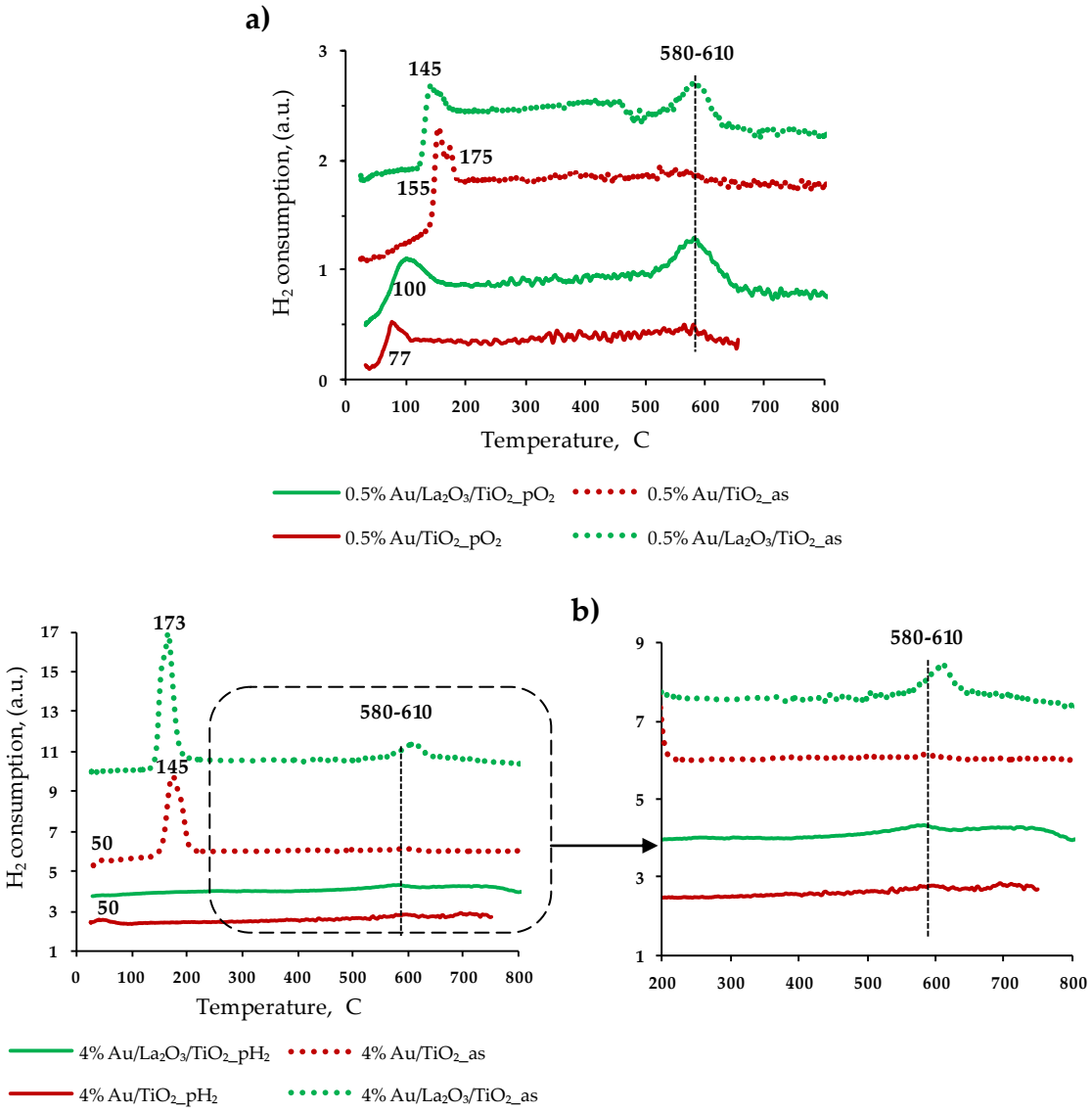

Figure 10. TPR profiles of Au/TiO_2 and $Au/La_2O_3/TiO_2$ catalysts with 0.5% of Au in as-prepared and after oxygen pretreatment **(a)** or with 4% of gold in as-prepared and after hydrogen pretreatment **(b).**

Additionally, in order to prove the existence of stable gold ions directly responsible for the best catalytic performance, the most active sample, 0.5% $Au/La_2O_3/TiO_2\_pO_2$, was analysed by XPS after *aerobic oxidation of n-octanol*. It was found that the concentration of Au^{+} ions decreased to 13%, compared with a 35% content of these gold monovalent ions before the reaction (Table 11, Entry 2 and Figure 11 b). In parallel, the activity of this sample also decreased in the second octanol oxidation cycle performed. After 15 min of the second run,

alcohol conversion was 11% after 15 min, compared to 22% of the first run reaction. The final conversion in the second cycle after 6 h was 31%, while in the first cycle it was 63%. However, it should be emphasized that these are very stable ionic species, $Au^{\delta+}$. Their contribution was determined by H_2-TPR (Figure 10) namely, by the area of the hydrogen consumption peak at 500-650 °C, attributed to high stability of $Au^{\delta+}$ species strongly bonded to the support, which was only 25-35 μmol/g, corresponding to 12-15% of the total amount of gold (204 μmol/g). The remaining 20-23% of gold ions is unstable, being reduced during the reaction. These gold species can be identified on the low-temperature region, up to 200 °C, of the TPR profiles (Figure 10 a).

Moreover, in order to check the stability of the mentioned gold ions and confirm that they are the active sites, 0.5% $Au/La_2O_3/TiO_2\_pO_2$ sample was treated in a hydrogen atmosphere at higher temperature (500 °C), for reducing unstable gold ions. According to the XPS analysis of this sample, it was found a decrease of 22% in the surface concentration of $Au^{\delta+}$ ions (Figure 11 c and Table 11, Entry 3). This reduced sample was tested in an octanol oxidation reaction. The initial and final conversion of octanol on this sample was reduced almost two times, as the activity of the sample after the recycling test, where it was also observed 13% of gold monovalent ions. Thus, this confirmed once again a direct correlation between surface concentration of monovalent gold ions and catalytic activity in n-octanol oxidation.

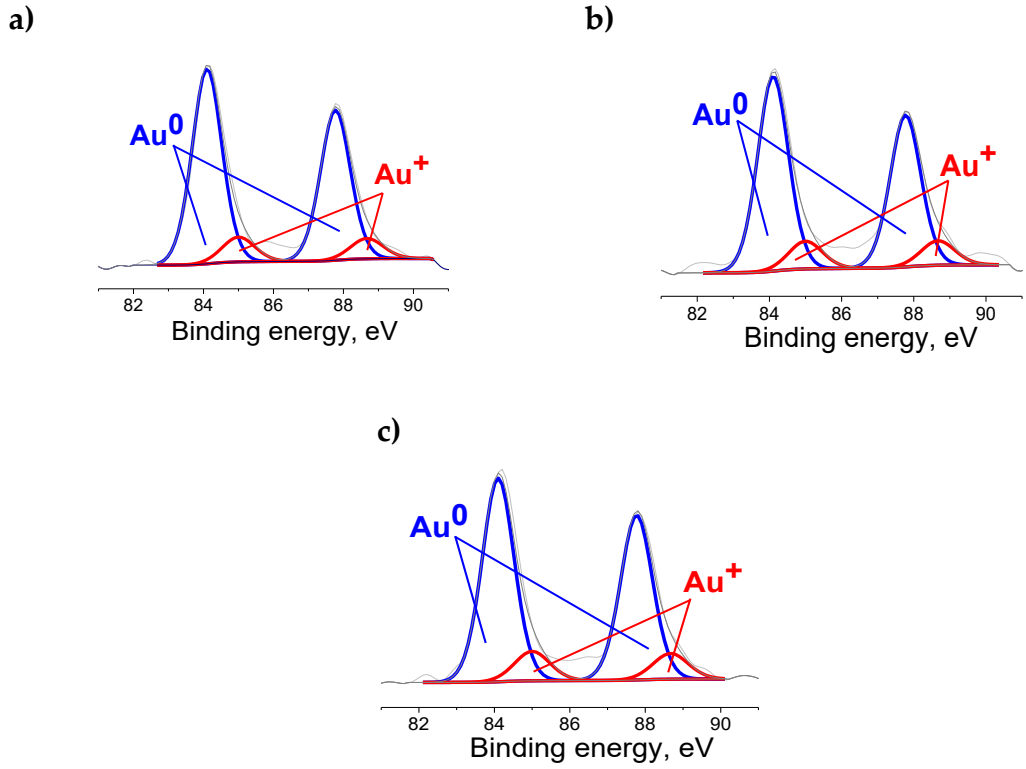

Figure 11. Au4f XP spectra of 0.5% $Au/La_2O_3/TiO_2\_pO_2$ samples after 15 min (**a**) and 6 h reaction in the aerobic oxidation of n-octanol (**b**) and after pretreatment in H_2 at 500 °C for 1 h (**c**).

Table 11. Catalytic performance of 0.5% $Au/La_2O_3/TiO_2$ catalyst in the aerobic oxidation of n-octanol and contribution of various electronic states of gold in this catalyst, calculated by XPS.

Entry	Sample	Conversion of n-octanol after 6 h, ca.%	Relative Au content, %	
			Au^0	Au^+
1	0.5% $Au/La_2O_3/TiO_2$_pO_2 [1]	63	65	35
2	0.5% $Au/La_2O_3/TiO_2$_pO_2 [2,a]	31	87	13
3	0.5% $Au/La_2O_3/TiO_2$_pH_2 [1,b]	34	87	13

XPS performed for the catalyst: [1] before reaction; [2] after reaction; [a] used, after 6 h of reaction; [b] pretreated in H_2 at 500 °C for 1 h.

The catalyst recyclability in *the peroxidative oxidation of 1-phenylethanol* was investigated up to six consecutive cycles, as described in the Experimental part, for the best performing catalyst, i.e., 4% $Au/La_2O_3/TiO_2$_pH_2. As can be seen in Figure 12, there was a gradual catalyst deactivation during the recycling tests. Particularly, in the second cycle, the catalyst maintained 90% of activity, whereas in the third cycle a loss of 23% of its initial activity was observed. Consecutive decreasing of activity stopped at the sixth cycle where the yield of acetophenone kept the same level as in the fifth cycle (58–59%). Nevertheless, high selectivity to acetophenone was preserved in each cycle.

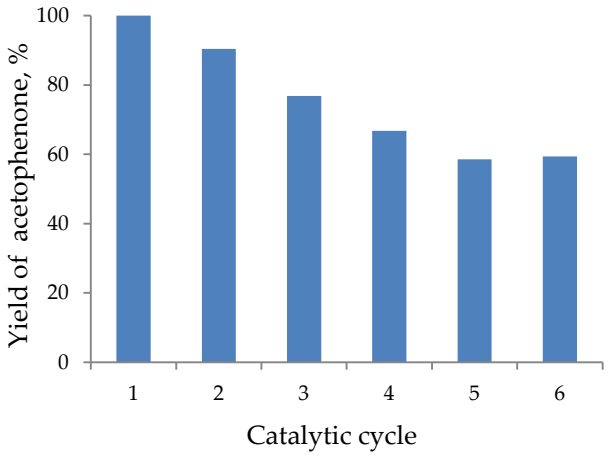

Figure 12. Peroxidative oxidation of 1-phenylethanol catalyzed by 4% $Au/La_2O_3/TiO_2$_pH_2: Effect of the catalyst recycling on the yield of acetophenone (R = 5000, TBHP: 1-phenylethanol = 2.43, 2 h, T = 80 °C).

To find out the cause of the observed catalyst deactivation, XPS analysis of the catalyst after the first and the last (6^{th}) cycle was performed (Figure 13, Table 12) and compared with the XPS results for the catalyst before reaction. Two electronic states of gold were found in the catalyst before reaction (Entry 1, Table 12) and in the used catalysts: metallic Au^0 (with BE ($Au4f_{7/2}$) 84.2 eV) and single charged ions Au^+ (with BE ($Au4f_{7/2}$) 85.2 eV) in catalyst after first cycle and Au^0 with (BE ($Au4f_{7/2}$) 84.1 eV) and Au^+ (with BE ($Au4f_{7/2}$) 85 eV) [177-179] in the

catalyst after 6 cycles. However, according to XPS measurements, the surface concentration of gold is different among the studied samples. It can be seen from Table 12 that, after first and after the sixth cycle, the catalytic activity decreased proportionally to the contribution of monovalent gold. That can probably be the reason for deactivation, as also in the case of n-octanol (Table 11 and Figure 11), since gold monovalent ions were the proposed active species for the reaction.

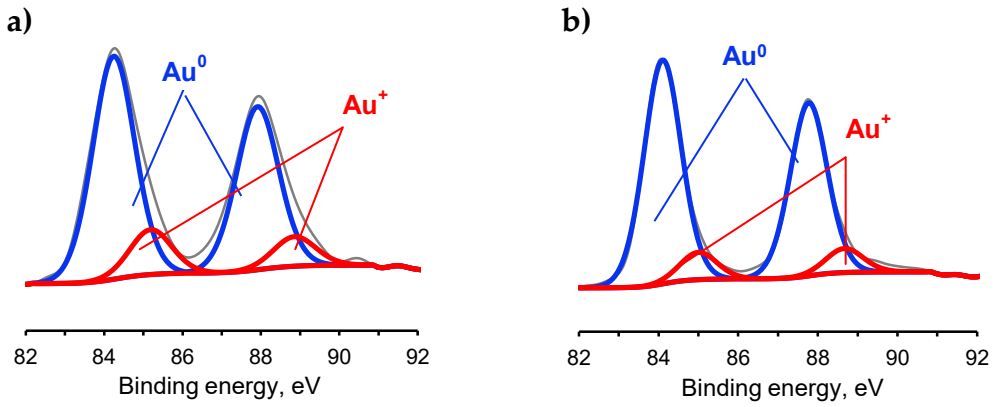

Figure 13. XPS of used 4% $Au/La_2O_3/TiO_2\_pH_2$ catalyst after the 1st (**a**) and 6th (**b**) cycles of 1-phenylethanol peroxidative oxidation (reaction conditions as in Table 3).

Table 12. Catalytic results[1] of the most active catalyst in the peroxidative oxidation of 1-phenylethanol and contribution of gold electronic states of in these catalysts, calculated by XPS.

Entry	Sample	Yield of acetophenone in 2 h, mol %	Relative Au content, %	
			Au^0	Au^+
1	$4\% Au/La_2O_3/TiO_2\_pH_2$ [a]	100	81	19
2	$4\% Au/La_2O_3/TiO_2\_pH_2\_1c$ [b]	90	83	17
3	$4\% Au/La_2O_3/TiO_2\_pH_2\_6c$ [c]	59	89	11

[1] $R = 5000$, TBHP:1-phenylethanol, $T = 80$ °C, stirring. XPS performed for the catalyst: [a] before reaction; [b] used, after 1 cycle of reaction; [c] used, after 6 cycles of reaction.

Additionally, for the most active samples in both reactions, in terms of support, i.e., Au supported on unmodified and La modified titania, with different gold contents and treatment atmospheres, *DRIFT spectroscopy of adsorbed CO at different pressures 5, 20, and 50 Torr* was applied to estimate the strength and the stability of the adsorption centers related to the complexes of ions Au^+-CO (Figure 14).

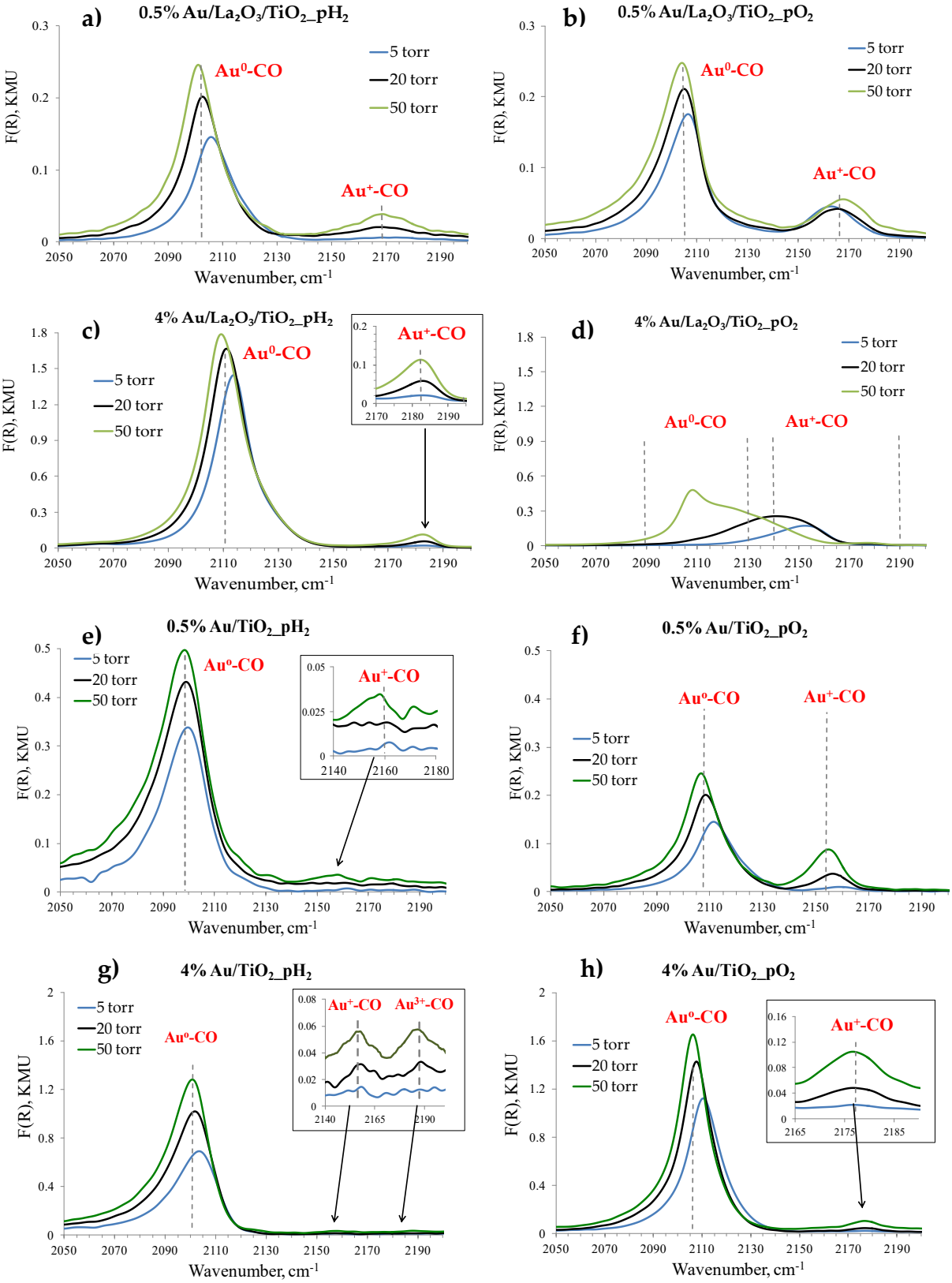

Figure 14. DRIFT spectra of CO adsorbed at different CO pressures on $Au/La_2O_3/TiO_2$ catalysts (**a-d**) and Au/TiO_2 (**e-h**) with different gold contents (0.5 or 4%) and pretreated at 300 °C for 1 h under a H_2 or O_2 atmosphere. Graphs **c,d,g,h** reproduced from [198] with permission from the Royal Society of Chemistry.

For the most active sample, 0.5% Au/La_2O_3/TiO_2_pO_2 (Figure 14 b), the intensity of this absorption slightly changed with a modification in the CO pressure, that indicates the presence of strong and stable Au^+ sites, and their concentration is about 1/3 of the total gold content, which correlates well with the XPS data (Table 7). For other samples, this absorption is less intense, with the exception of 4% Au/La_2O_3/TiO_2_pH_2, and strongly depends on the pressure of CO. The intensity increases with increasing pressure, and, accordingly, these sites are less strong than in 0.5% Au/La_2O_3/TiO_2_pO_2.

It is interesting to note that for 4% Au/La_2O_3/TiO_2_pO_2 (Figure 14 d), reduction of Au^+ sites is observed in the CO atmosphere, which indicates their very low stability and most probably most of them are reduced during the reaction. The stability of gold active sites can be clearly seen in the example of n-octanol peroxidative oxidation (Figure 3). Only for 0.5% Au/La_2O_3/TiO_2_pO_2 and 4% Au/La_2O_3/TiO_2_pH_2 n-octanol conversion did not reach a plateau with the reaction time, in comparison with the other two catalysts. This means that 0.5% Au/La_2O_3/TiO_2_pO_2 and 4% Au/La_2O_3/TiO_2_pH_2 catalysts are deactivated much slower than the others. Also, in 1-phenylethanol peroxidative oxidation (Table 3), the fastest acetophenone formation was observed on 0.5% Au/La_2O_3/TiO_2_pO_2 and 4% Au/La_2O_3/TiO_2_pH_2.

In contrast, for unmodified catalysts (Figure 14 e-h), the clear presence of the band related to Au^+ sites was found only in 0.5% Au/TiO_2_pO_2 (Figure 14 f), in a good agreement with XPS data, which shows that this sample has the largest amount of Au^+ ions (16%) among all unmodified samples (Table 8). However, the intensity of this band strongly depends on CO pressure, which possibly indicates weak adsorption on these ions. In the remaining unmodified samples, this band could only be seen by zooming of adsorption intensity in the region at 2170-2185 cm^{-1}, as well as the band related to Au^{3+} sites in the case of 4% Au/TiO_2_pH_2 (Figure 14 g). It can be due to the presence of only weak Au^+ sites, because even a 50 Torr CO pressure is not enough for their clear identification by DRIFT CO, while according to XPS (Table 8), Au^+ present in these samples stands for 9 to 14% of the total gold amount.

Thus, although the number of Au^+ ions (determined by XPS) for some materials was comparable and even higher than those found for lanthanum-modified catalysts, strong and stable ions were only found for lanthanum-modified samples, according to the results of the DRIFT CO method.

3.2.5. Study of acid-base properties of catalysts

NH_3-TPD and CO_2-TPD methods were applied to the study of acid and basic properties of the catalysts and their corresponding supports. Three types of acid and basic sites with different concentration and strength (weak, medium and strong), depending on the temperature range where CO_2 or NH_3 desorption

occurs, reflecting their nature, were detected for studied catalysts (Tables 13 and 14).

According to literature [198-206], both basic and acid centers with weak (25 – 200 or 100 – 200 °C) and medium strength (200 – 400 °C) are usually associated with surface hydroxyl groups, i.e., the Brønsted basic centers (BBC) and Brønsted acid centers (BAC). Strong acid centers (400 – 600 °C) along with protonated sites (hydroxyl groups) can also have aprotic nature and represent Lewis acid centers (LAC), which could include cations of gold, or titanium or modifiers in the studied $Au/M_xO_y/TiO_2$ catalysts. Strong basic centers (400 – 600 °C) are associated with low-coordinated oxygen anions or surface hydroxyl groups.

Study of acid properties by TPD method of ammonia

The TPD of NH_3 was used to determine the acidity of supports and respective gold catalysts, namely the concentration and strength of acid sites (Table 13). Physical adsorption can take place in preparation of ammonia TPD, its desorption being, however, typical of low temperatures. Therefore, to avoid the contribution of physical adsorption, the analysis started at 100 °C.

Table 13. Acidic properties of catalysts and their corresponding supports.

Entry	Sample	Concentration of acid centers, μmol/g			
		Weak	Medium	Strong	Total amount
1	TiO_2	208	79	30	317
2	Fe_2O_3/TiO_2		**244**		244
3	CeO_2/TiO_2	146	43	55	244
4	MgO/TiO_2		**201**		**201**
5	La_2O_3/TiO_2	145	43	4	192
6	0.5% $Au/TiO_2\_pH_2$	100	313	110	523
7	0.5% $Au/TiO_2\_pO_2$	167	250	337	754
8	4% $Au/TiO_2\_pH_2$	264	81	8	353
9	4% $Au/TiO_2\_pO_2$	260	66	9	335
10	0.5% $Au/CeO_2/TiO_2\_pH_2$	149	188	299	636
11	0.5% $Au/CeO_2/TiO_2\_pO_2$	108	293	269	670
12	4% $Au/CeO_2/TiO_2\_pH_2$	228	164	37	429
13	4% $Au/CeO_2/TiO_2\_pO_2$	194	86	32	312
14	0.5% $Au/Fe_2O_3/TiO_2\_pH_2$	86	114	41	241
15	0.5% $Au/Fe_2O_3/TiO_2\_pO_2$	189	440	234	863
16	4% $Au/Fe_2O_3/TiO_2\_pH_2$	298		54	352
17	4% $Au/Fe_2O_3/TiO_2\_pO_2$	176	398	320	894
18	0.5% $Au/MgO/TiO_2\_pH_2$	108	69	17	194
19	0.5% $Au/MgO/TiO_2\_pO_2$	203	177	36	416
20	4% $Au/MgO/TiO_2\_pH_2$	262		65	327
21	4% $Au/MgO/TiO_2\_pO_2$	369		67	436
22	0.5% $Au/La_2O_3/TiO_2\_pH_2$	208	50	78	336
23	0.5% $Au/La_2O_3/TiO_2\_pO_2$	217	81	100	398
24	4% $Au/La_2O_3/TiO_2\_pH_2$	63	58	103 83	307
25	4% $Au/La_2O_3/TiO_2\_pO_2$	119	123	73	315

Three types of acid sites were detected for the supports, but their concentration and strength were different (Table 13). The pristine titania showed

the highest acidity among the used supports with the majority of acid sites being of weak strength, while the concentrations of the medium and strong acid sites were 2.6 and 6.9-fold lower than the weaks ones. Therewith, they were all Brønsted acid sites (acidic OH groups) [198-201]. However, it is possible that the strong acid sites were of aprotic nature and were Lewis acid sites (e.g., tetrahedral coordinated Ti^{4+}) [198, 202]. Modification of titania with ceria and lanthana led to a decrease in the concentration of weak and medium acid sites. Alongside, the amount of strong acid sites increased for Ce-modified titania but decreased for La-modified titania.

Because of the broad ammonia desorption peak found in TPD profiles of magnesium and iron modified supports, it became problematic to determine the concentration of sites of certain strengths for these materials. However, it can be seen that the total number of acid sites for Fe and Mg-modified supports (244 and 201 μmol/g, respectively) decreased in comparison to pristine titania. Considering that these maxima are shifted to the low-temperature region, it can be assumed that most of acid sites belong preferentially to sites with weak and medium strength (maxima at 200 and 230 °C).

Such decrease in the concentration of acid sites, after modification of titania with metal oxides, is most likely a consequence of surface dehydration after calcination at 550 °C during preparation.

It should be noted separately that, in the case of CeO_2/TiO_2 and Fe_2O_3/TiO_2, partly medium and strong acid sites can be associated with the desorption of ammonia from aprotic Lewis sites due to the presence of Ce^{4+}/Ce^{3+} and $Fe^{3+,2+}/Fe^{2+}$, respectively, whose existence was indirectly confirmed by TPR (Figures 6 b and c).

After gold deposition, in all cases, there was a redistribution of acid sites.

For 0.5% $Au/TiO_2\_pO_2$ and 0.5% $Au/TiO_2\_pH_2$ catalysts, a significant increase in concentration of medium and strong sites was observed, while the number of sites with weak strength decreased in comparison to the pure titania support. For unmodified samples with 4% Au, an opposite behaviour in the distribution of acid sites was found: increasing of weak and decreasing of strong acid sites, however, the amount of medium sites was almost unchanged.

For Ce-modified catalysts with 0.5% Au, regardless of the pretreatment, there was an increase in the concentration of medium and strong acid sites, while weak sites remained unchanged for 0.5% $Au/CeO_2/TiO_2\_pH_2$ and decreased for 0.5% $Au/CeO_2/TiO_2\_pO_2$. For samples with 4% Au, after both pretreatments, the amount of weak and medium sites was increased, however, as in the case of unmodified samples, the concentration of strong acid sites decreased after gold deposition on ceria support.

For all Fe-modified catalysts, there was increased amount of weak and medium sites, with the exception of 0.5% $Au/Fe_2O_3/TiO_2\_pH_2$, in comparison

with Fe_2O_3/TiO_2. Meanwhile, a high amount of strong sites was found on 0.5% $Au/Fe_2O_3/TiO_2\_pO_2$ and 4% $Au/Fe_2O_3/TiO_2\_pO_2$.

Almost the same behavior in acid sites alteration was observed after gold loading on MgO/TiO_2: increase in the amount of weak and medium sites with the exception of 0.5% $Au/MgO/TiO_2\_pO_2$. However, the same concentration of strong acid sites was found for 4% $Au/MgO/TiO_2\_pH_2$ and 4% $Au/MgO/TiO_2\_pO_2$, while for 0.5% $Au/MgO/TiO_2\_pH_2$ and 0.5% $Au/MgO/TiO_2\_pO_2$, the amount of these sites was 2 and 4-fold lower, respectively, then in the higher gold loading samples.

An increase of medium and especially strong acid sites was found for lanthana-modified catalysts, where concentration significantly augmented 18 to 47-fold in all samples, regardless of the gold content and pretreatment atmosphere. Meanwhile, the increased amount of weak acid sites was found in 0.5% Au samples, while for 4% Au catalysts, especially 4% $Au/La_2O_3/TiO_2\_pH_2$, these sites decreased in comparison to the La_2O_3/TiO_2 support.

In general, there was an increase in the total acidity after gold deposition almost for all samples, and the following order of acid properties in terms of support was found: $Au/La_2O_3/TiO_2 < Au/MgO/TiO_2 < Au/CeO_2/TiO_2 < Au/TiO_2 < Au/Fe_2O_3/TiO_2$.

Such changes in acidity after metal deposition may originate from several causes. One can be associated with a change in the support properties during catalyst preparation resulting in the mutual influence of the support and the metal precursor, as previously discussed [198, 207-209]. Another possibility is blocking the acid sites, previously existing on the surface, by newly formed metal nanoparticles, as well as the formation of new sites due to metal-support interaction.

It should be also noted that due to the presence of Au^+/Au^{3+} ions, found by H_2-TPR, XPS and DRIFT CO in the samples, some of the strong acid sites (37-639 μmol/g) could also be associated with the desorption of ammonia from gold cations, which are Lewis acid sites.

Study of basic properties by TPD method of carbon dioxide

All types of basic sites mentioned above were present in the supports studied in this work (Table 14). Pristine titania exhibited an average total basicity among the studied supports, with the dominance of the basic sites of medium strength and almost absence of strong sites. A similar distribution of the basic sites was also observed for Ce modified titania, while the amount of these sites was lower. MgO/TiO_2 and especially Fe_2O_3/TiO_2 have abundance of basic sites with medium strength among all supports, while MgO/TiO_2 has the highest concentration of weak sites. The amount of strong basic sites was increased 1.6 and 2 times after modification of titania with MgO and Fe_2O_3, respectively. After

modification of titania by lanthana, there was an increase in the concentration of weak and especially strong basic sites (by 3.4 times), while the number of medium sites remained almost unchanged.

Gold deposition on the support surface led to a redistribution of the basic sites similar to that of the acidic ones (Table 14). For almost all studied catalysts, there was an increase in the number of basic sites while, in all cases, the strong basic sites increased.

For unmodified catalysts, similar redistribution of acid sites was observed upon Au loading for 0.5% Au/TiO_2_pO_2 and 4% Au/TiO_2_pO_2: increasing of weak and strong sites with decreasing of medium centers. In case of 0.5% Au/TiO_2_pH_2, the amount of sites with weak and medium strength was increased, while, in contrast, for 4% Au/TiO_2_pH_2, the concentration of these sites decreased.

Increase of weak and strong sites with decrease of medium centers was observed for ceria-modified samples with 0.5% Au after both treatments. Meanwhile, weak and medium sites increased in 4% Au/CeO_2/TiO_2_pH_2 catalyst, and decreased for 4% Au/CeO_2/TiO_2_pO_2.

Almost for all iron-modified catalysts, there was a significant increase of all type of sites, especially weak and medium ones (3-fold) in case of hydrogen treated samples.

Table 14. Basic properties of catalysts and their corresponding supports.

Entry	Sample	Concentration of basic centers, μmol/g			
		Weak	Medium	Strong	Total amount
1	TiO_2	29	51	5	85
2	Fe_2O_3/TiO_2	50	72	8	130
3	CeO_2/TiO_2	27	40	3	70
4	MgO/TiO_2	115	66	10	**191**
5	La_2O_3/TiO_2	56	46	17	119
6	0.5% Au/TiO_2_pH_2	40	66	15	121
7	0.5% Au/TiO_2_pO_2	46	20	13	79
8	4% Au/TiO_2_pH_2	15	41	17	73
9	4% Au/TiO_2_pO_2	34	29	21	84
10	0.5% Au/CeO_2/TiO_2_pH_2	31	23	15	69
11	0.5% Au/CeO_2/TiO_2_pO_2	35	23	16	74
12	4% Au/CeO_2/TiO_2_pH_2	60	63	31	154
13	4% Au/CeO_2/TiO_2_pO_2	20	31	24	75
14	0.5% Au/Fe_2O_3/TiO_2_pH_2	22 121	130	21	294
15	0.5% Au/Fe_2O_3/TiO_2_pO_2	37	91	47	175
16	4% Au/Fe_2O_3/TiO_2_pH_2	33 138	180	23	374
17	4% Au/Fe_2O_3/TiO_2_pO_2	20	74	30	124
18	0.5% Au/MgO/TiO_2_pH_2	23 163	126	32	344
19	0.5% Au/MgO/TiO_2_pO_2	44	38	26	108
20	4% Au/MgO/TiO_2_pH_2	23 78	66	69	236
21	4% Au/MgO/TiO_2_pO_2	51	41	21	113
22	0.5% Au/La_2O_3/TiO_2_pH_2	52	73	36	161
23	0.5% Au/La_2O_3/TiO_2_pO_2	41	58	60	159
24	4% Au/La_2O_3/TiO_2_pH_2	38	46	76	160
25	4% Au/La_2O_3/TiO_2_pO_2	22	38	32	92

For 0.5% Au/MgO/TiO_2_pO_2, 4% Au/MgO/TiO_2_pH_2 and 4% Au/MgO/TiO_2_pO_2 samples, there was a decrease of weak and medium sites, while an increase of these sites was found for 0.5% Au/MgO/TiO_2_pH_2. Increasing of strong acid sites was observed for all Mg-modified materials, especially for 4% Au/MgO/TiO_2_pH_2.

Almost the same trend in basic sites change was found for La-modified samples, as in Mg-modified materials. However, it should be mentioned that La-modified catalysts, especially 0.5% Au/La_2O_3/TiO_2_pO_2 and 4% Au/La_2O_3/TiO_2_pH_2, have the largest amount of strong basic sites among all materials.

The following order of basic properties (total basicity) in terms of support is found: Au/TiO_2 < Au/CeO_2/TiO_2 < Au/La_2O_3/TiO_2 < Au/MgO/TiO_2 < Au/Fe_2O_3/TiO_2. Therefore, higher amounts of basic sites are found in magnesium and iron-modified catalysts.

The reasons for the changes in basicity after gold deposition are apparently the same as for acidity, as they originate from the exposure of the support to the metal precursor during preparation, mutual influence of the support and the precursor, and basic sites blocking. Redistribution may also be due to the exchange of electrons between gold and the support, new metal-oxide pairs and low-coordination oxygen anions appear [198].

Predominance of basic sites with weak and medium strength observed only for Au/MgO/TiO_2 and especially for Au/Fe_2O_3/TiO_2 catalysts is likely caused by formation of the hydroxides due to the interaction with water during catalyst preparation, providing hydroxyl groups [173-175, 210].

It should be noted that one cannot say unambiguously that the newly formed OH groups, due to the transformation of magnesium and iron oxides to hydroxides, have only a basic character ($OH^{\delta-}$), since one can not exclude that some of them may have acidic character ($OH^{\delta+}$) as well.

Comparison of the catalytic and acid-base properties results

Since in case of 1-phenylethanol oxidation only one product (acetophenone) is formed, the acid-base properties (Table 13 and 14) can be compared with the catalytic results using n-octanol as an example. The oxidation of n-octanol can proceed along two paths (Scheme 2), resulting in two final products, namely acid or ester (see Section 3.3.1).

It is known that the esterification reaction is catalyzed by H^+. On the catalyst surface, most likely, the Brønsted acid centers act as the source of H^+. At the same time, the formation of acid requires the presence of water, which on the catalyst surface, can be in the form of pairs of Brønsted basic and acid centers (BBC and BAC), not excluding adsorbed water, which in turn, can dissociate on the catalyst surface with the formation of a pair of BBC and BAC. Accordingly, both

acidic and basic Brønsted centers must be present on the surface of the catalyst for the reaction to proceed along route A, including the esterification reaction (Scheme 2). In turn, mainly BAC should be on the surface of the catalyst for the reaction to proceed along route B.

Concerning the studied catalysts, no direct correlation was found between the acid-base properties, determined by the TPD methods of ammonia and CO_2, and the selectivity for acid or ester (Table 15). This is most likely due to a combination of a number of factors, namely, different activity of the catalysts, as well as the presence of trivalent gold and metallic gold. The adsorption of the solvent on trivalent gold and metallic gold causes not only the deactivation of the catalyst, but also a change in selectivity, which leads to disconformities between the acid-base properties and ester and/or acid selectivity. In addition, some features of desorption methods for determining acid-base properties, in particular TPD of ammonia and CO_2 can also contribute to the discrepancy.

Firstly, one should take into account the different temperatures: in this case, that of tests of oxidation of n-octanol (T = 80 °C) and the temperature range at which TPD study is carried out (CO_2 desorption starts at 25 °C while NH_3 desorption starts at 100 °C, to exclude the contribution of ammonia's physical adsorption). It should also be noted that mainly due to this reason only the concentrations of weak acid and basic centers are taken into account. It is also well known that strong BAC and BBC are active participants in the catalytic process only at elevated temperatures (high-temperature gas-phase reactions).

Table 15. Acid-base properties of Au/(M_xO_y)/TiO_2 catalysts and product selectivity for n-octanol aerobic oxidation on them.

Entry	Catalyst	Concentration of weak centers, μmol/g		BAC/BBC	Selectivity after 6 h, %	
		Acid	Basic		Ester	Acid
1	0.5% Au/TiO_2_pH_2	100	46	2.2	12	39
2	0.5% Au/TiO_2_pO_2	167	56	3.0	20	52
3	4% Au/TiO_2_pH_2	264	15	18	16	3
4	4% Au/TiO_2_pO_2	260	34	7.6	42	3
5	0.5% Au/CeO_2/TiO_2_pH_2	86	31	2.8	20	54
6	0.5% Au/CeO_2/TiO_2_pO_2	108	35	3.0	30	43
7	4% Au/CeO_2/TiO_2_pH_2	298	60	5.0	32	2
8	4% Au/CeO_2/TiO_2_pO_2	194	20	9.7	63	2
9	0.5% Au/Fe_2O_3/TiO_2_pH_2	86	143	0.6	17	29
10	0.5% Au/Fe_2O_3/TiO_2_pO_2	189	37	5.1	43	21
11	4% Au/Fe_2O_3/TiO_2_pH_2	298	171	1.7	42	0
12	4% Au/Fe_2O_3/TiO_2_pO_2	176	20	8.8	51	1
13	0.5% Au/MgO/TiO_2_pH_2	108	185	0.6	16	**53**
14	0.5% Au/MgO/TiO_2_pO_2	203	44	4.6	42	20
15	4% Au/MgO/TiO_2_pH_2	262	101	2.6	31	2
16	4% Au/MgO/TiO_2_pO_2	369	51	7.2	42	0
17	0.5% Au/La_2O_3/TiO_2_pH_2	208	52	4.0	48	24
18	0.5% Au/La_2O_3/TiO_2_pO_2	217	41	5.3	63	11
19	4% Au/La_2O_3/TiO_2_pH_2	262	38	6.9	64	0
20	4% Au/La_2O_3/TiO_2_pO_2	119	22	5.4	75	0

Secondly, the probe molecules can change the chemical properties of the surface due to chemical transformations. Representative examples are: ammonia dissociation at elevated temperatures on NH_2^- and H^+, giving false centers [211], in addition, as was shown by several authors [212, 213], a carbon dioxide molecule adsorbed on small gold nanoparticles can react with gold at room temperature (i.e., oxidize metallic gold: $2Au^0 + CO_2 \rightarrow Au^+–O^{2-}–Au^+ + CO$), and, accordingly, provide new basic sites, not directly related to the catalyst.

Thirdly, the probe molecules do not coincide in size with the reagent molecules and there will always remain the question of comparing the results of measuring acidity (basicity) and catalytic behavior.

Lastly, the TPD methods of NH_3 and CO_2 give information only about the strength and concentration of acid and basic centers, but not about their nature (Brønsted acid centers, Brønsted basic centers, Lewis acid centers and Lewis basic centers).

Nevertheless, for most of the studied systems, except for samples with a high content of Au^{3+} (0.5% $Au/Fe_2O_3/TiO_2\_pH_2$, 4% $Au/Fe_2O_3/TiO_2\_pH_2$ and 4% $Au/MgO/TiO_2\_pH_2$) there is a general tendency in the selectivity for acid and/or ester, depending on the acid-base properties of the catalysts (Table 15), namely:

For catalysts with 0.5% Au, acid and ester are observed in the reaction products, and the higher the ratio of BAC to BBC, the higher ester formation. For example, 0.5% $Au/TiO_2\_pH_2$ and 0.5% Au/TiO_2_pO, 0.5% $Au/CeO_2/TiO_2\_pH_2$ and 0.5% $Au/CeO_2/TiO_2\_pO_2$, exhibited BAC/BBC ≤ 3 and their selectivity to ester did not exceed 30% and acid prevailed in the reaction products. Meanwhile, 0.5% $Au/Fe_2O_3/TiO_2\_pO_2$ and 0.5% $Au/MgO/TiO_2\_pO_2$, 0.5% $Au/La_2O_3/TiO_2\_pO_2$ and 0.5% $Au/La_2O_3/TiO_2\_pH_2$, with BAC/BBC > 4.5 gave ester selectivity higher than 40%. Also, it can be concluded that, since octanoic acid was observed in the products for all catalysts with low gold content, the reaction proceeds along route A (Scheme 2).

There is a significant predominance of BAC compared to BBC for samples with 4% Au (BAC/BBC > 5.4), where the acid formation does not exceed 3%. Thus, one can assume that the reaction on these catalysts proceeds mainly along acid-free route B (Scheme 2). Therefore, using catalysts with 4% Au, an octyl octanoate is formed, its selectivity being higher for materials with an oxidative pretreatment.

3.2.6. Study of oxygen chemisorption

The analysis of the XPS of O 1s peak was used to investigate oxygen species on catalyst surface, since they can play a special role in oxidation reaction.

The O 1s spectra (Figure 15) is asymmetrical for almost all studied catalysts, with a tail extending towards higher energies, that is typical of titania based

catalysts [211]. Exceptions were Fe-modified samples after hydrogen treatment (Figure 15 i and k) that have a different band shape.

For all studied catalysts, the O 1s peak can be deconvoluted into three bands: first at BE 530–531 eV (denoted as O_I), associated with the lattice oxygen O^{2-}; second at BE 531–532 eV (denoted as O_{II}), associated with the low coordination oxygen species O^-, surface defects/vacancies; and third at BE 532–534 eV (denoted as O_{III}) assigned to hydroxyl groups carbonate species and/or adsorbed water [214-219].

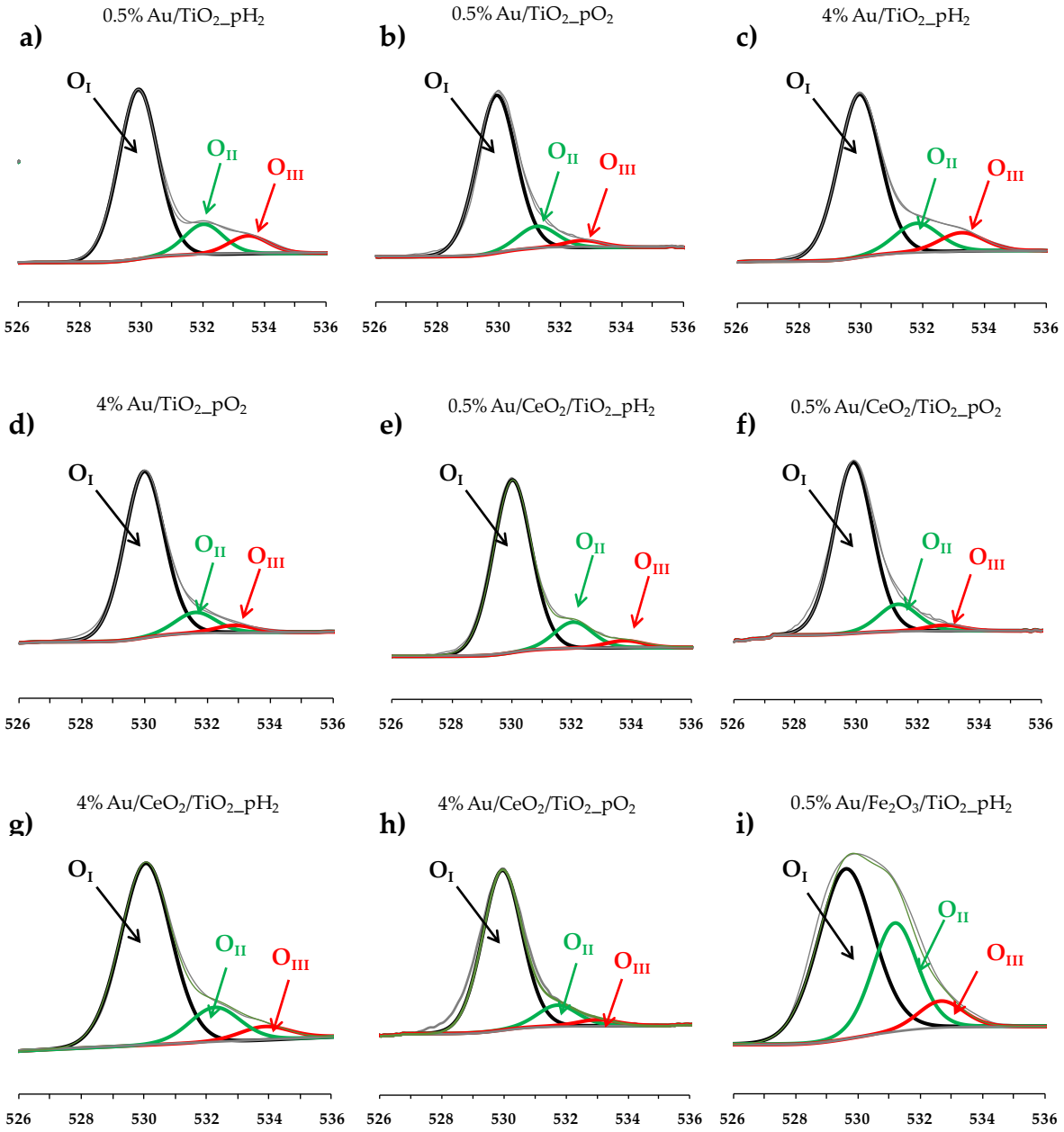

Figure 15. *Cont.*

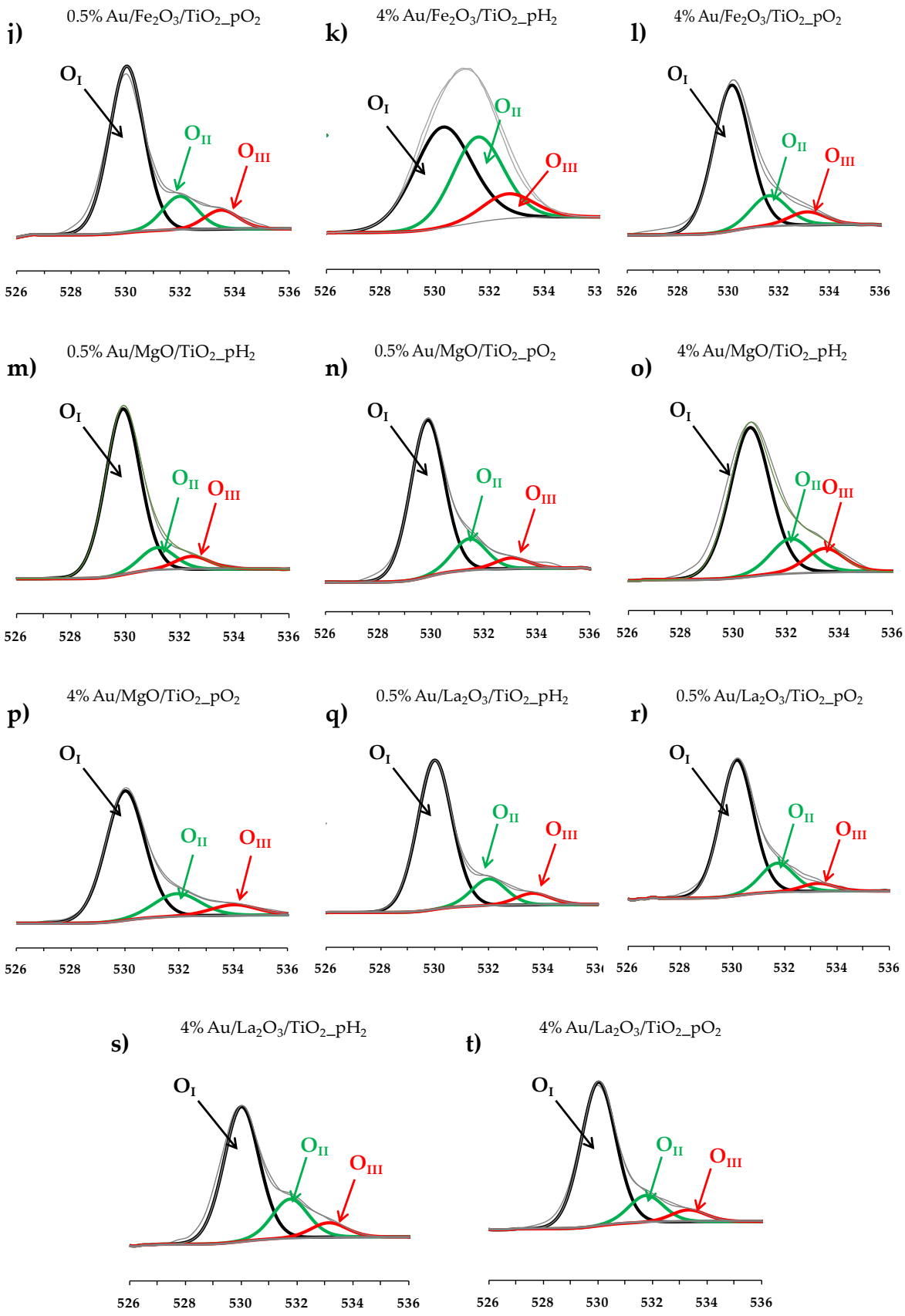

Figure 15. O 1s XP spectra of samples with different gold contents (0.5 or 4 wt.%), pretreated in H_2 or O_2 flow, at 300 °C, for 1 h: Au/TiO_2 (**a–d**), $Au/CeO_2/TiO_2$ (**e–h**), $Au/Fe_2O_3/TiO_2$ (**i–l**), $Au/MgO/TiO_2$ (**m–p**) and $Au/La_2O_3/TiO_2$ (**q–t**).

Surface chemisorbed oxygen O^-, species of O_{II} group, is very active in oxidation reactions because its mobility is higher than that of lattice oxygen (O_I) [220], and the high activity could be correlated with the high content of chemisorbed oxygen on the catalyst surface. The relative contribution of each oxygen species and the $O_{II}/(O_I + O_{II})$ ratios are presented in Table 16. According to these results, the O_{II} contribution of the catalysts shows the following order: $Au/TiO_2 < Au/CeO_2/TiO_2 < Au/MgO/TiO_2 \leq Au/La_2O_3/TiO_2 < Au/Fe_2O_3/TiO_2$.

Thus, a higher amount of species related to O_{II} is observed in La-, Mg-, and notably in Fe-modified catalysts, compared to unmodified and Ce-modified samples. Significant contribution of O_{II} in Fe-modified catalysts may be caused by predominant hydroxyl groups (which presence was determined with CO_2-TPD and NH_3-TPD) from $Fe(OH)_2$, and/or FeOOH (its transformation was observed in TPR profiles at 336 °C, Figure 6 c) [221]. In case of Mg-modified samples, part of O_{II} can also be attributed to OH groups, due to the fact that magnesium oxide can be transformed into hydroxide and there is an increase in acidic and/or basic sites after the deposition of gold on Mg/TiO_2, according to CO_2-TPD and NH_3-TPD results.

Table 16. Contribution of oxygen species calculated by XPS for the studied catalysts.

Entry	Catalyst	O 1s relative content, %			
		O_I (530 – 531) BE	O_{II} (531 – 532) BE	O_{III} (532 – 534) BE	$O_{II}/O_{II}+O_I$
1	0.5% $Au/TiO_2\_pH_2$	78	14	8	15
2	0.5% $Au/TiO_2\_pO_2$	85	12	3	12
3	4% $Au/TiO_2\_pH_2$	76	15	9	15
4	4% $Au/TiO_2\_pO_2$	85	11	4	12
5	0.5% $Au/CeO_2/TiO_2\_pH_2$	84	13	3	13
6	0.5% $Au/CeO_2/TiO_2\_pO_2$	85	13	2	13
7	4% $Au/CeO_2/TiO_2\_pH_2$	79	15	6	16
8	4% $Au/CeO_2/TiO_2\_pO_2$	87	10	3	10
9	0.5% $Au/Fe_2O_3/TiO_2\_pH_2$	61	31	8	34
10	0.5% $Au/Fe_2O_3/TiO_2\_pO_2$	76	15	9	16
11	4% $Au/Fe_2O_3/TiO_2\_pH_2$	51	38	11	43
12	4% $Au/Fe_2O_3/TiO_2\_pO_2$	83	15	2	15
13	0.5% $Au/MgO/TiO_2\_pH_2$	82	11	7	12
14	0.5% $Au/MgO/TiO_2\_pO_2$	79	16	5	17
15	4% $Au/MgO/TiO_2\_pH_2$	69	19	12	22
16	4% $Au/MgO/TiO_2\_pO_2$	76	16	8	17
17	0.5% $Au/La_2O_3/TiO_2\_pH_2$	80	14	6	15
18	0.5% $Au/La_2O_3/TiO_2\_pO_2$	78	17	5	18
19	4% $Au/La_2O_3/TiO_2\_pH_2$	71	21	8	22
20	4% $Au/La_2O_3/TiO_2\_pO_2$	79	15	6	16

Based on the chemical nature (properties) of lanthanum oxide, one can assume that the O_{II} contribution in La-modified samples can be mostly related to the low-coordinated oxygen (O^- species), which are strong basic sites. These samples, notably 0.5% $Au/La_2O_3/TiO_2\_pO_2$ and 4% $Au/La_2O_3/TiO_2\_pH_2$, showed the highest concentration of O^- species among all samples, as determined by CO_2-TPD. At the same time, weak and medium Brønsted basic centers ($OH^{\delta-}$) in

La-modified samples were found by CO_2-TPD in moderate amounts, in contrast to the larger OH amount in Mg- and Fe-modified catalysts.

Thus, it can be concluded that the highest contribution of surface chemisorbed oxygen O^- was found in La-modified samples, while the increased content of O_{II} in Mg- and Fe-modified catalysts was predominantly associated with the formation of magnesium or iron hydroxides occurring during catalyst preparation.

Additionally, O_2-TPD was used to assess the nature of the interaction of oxygen with the surface of the catalyst and the support (Figure 16). Since the existence of hydroxides on Mg- and Fe-modified catalysts may contribute to oxygen on the O_2-TPD profiles, thereby giving a false signal, this analysis was used only for unmodified, and Ce- and La-modified materials.

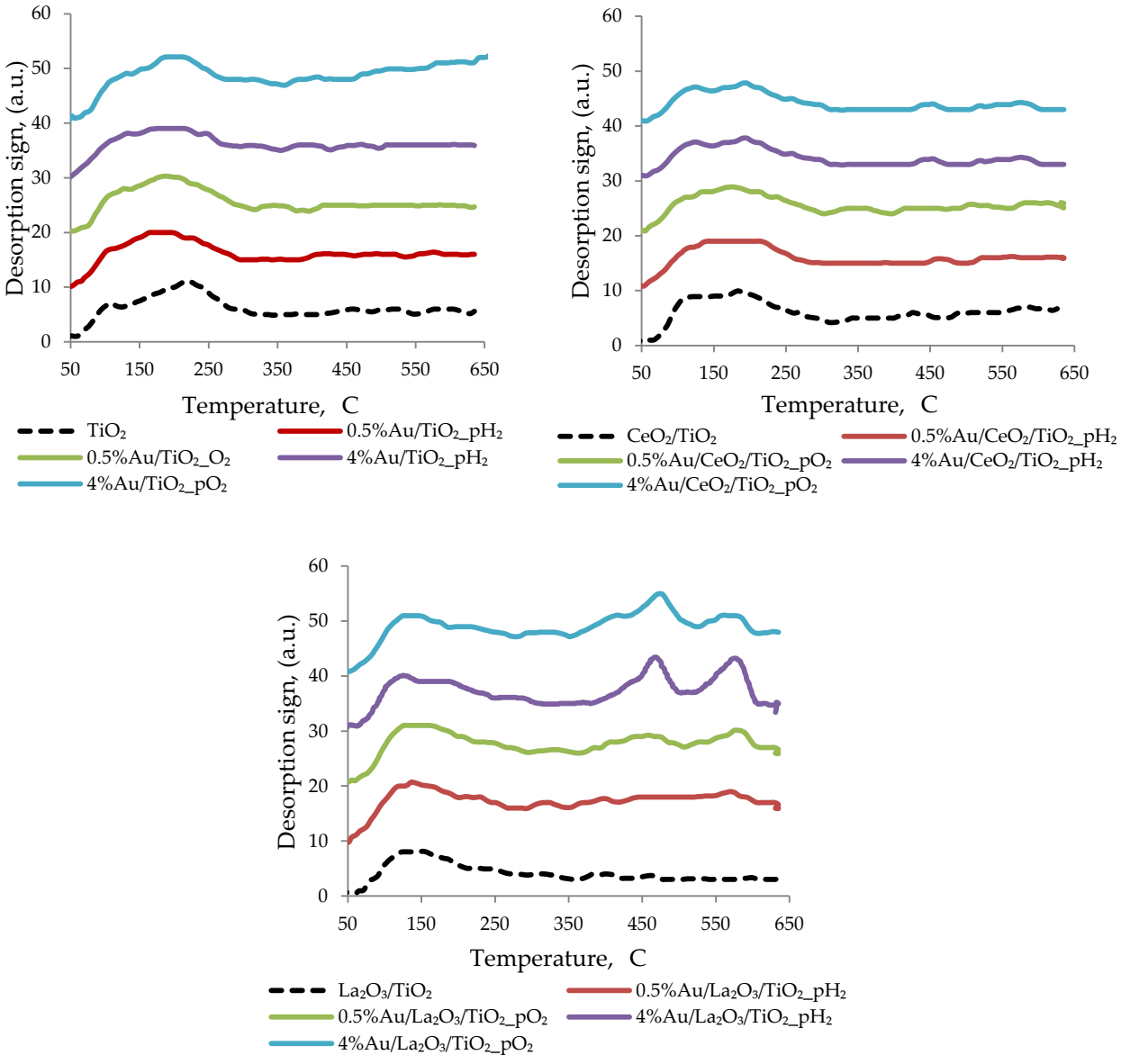

Figure 16. O_2-TPD profiles for Au catalysts supported on TiO_2, CeO_2/TiO_2 and La_2O_3/TiO_2 with different pretreatments and their supports.

The O_2-TPD profiles obtained for the catalysts and their corresponding supports (Figure 16) show the presence of several peaks of oxygen desorption, corresponding to different forms of adsorbed oxygen.

All the catalysts showed a broad peak of oxygen desorption in the range of 50–350 °C, which may be due to the adsorption of O_2^- on TiO_2, according to Yu et al. [222]. It should be noted that pure titania showed three overlapping peaks (at 95, 205 and 292 °C) in this temperature range. After gold deposition on TiO_2, a slight change in the shape of these peaks was observed. After titania was modified with ceria and lanthana, the shape and position of the wide peak in the low-temperature region changed, and overlapping maxima were observed at 100, 190 and 265 °C for CeO_2/TiO_2 and at 110, 230 and 310 °C for La_2O_3/TiO_2.

The deposition of gold on the ceria-modified support did not cause a significant change in the O_2-TPD profiles. However, after the deposition of gold on the surface of La-modified titania, high-temperature peaks appeared in the range of 400–600 °C, and catalysts with 4% Au had a noticeably high intensity, with peaks at 460 and 560 °C. These desorption peaks are likely to occur at higher temperatures and correspond to adsorbed O^- on the surface of TiO_2, as described by different authors [222, 223]. Addition of lanthana and gold effectively stimulate the dissociation of O_2 to O^-, which has a higher activity than the super-oxo form O_2^- in the oxidation reaction [222, 224, 225].

Thus, these results support the previously established favorable features of doping titania with lanthana (formation and stabilization of single charged gold ions through their localization on strong basic sites of La_2O_3/TiO_2). Besides they revealed another promoting role of modifying lanthana additives: providing the most active type of oxygen for effective oxidation of alcohols. This also confirms the conclusions taken from XPS O 1s results for La-modified samples.

SUMMARY

Based on the comparison of catalytic and characterization results, it can be concluded that, despite the different chemical nature of the alcohols studied, mono-charged gold ions seem to be the catalytically active states in the both studied processes, while Au^0 and, especially, Au^{3+} had negative effects. Herein, the concentration, adsorption strength and stability of active sites can be determined by the gold content, the nature of the support and modifier, and the pretreatment atmosphere.

Regardless of the alcohol and the type of oxidizing agent, the best catalytic characteristics were shown by catalysts modified with lanthanum oxide, which possesses electron-donor properties. Notably, the most active catalysts (0.5% $Au/La_2O_3/TiO_2$_pO_2 and 4% $Au/La_2O_3/TiO_2$_pH_2) shared a high concentration of stable monovalent gold ions without the presence of Au^{3+}, and their deactivation in oxidation of n-octanol and 1-phenylethanol was parallel to the

reduction of $Au^{+}(Au^{\delta+})$ states, what confirmed the cationic nature of the active sites.

The only difference was that, in the absence of solvent and using TBHP as an oxidizing agent, the most active catalysts are those with a high load of gold and with hydrogen treatment. In the case of using a solvent and oxygen as oxidizing agent, as in the oxidation of n-octanol, the catalysts with the lowest gold content after oxidative pretreatment showed the highest activity. The reason for such difference is, most likely, the reduction of some part of unstable gold ions to the metallic state in the 0.5% $Au/La_2O_3/TiO_2\_pO_2$ catalyst by electron transfer, under the influence of TBHP (even catalysts in «as prepared state» could provide high activity in 1-phenylethanol oxidation with TBHP after 6 h). Moreover, it was previously shown that 0.5% $Au/La_2O_3/TiO_2\_pO_2$ and 4% $Au/La_2O_3/TiO_2\_pH_2$ have the same contribution of stable gold ions; furthermore, the difference in catalytic activity of 1-phenylethanol oxidation on these catalysts was not so noticeable.

The promoting role of lanthanum additives consists not only in the formation of the most stable Au^{+} $(Au^{\delta+})$ species on the surface of La-modified TiO_2, due to their localization at the strong basic Lewis sites, but also in the presence of the most active type of oxygen, so contributing to a more efficient oxidation of alcohols.

It was found that reaction product distribution, notably, the formation of acid and/or ester, depends on the ratio of Brønsted acid centers to Brønsted basic centers: with a high ratio, no acid is formed; with a low BAC/BBC ratio, selectivity to acid is higher than to ester; intermediate values of BAC/BBC ratio produce a mixture of acid and ester. It should be mentioned that such a trend in the dependence of the selectivity with the BAC/BBC ratio was not observed only for the catalysts with high content of trivalent gold (0.5% $Au/Fe_2O_3/TiO_2\_pH_2$, 4% $Au/Fe_2O_3/TiO_2\_pH_2$ and 4% $Au/MgO/TiO_2\_pH_2$), where mainly the adsorption of solvent occurs.

3.3. Theoretical Calculations

Quantum chemistry simulations were applied to reveal the role of different gold states (active sites and inhibitors) in n-octanol and 1-phenylethanol oxidation.

3.3.1. Quantum chemical simulation of n-octanol adsorption on tetrahedral gold cluster

The n-octanol adsorption was simulated as these reactions:

$$Au_{20} + C_7H_{15}CH_2OH \rightarrow (C_7H_{15}CH_2OH)Au_{20} \quad (3.1)$$

$$Au_{20}^{+} + C_7H_{15}CH_2OH \rightarrow (C_7H_{15}CH_2OH)Au_{20}^{+} \quad (3.2)$$

Different coordinations of alcohol on Au_{20} were considered. The structures of $(C_7H_{15}CH_2OH)Au_{20}$ were optimized, and the total energies of the reagents and products were calculated considering the energy of zero vibrations. The change in total energy and standard enthalpies of the reactions (3.1) and (3.2) at 100 °C were determined according to the formulas:

$$\Delta E_1 = E(\text{octanol-}Au_{20}) - E(Au_{20}) - E(\text{octanol}) \quad (3.3)$$

$$\Delta E_2 = E(\text{octanol-}Au_{20}^{+}) - E(Au_{20}^{+}) - E(\text{octanol}) \quad (3.4)$$

The optimized structures of octanol-Au_{20} complexes with alcohol coordination on different gold atoms are shown in Figure 17. The energy changes during the formation of the complexes and the corresponding standard enthalpies are shown in Table 17.

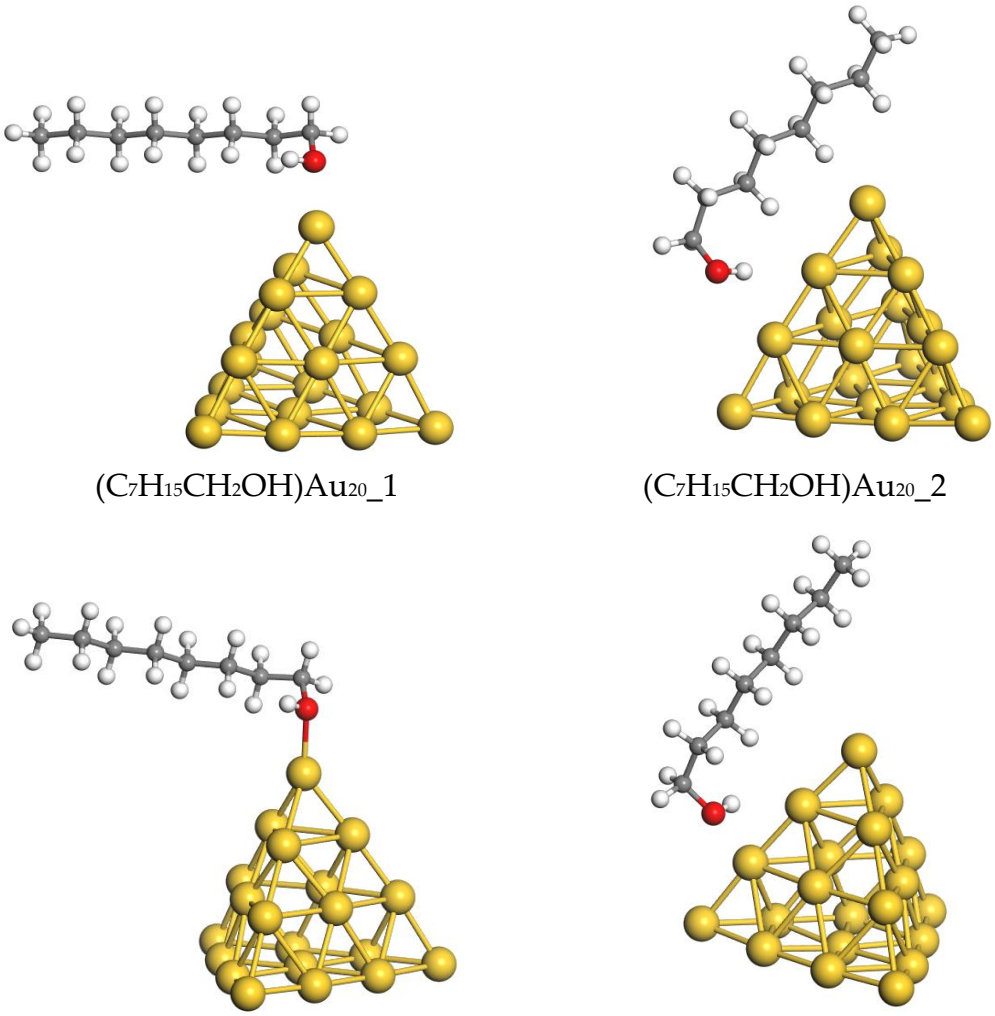

$(C_7H_{15}CH_2OH)Au_{20}$_1 $(C_7H_{15}CH_2OH)Au_{20}$_2

$(C_7H_{15}CH_2OH)Au_{20}^{+}$_1 $(C_7H_{15}CH_2OH)Au_{20}^{+}$_2

Figure 17. Optimized structures of n-Octanol-Au_{20} and n-Octanol-Au_{20}^{+} complexes.

Table 17. Calculated energy change (ΔE, kJ/mol) and standard enthalpy (ΔH, kJ/mol) in reactions (3.1) and (3.2) of n-octanol with Au_{20}^{z} cluster (z=0, +1).

z	Complex	Type of coordination	ΔE_1, ΔE_2	ΔH_1, ΔH_2
0	$(C_7H_{15}CH_2OH)Au_{20}$_1	top	-40	-36
0	$(C_7H_{15}CH_2OH)Au_{20}$_2	edge	-23	-20
+1	$(C_7H_{15}CH_2OH)Au_{20}^{+}$_1	top	-81	-78
+1	$(C_7H_{15}CH_2OH)Au_{20}^{+}$_2	edge	-55	-51

Optimization of octanol-Au_{20} complex, in which alcohol is coordinated on the facet of the cluster, led to the $(C_7H_{15}CH_2OH)Au_{20}$_2 complex with edge coordination. The OH group is involved in the interaction of the alcohol and the cluster. The calculated Au-O distances are 0.243 nm and 0.338 nm in $(C_7H_{15}CH_2OH)Au_{20}$_1 and $(C_7H_{15}CH_2OH)Au_{20}$_2, respectively. According to the calculated data, the most favorable coordination of n-octanol on Au_{20} is at the cluster's top. The binding energy of alcohol on the edge atoms is significantly lower.

Optimized structures of octanol-Au_{20}^{+} have features similar to those of neutral octanol-Au_{20}. In contrast, the calculated energy changes in reaction 3.2 (Table 17) are larger than in reaction 3.1. Binding energy of n-octanol with low-coordinated cationic gold atoms through OH group is twofold as much than that of low-coordinated gold atoms of neutral cluster. So, it can be concluded that the cationic sites play an important role in n-octanol activation on gold nanoparticles.

Thus, it was shown that the low-coordinated gold atoms on the clusters top are the most active in the activation of n-octanol. Binding energy of n-octanol with low-coordinated cationic gold atoms is sufficiently higher than on the neutral cluster. Therefore, based on the quantum chemistry, it can be concluded that the cationic sites play an important role in n-octanol adsorption.

3.3.2. Quantum chemical simulation of n-heptane adsorption on Au^0, Au^+ and Au^{+3}

To reveal which gold sites act as inhibitors of the catalytic reaction, a quantum chemical simulation of the adsorption of a solvent (heptane) on simple models containing Au^0, Au^+ and Au^{3+} was performed. $(Au^0O)^{2-}$, $(Au^+O)^-$ and $(Au^{3+}O)^+$ molecules were considered as models. Optimized structures of C_7H_{16}-$(Au^0O)^{2-}$, C_7H_{16}-$(Au^+O)^-$ and C_7H_{16}-$(Au^{3+}O)^+$ complexes and calculated values of adsorption energies are presented in Figure 18.

C_7H_{16} adsorption was simulated through reactions 3.5-3.7:

$$(Au^0O)^{2-} + C_7H_{16} \rightarrow (Au^0O)^{2-} \quad (3.5)$$

$$(Au^+O)^- + C_7H_{16} \rightarrow C_7H_{16}\text{-}(Au^+O)^- \quad (3.6)$$

$$(Au^{3+}O)^+ + C_7H_{16} \rightarrow C_7H_{16}\text{-}(Au^{3+}O)^+ \quad (3.7)$$

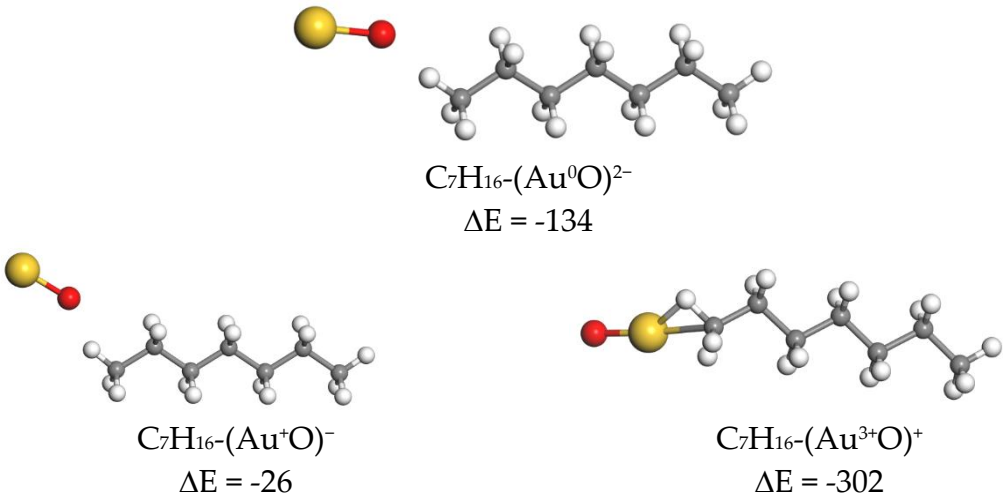

Figure 18. Optimized structures of C_7H_{16}-$(Au^0O)^{2-}$, C_7H_{16}-$(Au^+O)^-$ and C_7H_{16}-$(Au^{+3}O)^+$. Calculated adsorption energies are given in kJ/mol.

Heptane can interact with $(Au^0O)^{2-}$ with an adsorption energy of -134 kJ/mol. This suggests that the Au^0 sites may be partially occupied by solvent molecules. In contrast, heptane forms the most stable complex with $(AuO)^+$, in which gold is Au^{3+} state. The calculated adsorption energy in C_7H_{16}-$(Au^{3+}O)^+$ is -302 kJ/mol.

Therefore, using small models of active sites containing Au^0, Au^+ and Au^{3+}, it was shown that $(Au^{3+}O)^+$ cations can strongly bind heptane.

3.3.3. Quantum chemical simulation of phenylethanol adsorption on a gold cluster

The following issues, related to the nature of the active sites of the gold nanoparticles in the activation of phenylethanol at the atomic level, were considered in this section:

(*i*) Which coordination of phenylethanol to the gold cluster is preferred: by OH– or by C_6H_5– groups?
(*ii*) How do the structural features of the catalyst surface, including availability of low coordinated gold atoms, affect the adsorption of the alcohol?
(*iii*) What is the effect of gold cationic sites on alcohol activation?

The interaction of two phenylethanols with Au_{20} cluster was simulated:

$$Au_{20} + CH_3–CH(OH)–Ph \rightarrow (CH_3–CH(OH)–Ph)Au_{20} \quad (3.8)$$

$$Au_{20} + OH–CH_2–CH_2–Ph \rightarrow (HO–CH_2–CH_2–Ph)Au_{20} \quad (3.9)$$

Different coordination modes of alcohol on Au_{20} by the OH group or the phenyl fragment were considered. The structures of $(HO–CH_2–CH_2–Ph)Au_{20}$ isomers were optimized, and the total energies of the reagents and products were calculated considering the energy of zero vibrations.

The change in total energy and standard enthalpies of the reaction (3.8) were determined according to the formula:

$$\Delta E = E(\text{phenylethanol–Au}_{20}) - E(\text{Au}_{20}) - E(\text{phenylethanol}) \quad (3.10)$$

The optimized structures of phenylethanol-Au_{20} complexes, in which the alcohol is coordinated to a gold atom by the OH group, are shown in Figure 19. The energy changes during the formation of the complexes and the corresponding standard enthalpies are collected in Table 18.

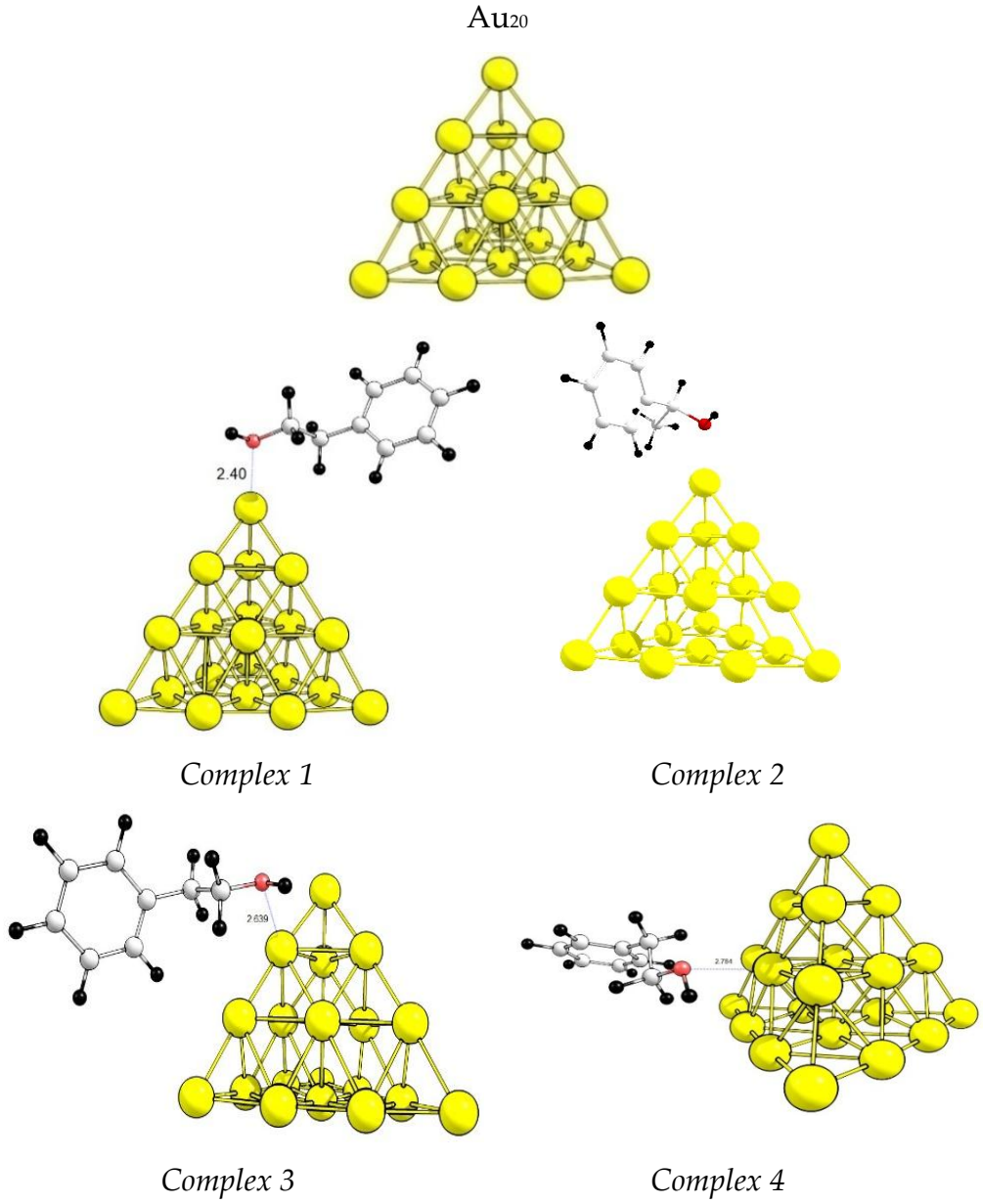

Figure 19. Optimized structures of Au_{20} clusters and phenylethanol-Au_{20} complexes (coordination by OH group).

According to the calculated data, the most favorable coordination during the interaction of phenylethanols with Au_{20} is carried out at the top of the cluster. Both 1-phenylethanol and 2-phenylethanol bind to the top gold atom with

similar values of adsorption energy (57–60 kJ/mol). The binding energies of alcohol on the edge and facet gold atoms are significantly lower (considering 1-phenylethanol as an example).

Table 18. The calculated values of the energy change (Δ*E*, kJ/mol) and standard enthalpy (Δ*H*, kJ/mol) in the reactions of 1-phenylethanol (3.8) or of 2-phenylethanol (3.9) with the Au_{20}^{z} cluster (z = 0, +1).

z	Complex	Isomer	Type of coordination		Δ*E*	Δ*H*
0	1	2	OH–	top	−57	−54
0	2	1	OH–	top	−60	−57
0	3	2	OH–	edge	−33	−29
0	4	2	OH–	facet	−30	−31
0	5	2	C_6H_5–	top	−49	−45
0	6	2	C_6H_5–	edge	−23	−21
+1	1	2	OH–	top	−97	−92
+1	2	1	OH–	top	−112	−108
+1	3	2	OH–	edge	−75	−70
+1	4	2	OH–	facet	−56	−54
+1	5	2	C_6H_5–	top	−102	−100
+1	6	2	C_6H_5–	edge	−75	−72

When alcohol is coordinated on the cluster through a benzene fragment (Figure 20), the adsorption energies decrease at all sites of Au_{20}, compared to OH– group coordination. Between two different ways of alcohol coordination (OH– or C_6H_5–), coordination by the OH– group is advantageous (Complex 2, Figure 19). In this case, low-coordinated gold atoms are the most active in the activation of alcohol.

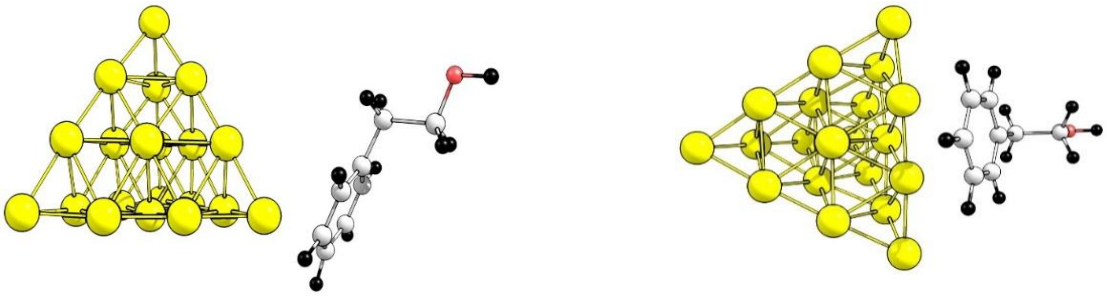

Complex 5 *Complex 6*

Figure 20. Optimized structures of phenylethanol-Au_{20} complexes (coordination by C_6H_5 fragment).

Then, how the gold cationic sites affect alcohol adsorption was examined. The interaction of 1-phenylethanol or 2-phenylethanol with an Au_{20}^{+} cluster was simulated at different coordinations (by the OH group or the phenyl fragment):

$$Au_{20}^{+} + CH_3–CH(OH)–Ph \rightarrow (CH_3–CH(OH)–Ph)Au_{20}^{+} \quad (3.11)$$

$$Au_{20}^{+} + HO–CH_2–CH_2–Ph \rightarrow (HO–CH_2–CH_2–Ph)Au_{20}^{+} \quad (3.12)$$

The optimized structures of phenylethanol-Au_{20}^{+}complexes have similar features with neutral phenylethanol-Au_{20}. In contrast, the calculated energy changes in reaction 3.11 (Table 18) are larger than in reaction 3.8. The binding energy of phenylethanol to low-coordinated cationic gold atoms through the OH– group is significantly higher than on the neutral cluster. When 1-phenylethanol is coordinated by the aromatic ring on Au_{20}^{+}, the adsorption energy increases and becomes almost the same as the coordination of alcohol with the OH group. Thus, it can be concluded that the cationic sites play a decisive role in phenylethanol adsorption.

SUMMARY

Therefore, based on the simulation of adsorption of n-octanol and 1-phenylethanol on Au clusters using DFT calculations, it can be concluded that low-coordinated gold atoms are the most active in the activation of both alcohols. Thus, the cationic sites play an important role in alcohol oxidation, what confirms the suggestions on the gold cationic nature based on the experimental results.

Besides that, based on the quantum chemical calculations, it was revealed that, in case of using heptane as solvent in aerobic oxidation of n-octanol, Au^{0} had negative effect, due to a partial blocking of Au^{0} by the solvent. Au^{3+} also inhibited the oxidation process, due to the strong adsorption of the solvent and/or water formed during the reaction.

CONCLUSIONS

Based on the research results presented in this Thesis, the following conclusions can be drawn:

1. The efficiency of Au/(M_xO_y)/TiO_2 catalysts (where M_xO_y are CeO_2, Fe_2O_3, La_2O_3 or MgO) with different gold contents (0.5 or 4 wt.%), and thermal redox pretreatment conditions (H_2 or O_2), have been investigated in the aerobic and peroxidative oxidation of n-octanol and 1-phenylethanol under mild conditions. It has been found that the catalytic behavior of gold-based systems is primarily determined by the electronic state of the deposited gold; namely, the ratio between the Au^0, Au^+ and Au^{3+} states, which, in turn, is determined by the nature of the support and modifier, pretreatment conditions and gold concentration.

2. The comparative study revealed that, despite the different chemical nature of the studied alcohols and the oxidants used, Au^+ ions play a decisive role in the aerobic and peroxidative oxidation of n-octanol and 1-phenylethanol, and act as the active sites of Au/M_xO_y/TiO_2 catalysts. Au^{3+} ions play an inhibitory role in the oxidation of n-octanol, due to the strong adsorption of the solvent and/or the blocking of highly charged trivalent gold ions by water molecules produced by the reaction. The low catalytic activity of the samples where only metallic gold was detected was probably due to the partial blocking of the Au^0 sites by the solvent that also led to inhibition of the oxidation of n-octanol, as in the case of Au^{3+}.

3. The concentration, stability, and adsorption strength of Au^+ sites are highly dependent on the nature of the support and the pretreatment atmosphere. The strongest and most stable $Au^+(Au^{\delta+})$ states are formed on the surface of La-modified TiO_2 through their localization at strong basic Lewis centers. The promoting role of lanthanum additives also consists in the formation of the most active type of oxygen, contributing to a more efficient oxidation of alcohols. The effects of pretreatment atmosphere and gold concentration are mutually dependent: in the case of Au/La_2O_3/TiO_2 samples, the most stable Au^+ centers were formed after pretreatment in an H_2 atmosphere when gold content was 4 wt.%, but after pretreatment in an O_2 atmosphere when gold content was 0.5 wt.%.

4. The deactivation of the studied catalysts in both reactions is caused by the reduction of a part of the $Au^+(Au^{\delta+})$ states, which confirms the cationic nature of the active site.

5. The functional groups of the support surface (Brønsted and Lewis acid and basic centers) not only act as a tool for the formation and stabilization of Au^+

centers, but also participate in the alcohol conversion process; in particular, they determine the products distribution and selectivity in the oxidation of n-octanol.
6. The catalytic systems based on gold nanoparticles supported on La-modified TiO_2 are promising catalysts for selective liquid-phase oxidation of alcohols with quite different reactivity. This should motivate the interest in future research of their use for the oxidation of more complex, polyfunctional alcohols.

CONCLUSIONES

A partir de los resultados de la investigación presentados en esta Tesis, se pueden extraer las siguientes conclusiones:

1. Se ha investigado la eficiencia de los catalizadores $Au/(M_xO_y)/TiO_2$ (donde M_xO_y son CeO_2, Fe_2O_3, La_2O_3 o MgO) con diferentes contenidos de oro (0,5 o 4% en peso) y condiciones de pretratamiento térmico (H_2 u O_2), en la oxidación aerobia y peroxidativa de n-octanol y 1-feniletanol en condiciones suaves. Se ha encontrado que el comportamiento catalítico de los sistemas a base de oro está determinado principalmente por el estado electrónico del oro depositado; a saber, la proporción entre los estados Au^0, Au^+ y Au^{3+}, que, a su vez, está determinada por la naturaleza del soporte y el modificador, las condiciones de pretratamiento y la concentración de oro.
2. El estudio comparativo reveló que, a pesar de la diferente naturaleza química de los alcoholes estudiados y de los oxidantes empleados, los iones Au^+ juegan un papel decisivo en la oxidación aerobia y peroxidativa del n-octanol y el 1-feniletanol, y actúan como sitios activos de los catalizadores $Au/(M_xO_y)/TiO_2$. Los iones Au^{3+} juegan un papel inhibidor en la oxidación del n-octanol, debido a la fuerte adsorción del solvente y/o al bloqueo de los iones de oro trivalentes altamente cargados por las moléculas de agua producto de la reacción. La baja actividad catalítica de las muestras donde solo se detectó oro metálico probablemente se debió al bloqueo parcial de los sitios Au^0 por el solvente, que también condujo a la inhibición de la oxidación del n-octanol, como en el caso del Au^{3+}.
3. La concentración, estabilidad y fuerza de adsorción de los sitios de Au^+ dependen en gran medida de la naturaleza del soporte y la atmósfera de pretratamiento. Los estados $Au^+(Au^{\delta+})$ más fuertes y más estables se forman en la superficie del TiO_2 modificado con La a través de su localización en centros de Lewis básicos fuertes. El papel promotor del lantano como aditivo también consiste en la formación de un tipo de oxígeno más reactivo, lo que contribuye a una oxidación más eficiente de los alcoholes. Los efectos de la atmósfera de pretratamiento y la concentración de oro son mutuamente dependientes: en el

caso de los catalizadores $Au/La_2O_3/TiO_2$, los centros de Au^+ más estables se formaron tras el pretratamiento en atmósfera de H_2 cuando el contenido de oro fué del 4% en peso, pero tras el pretratamiento en atmósfera de O_2 cuando el contenido de oro fué del 0,5% en peso.

4. La desactivación de los sistemas estudiados en ambas reacciones es causada por la reducción de una parte de los estados $Au^+(Au^{\delta+})$, lo que confirma la naturaleza catiónica del sitio activo;

5. Los grupos funcionales de la superficie de soporte (centros ácidos y básicos de Brønsted y Lewis) actúan no solo como una herramienta para la formación y estabilización de los centros Au^+, sino que también participan en el proceso de la conversión del alcohol; en particular, determinan la distribución de productos y la selectividad en la oxidación de n-octanol.

6. Los sistemas catalíticos basados en nanopartículas de oro soportadas en TiO_2 modificado con La son catalizadores prometedores para la oxidación selectiva en fase líquida de alcoholes de reactividad química bastante diferente. Esto motiva el interés de futuras investigaciones de su uso para la oxidación selectiva de alcoholes polifuncionales más complejos.

ABBREVIATIONS

Au/TiO_2 – unmodified titania-supported gold catalyst;

$Au/M_xO_y/TiO_2$ (M_xO_y = CeO_2, La_2O_3, Fe_2O_3 or MgO) – gold catalyst supported on titania modified with cerium, lanthanum, iron or magnesium oxides;

Au NPs – gold nanoparticles;

BAC – Brønsted acid centers;

BBC – Brønsted basic centers;

BE – Binding energy (eV);

BET – Brunauer–Emmett–Teller theory;

CO_2-TPD – temperature-programmed desorption of carbon dioxide;

C_{OL} – alcohol conversion, mol%;

DRIFT CO – diffuse reflectance infrared Fourier transform spectroscopy of CO adsorption;

DFT – density functional theory;

DP – deposition-precipitation method;

HRTEM – high resolution transmission electron microscopy;

H_2-TPR – temperature-programmed reduction with hydrogen;

LAC – Lewis acid centers;

LBC – Lewis basic centers;

NH_3-TPD – temperature-programmed desorption of ammonia;

O_2-TPD – temperature-programmed desorption of oxygen;

R (A/M) – alcohol/active metal ratio mol/mol;

S_x – selectivity to product x subscripts: (AC, carboxylic acid or acetophenone; AL, aldehyde; ES: ester), mol%;

STEM-HAADF – scanning transmission electron microscopy-high angle annular dark field;

T – reaction temperature;

TBHP, *t*-BuOOH – tert-butyl hydroperoxide;

XRD – X-ray diffraction;

XPS – X-ray photoelectron spectroscopy;

Y_x – yield to product x subscripts: (AC, carboxylic acid or acetophenone; AL, aldehyde; ES: ester), mol%.

BIBLIOGRAPHY

1. Barati, B.; Moghadam, M.; Rahmati, A.; Mirkhani, V.; Tangestaninejad, S.; Mohammadpoor-Baltork, I. Direct oxidation of alcohols to carboxylic acids over ruthenium hydride catalyst with diphenylsulfoxide oxidant. *Inorg. Chem. Commun.* **2013**, *29*, 1.
2. Corberán, V.C.; González-Pérez, M.E.; Martínez-González, S.; Gómez-Avilés, A. Green oxidation of fatty alcohols: Challenges and opportunities. *Appl. Catal. A-Gen.* **2014**, *474*, 211–223.
3. Tojo, G.; Fernández, M. *Oxidation of Primary Alcohols to Carboxylic Acids: A Guide to Current Common Practice*; Springer: Berlin, Germany, 2006.
4. Zhao, M.; Li, J.; Song, Z.; Desmond, R.; Tschaen, D.M.; Grabowski, E.J.J.; Reider, P.J. A novel chromium trioxide catalyzed oxidation of primary alcohols to the carboxylic acids. *Tetrahedron Lett.* **1998**, *39*, 5323–5326.
5. Augustine, R.L. *Heterogeneous Catalysis for The Synthetic Chemist*; Dekker: New York, NY, USA, 1996.
6. Sheldon, R.A. Catalysis: The key to waste minimization. *J. Chem. Tech. Biotechnol.* **1997**, *68*, 381–388.
7. Schmieder-van de Vondervoort, L.; Bouttemy, S.; Padron, J.M.; Le Bras, J.; Muzart, J.; Alsters, P.L. Chromium catalyzed oxidation of (homo)allylic and (homo)propargylic alcohols with sodium periodate to ketones or carboxylic acids. *Synlett* **2002**, *2*, 243–246.
8. Sheldon, R.A.; Arends, I.W.C.E.; Dijksman, A. New developments in catalytic alcohol oxidation for fine chemicals synthesis. *Catal. Today* **2000**, *57*, 157–166.
9. Werpy, T.; Petersen, G. *Top Value Added Chemicals from Biomass: Volume I—Results of Screening for Potential Candidates from Sugars and Synthesis Gas*; U. S. Department of Energy: Oak Ridge, CO, USA, 2004.
10. Mori, K.; Yamaguchi, K.; Hara, T.; Mizugaki, T.; Ebitani, K.; Kaneda, K. Controlled synthesis of hydroxyl apatite-supported palladium complexes as highly efficient heterogeneous catalysts. *J. Am. Chem. Soc.* **2002**, *124*, 11572–11573.
11. Nishimura, T.; Onoue, T.; Ohe, K.; Uemura, S. Palladium(II)-catalyzed oxidation of alcohols to aldehydes and ketones by molecular oxygen. *J. Org. Chem.* **1999**, 64, 6750–6755.
12. Hasan, M.; Musawir, M.; Davey, P.N.; Kozhevnikov, I.V. Oxidation of primary alcohols to aldehydes with oxygen catalyzed by tetra-n-propyl-ammonium-perruthenate. *J. Mol. Catal. A-Chem.* **2002**, *180*, 77–84.
13. Yamaguchi, K.; Mori, K.; Mizugaki, T.; Ebitani, K.; Kaneda, K. Creation of a monomeric Ru species on the surface of hydroxyapatite as an effricient heterogeneous catalyst for aerobic alcohol oxidation. *J. Am. Chem. Soc.* **2000**, *122*, 7144–7145.

14. Wang, H.; Fan, W.; He, Y.; Wang, J.; Kondo, J.N.; Tatsumi, T. Selective oxidation of alcohols to aldehydes/ketones over copper oxide-supported gold catalysts. *J. Catal.* **2013**, *299*, 10–19.
15. Hashmi, A.S.K.; Lothschutz, C.; Ackermann, M.; Doepp, R.; Anantharaman, S.; Marchetti, B.; Bertagnolli, H.; Rominger, F. Gold Catalysis: In situ EXAFS study of homogeneous oxidative esterification. *Chem. Eur. J.* **2010**, *16*, 8012–8019.
16. Enache, D.I.; Edwards, J.K.; Landon, P.; Solsona-Espriu, B.; Carley, A.F.; Herzing, A.A.; Watanabe, M. Solvent-free oxidation of primary alcohols to aldehydes using Au-Pd/TiO_2 catalysts. *Science* **2006**, *311*, 362–365.
17. Martins, L.M.D.R.S.; Carabineiro, S.A.C.; Wang, J.; Rocha, B.G.M.; Maldonado-Hodar, F.J.; Latourrette de Oliveira Pombeiro, A.J. Supported gold nanoparticles as reusable catalysts for oxidation reactions of industrial significance. *ChemCatChem* **2017**, *9*, 1211–1221.
18. Overbury, S.; Schwartz, M.; Mullins, D.; Yan, W.; Dai, S. Evaluation of the Au size effect: CO oxidation catalyzed by Au/TiO_2. *J. Catal.* **2006**, *241*, 1, 56–65.
19. Schubert, M.M.; Hackenberg, S.; van Veen, A.C.; Muhler, M.; Plzak, V.; Behm, R.J. Evaluation of the Au size effect: CO oxidation over supported gold catalysts –"Inert" and "active" support materials and their role for the oxygen supply during reaction. *J. Catal.* **2001**, *197*, 113–122.
20. Molina, L.M.; Rasmussen, M.D.; Hammer, B. Adsorption of O_2 and oxidation of CO at Au nanoparticles supported by TiO_2 (110). *J. Chem. Phys.* **2004**, *120*, 7673–7680.
21. Hashmi, A.S.K.; Hutchings, G. J. Gold catalysis. *Angew. Chem. Int. Ed.* 2006, *45*, 7896–7936.
22. Kotolevich, Y.; Kolobova, E.; Khramov, E.; Farıas, M.H.; Zubavichus, Y.; Tiznado, H.; González-Pérez, M.E.; Corberán, V.C.; Mota-Morales, J.D.; Pestryakov, A.N.; et al. n-Octanol oxidation on Au/TiO_2 catalysts promoted with La and Ce oxides. *J. Mol. Catal.* **2017**, *427*, 1–10.
23. Kotolevich, Y.; Kolobova, E.; Mamontov, G.; Khramov, E.; Cabrera Ortega, J.E.; Tiznado, H.; Farias, M.H.; Bogdanchikova, N.; Zubavichus, Y.V.; Mota-Morales, J.D.; et al. Au/TiO_2 catalysts promoted with Fe and Mg for n-octanol oxidation under mild conditions. *Catal. Today* **2016**, *278*, 104–112.
24. Kohlpaintner, C.; Schulte, M.; Falbe, J.; Lappe, P.; Weber, J.; Frey, G.D. Aldehydes, Araliphatic. *In Ullmann's Encyclopedia of Industrial Chemistry*; Wiley-VCH Verlag GmbH: Weinheim, Germany, 2013.
25. Harrigan-Farrelly, J. *Caprylic (Octanoic) Acid registration review final decision.* Federal Register. 2009, *74*, 30080–30081.
26. Voller, B.; Lines, E.; McCrossin, G.; Tinaz, S.; Lungu, C.; Grimes, G.; Starling, J.; Potti, G.; Buchwald, P. Dose-escalation study of octanoic acid in patients with essential tremor. *J. Clin. Invest.* **2016**, *126*, 1451–1457.
27. Lowell, S.Y.; Kelley, R.T.; Monahan, M.; Hosbach-Cannon, C.J.; Colton, R.H.; Mihaila, D. The effect of octanoic acid on essential voice tremor: A Double-Blind, Placebo-Controlled Study. *Laryngoscope* **2018**, *129*, 1882–1890. [CrossRef]

28. PubChem. "Octanoic acid". Available online: https://pubchem.ncbi.nlm.nih.gov/compound/379 (accessed on 20 March 2020)
29. Kotolevich, Y.; Martynyuk, O.; Martínez-Gonzalez, S.; Tiznado, H.; Pestryakov, A.; Avalos Borja, M.; Cortes Corberan, V.; Bogdanchikova, N. Novel route of synthesis of ultra-small Au nanoparticles on SiO_2 supports. *Fuel* **2019**, *236*, 589–597.
30. Kotolevich, Y.; Martynyuk, O.; García Ramos, J.C.; Cabrera Ortega, J.E.; Velez, R. ; Maturano Rojas, V.; Aguilar Tapia, A. *et al.* Nanostructured silica-supported gold: Effect of nanoparticle size distribution and electronic state on its catalytic properties in oxidation reactions. *Catal Today* **2021,** *366*, 77-86.
31. Li, W.; Wang, A.; Liu, X.; Zhang, T. Silica-supported Au–Cu alloy nanoparticles as an efficient catalyst for selective oxidation of alcohols. *Appl. Catal. A-Gen.* **2012**, *433–434*, 146–151.
32. Su, F.-Z.; Chen, M.; Wang, L.-C.; Huang, X.-S.; Liu, Y.-M.; Cao, Y.; He, H.-Y.; Fan, K.-N. Aerobic oxidation of alcohols catalyzed by gold nanoparticles supported on gallia polymorphs. *Catal. Commun.* **2008**, *9*, 1027–1032.
33. Liu, H.; Liu, Y.; Li, Y.; Tang, Z.; Jiang, H. Metal-organic framework supported gold nanoparticles as a highly active heterogeneous catalyst for aerobic oxidation of alcohols. *J. Phys. Chem. C* **2010**, *114*, 13362–13369.
34. Haider, P.; Baiker, A. Gold supported on Cu–Mg–Al-mixed oxides: Strong enhancement of activity in aerobic alcohol oxidation by concerted effect of copper and magnesium. *J. Catal.* **2007**, *248*, 175–187.
35. Kaskow, I.; Sobczak, I.; Ziolek, M.; Corberan, V.C. The effect of support properties on n-octanol oxidation performed on gold–silver catalysts supported on MgO, ZnO and Nb_2O_5. *J. Mol. Catal.* **2020**, *482*, 110674.
36. Abad, A.; Almela, C.; Corma, A.; Garcıa, H. Efficient chemoselective alcohol oxidation using oxygen as oxidant. Superior performance of gold over palladium catalysts. *Tetrahedron* **2006**, *62*, 6666–6672.
37. Carabineiro, S.A.C.; Ribeiro, A.P.C.; Buijnsters, J.G.; Avalos-Borja, M.; Pombeiro, A.J.L.; Figueiredo, J.L.; Martins, L.M.D.R.S. Solvent-free oxidation of 1-phenylethanol catalysed by gold nanoparticles supported on carbon powder materials. *Catal.Today.* **2020**, *357*, 22-31.
38. Mitsudome, T.; Noujima, A.; Mizugaki, T.; Jitsukawa, K.; Kaneda, K. Efficient aerobic oxidation of alcohols using a hydrotalcite-supported gold nanoparticle catalyst. *Adv. Synth. Catal.* **2009**, *351*, 1890–1896.
39. Liang, W.; Xiangju, M.; Fengshou, X. Au nanoparticles supported on a layered double hydroxide with excellent catalytic properties for the aerobic oxidation of alcohols. *Chin. J. Catal.* **2010**, *31*, 943–947.
40. Haider, P.; Grunwaldt, J.D.; Baiker, A. Gold supported on Mg, Al and Cu containing mixed oxides: Relation between surface properties and behavior in catalytic aerobic oxidation of 1-phenylethanol. *Catal. Today* **2009**, *141*, 349–354.
41. Shanahan, A.E.; McNamara, J.A.; Sullivan, H.J.; Byrne, M. An insight into the superior performance of a gold nanocatalyst on single wall carbon nanotubes to

that on titanium dioxide and amorphous carbon for the green aerobic oxidation of aromatic alcohols. *New Carbon Mater.* **2017**, *32*, 242–251.

42. Wang, L.; He, L.; Liu, Q.; Liu, Y.; Chen, M.; Cao, Y.; He, H.; Fan, K. Solvent-free selective oxidation of alcohols by molecular oxygen over gold nanoparticles supported on β-MnO_2 nanorods. *Appl. Catal. A: Gen.* **2008**, *344*, 150–157.
43. Nepak, D.; Darbha, S. Selective aerobic oxidation of alcohols over Au–Pd/sodium titanate nanotubes. *Catal. Commun.* **2015**, *58*, 149–153.
44. Yang, X.; Wang, X.; Liang, C.; Su, W.; Wang, C.; Feng, Z.; Li, C.; Qiu, J. Aerobic oxidation of alcohols over Au/TiO_2: An insight on the promotion effect of water on the catalytic activity of Au/TiO_2. *Catal. Commun.* **2008**, *9*, 2278–2281.
45. Li, H.; Zheng, Z.; Cao, M.; Cao, R. Stable gold nanoparticle encapsulated in silica-dendrimers organic–inorganic hybrid composite as recyclable catalyst for oxidation of alcohol. *Microporous Mesoporous Mater.* **2010**, *136*, 42–49.
46. Mertens, P.G.N.; Corthals, S.L.F.; Yeb, X.; Poelman, H.; Jacobs, P.A.; Sels, B.F.; Vankelecom, I.F.J.; De Vos, D.E. Selective alcohol oxidation to aldehydes and ketones over base-promoted gold–palladium clusters as recyclable quasi homogeneous and heterogeneous metal catalysts. *J. Mol. Catal. A: Chem.* **2009**, *313*, 14–21.
47. Thurman, R.B.; Gerba, C.P. The molecular mechanisms of copper and silver ion disinfection of bacteria and viruses. *CRC Crit. Rev. Environ.Contr.* **1989**, 18, 295-315.
48. Parish, R.V. Gold in medicine-chrysotherapy. *Interdiscip. Sci. Rev.* **1992**, 17, 221-228.
49. Bau, R. Crystal structure of the antiarthritic drug gold thiomalate (myochrysine): a double-helical geometry in the solid state. *J. Am. Chem. Soc.* **1998**, *120*, 9380-9381.
50. Karthika, V.; Arumugam, A.; Gopinath, K.; Kaleeswarran, P.; Govindarajan, M.; Alharbi, N.S. *Guazuma ulmifolia* bark-synthesized Ag, Au and Ag/Au alloy nanoparticles: photocatalytic potential, DNA/protein interactions, anticancer activity and toxicity against 14 species of microbial pathogens. *J. Photochem. Photobiol.* B **2017**, *167*, 189–199.
51. Ding, X.; Yuan, P.; Gao, N.; Zhu, H.; Yang, Y.Y.; Xu, Q-H. Au-Ag core-shell nanoparticles for simultaneous bacterial imaging and synergistic antibacterial activity. *Nanomed. Nanotechnol.* **2017**, *13*, 297–305.
52. Haruta, M.; Kobayashi, T.; Sano, H.; Yamada, N. Novel gold catalysts for the oxidation of carbon monoxide at a temperature far below 0 C. *Chem. Lett.*, **1987**, *16*, 405–408.
53. Haruta, M.; Yamada, N.; Kobayashi, T.; Iijima, S. Gold catalysts prepared by coprecipitation for low-temperature oxidation of hydrogen and of carbon monoxide. *J. Catal.* **1989**, *115*, 301–309.
54. Kobayashi, T.; Haruta, M.; Sano, H.; Nakane, M. A selective CO sensor using Ti-doped α-Fe_2O_3 with coprecipitated ultrafine particles of gold. *Sens. Actuators* **1988**, *13*, 339–349.
55. Thompson, D. New advances in gold catalysis part I. *Gold Bull.* **1998**, 31, 111–118.
56. Thompson, D. New advances in gold catalysis part II. *Gold Bull.* **1999**, 32, 12–19.

57. Haruta, M. Gold as a novel catalyst in the 21st century: Preparation, working mechanism and applications. *Gold Bull.* **2004**, *37*, 27-36.
58. Hutchings, G.J.; Haruta, M. A golden age of catalysis: a perspective. *Appl. Catal., A*, **2005**, *291*, 2.
59. Carabineiro, S.A.C.; Thompson, D. *"Catalytic applications for gold nanotechnology"* in *Nanocatalysis.* Heiz, U., Landman, U., Eds.; Heidelberg: Springer, Berlin, 2007, pp. 377–489.
60. Mallat, T., Baiker, A. Potential of gold nanoparticles for oxidation in fine chemical synthesis. *Annu. Rev. Chem. Biomol. Eng*. **2012**, *3*, 11–28.
61. Ishida, T.; Koga, H.; Okumura, M.; Haruta, M. Advances in gold catalysis and understanding the catalytic mechanism. *Chem. Rec.* **2016**, *16*, 2278–2293.
62. Pestryakov, A.N. *Formation of active surface of catalysts based on* $d^n s^1$ *metals in alcohol oxidation.* Dr. Sc. Thesis (in Russian). Moscow State University, Moscow, Russia, 1998.
63. Haruta, M. Catalysis of Gold Nanoparticles Deposited on Metal Oxides. *CATTECH*, **2002**, *6*, 102-115.
64. Xie, X.; Li, Y.; Liu, Z.Q. Haruta, M. Low-temperature oxidation of CO catalysed by Co_3O_4 nanorods. *Nature* **2008**, *458*, 746-749.
65. Ishida, T.; Haruta, M. Gold catalysts: towards sustainable chemistry. *Angew. Chem. Int. Ed.* **2007**, *46*, 7154-7156.
66. Astruc, D., Ed., *Nanoparticles and Catalysis*, Wiley-VCH Verlag GmbH, Weinheim, Germany, 2008.
67. Herzing, A.A.; Kiely, C.J.; Carley, A.F.; Landon, P.; Hutchings, G.J. Identification of active gold nanoclusters on iron oxide supports for CO oxidation. *Science* **2008**, *321*, 1331–1335.
68. Chrétien, S.; Buratto, S.K.; Metiu, H. Catalysis by very small Au clusters. *Curr. Opin. Solid State Mater. Sci.* **2007**, *11*, 62–75.
69. Martynyuk, O.; Kotolevich, Y.; Velez, R.; Cabrera Ortega, J.E.; Tiznado, H.; Zepeda, T.; Mota-Morales, J.D.; Pestryakov, A.; Bogdanchikova, N. On the High Sensitivity of the Electronic States of 1 nm Gold Particles to Pretreatments and Modifiers. *Molecules* **2016**, *21*, 432.
70. Zhu, H.; Ma, Zh.; Clark, J.C.; Pan, Z.W.; Overbury, S.H.; Dai, S. Low-temperature CO oxidation on Au/fumed SiO_2-based catalysts prepared from $Au(en)_2Cl_3$ precursor. *Appl. Catal. A: Gen.* **2007**, *326*, 89–99.
71. Wang, H.P.; Liu, C.J. Preparation and characterization of SBA-15 supported Pd catalyst for CO oxidation. *Appl. Catal. B: Environ.* **2011**, *106*, 672–680.
72. Ma, Zh.; Overbury, S.H.; Dai, Sh. $Au/M_xO_y/TiO_2$ catalysts for CO oxidation: Promotional effect of main-group, transition, and rare-earth metal oxide additives. *J. Mol. Cat. A Chem.* **2007**, *273*, 186–197.
73. Molina, L.M.; Hammer, B. Some recent theoretical advances in the understanding of the catalytic activity of Au. *Appl. Catal. A: Gen* **2005**, *291*, 21-31.

74. Corma, A.; Concepción, P.; Carrettin, S. Stabilization of cationic gold species on Au/CeO_2 catalysts under working conditions. *Appl. Catal. A: Gen.* **2006**, *307*, 42-45.
75. Wang, F.; Ueda, W.; Xu, J. Detection and measurement of surface electron transfer on reduced molybdenum oxides (MoO(x)) and catalytic activities of Au/MoO(x). *Angew. Chem. Int. Ed.* **2012**, *51*, 3883-3887.
76. Haruta, M.; Kobayashi, T.; Ueda, A.; Nakahara, Y. Preparation of highly dispersed gold on titanium and magnesium oxide. *Stud. Surf. Sci. Catal.* **1991**, *63*, 695–704.
77. Prati, L.; Martra, G. New gold catalysts for liquid phase oxidation. *Gold Bull.* **1999**, *32*, 96–101.
78. Haruta, A. When gold is not noble: catalysis by nanoparticles. *Chem. Rec.* **2003**, *3*, 75–87.
79. Carabineiro, S.A.C., Thompson, D. *"Gold Catalysis"* in *Gold: Science and Applications,* Corti, C., Holliday, R., Eds., Boca Raton, FL; London, New York, NY: CRC Press; Taylor and Francis Group, 2010, 89–122.
80. Lin, J.-N.; Wan, B.-Z. Effects of preparation conditions on gold/Y-type zeolite for CO oxidation. *Appl. Catal. B: Environ.* **2003**, *41*, 83–95.
81. Zanella, R.; Delannoy, L.; Louis, C. Mechanism of deposition of gold precursors onto TiO_2 during the preparation by cation adsorption and deposition–precipitation with NaOH and urea. *Appl. Catal. A: Gen.* **2005**, *291*, 62–72.
82. Haruta, M. Novel catalysis of gold deposited on metal oxides. *Catal. Surv. Jpn.* **1997**, *1*, 61–73.
83. Park, E.D.; Lee, J.S. Effects of pretreatment conditions on CO oxidation over supported Au catalysts. *J. Catal.* **1999**, *186*, 1–11.
84. Lee, S.-J.; Gavriilidis, A.; Pankhurst, Q.A.; Kyek, A.; Wagner, F.E.; Wong, P.C.L.; King, L.Y. Effect of drying conditions of Au–Mn co-precipitates for low-temperature CO oxidation. *J. Catal.* **2001**, *200*, 298–308.
85. Minico, S.; Scire, S.; Crisafulli, C.; Maggiore, R.; Galvagno, S. Catalytic combustion of volatile organic compounds on gold/iron oxide catalysts. *Appl. Catal. B: Environ.* **2000**, *28*, 245–251.
86. Rodriguez, P.; Plana, D.; Fermin, D.J.; Koper, M.T.M. New insights into the catalytic activity of gold nanoparticles for CO oxidation in electrochemical media, *J. Catal.* **2014,** *311*, 182–189.
87. Abad, A.; Corma, A.; García, H. Catalyst Parameters Determining Activity and Selectivity of Supported Gold Nanoparticles for the Aerobic Oxidation of Alcohols: The Molecular Reaction Mechanism. *Chem. Eur. J.* **2007**, *14(1)*, 212–222.
88. Barakat, T.; Rooke, J.C. Genty, E.; Cousin, R.; Siffert, S.; Su, B-L. Gold catalysts in environmental remediation and water-gas shift technologies. *Energy Environ. Sci.* **2013**, *6*, 371–391.
89. Haruta, M. Size- and support-dependency in the catalysis of gold. *Catal. Today* **1997**, *36*, 153–160.
90. Campbell, C.T. The active site in nanopaticle gold catalysis. *Science* **2004**, 306, 234–235.

91. Carrettin, S.; Hao, Y.; Aguilar-Guerrero, V.; Gates, B.; Trasobares, S.; Calvino, J.; Corma, A. Increasing the number of oxygen vacancies on TiO_2 by doping with iron increases the activity of supported gold for CO oxidation. *Chem. Eur. J.* **2007**, 13, 7771–7779.
92. Guzman, J.; Gates, B.C. Catalysis by supported gold: correlation between catalytic activity for CO oxidation and oxidation states of gold. *J. Am. Chem. Soc.* **2004**, *126*, 2672–2673.
93. Lee, J.Y.; Schwank, J. Infrared spectroscopic study of NO reduction by H_2 on supported gold catalysts. *J. Catal.* **1986**, *102*, 207–215.
94. Hutchings, G.J.; Hall, M.S.; Carley, A.F.; Landon, P.; Solsona, B.E.; Kiely, C.J. *et al.* Role of gold cations in the oxidation of carbon monoxide catalyzed by iron oxide-supported gold. *J. Catal.* **2006**, 242, 71–81.
95. Bogdanchikova, N.; Pestryakov, A.; Tuzovskaya, I.; Zepeda, T.A.; Farias, M.H.; Tiznado, H.; Martynyuk, O. Effect of redox treatments on activation and deactivation of gold nanospecies supported on mesoporous silica in CO oxidation. *Fuel* **2013**, *110*, 40–47.
96. Pestryakov, A.N.; Lunin, V.V.; Bogdanchikova, N.; Temkin, O.N.; Smolentseva, E. Active states of gold in small and big metal particles in CO and methanol selective oxidation. *Fuel*, **2013**, *110*, 48–53.
97. Chen, M.S.; Goodman, D.W.; Catalytically active gold: from nanoparticles to ultrathin films. *Chen. Acc. Chem. Res.* **2006,** *39*, 739–746. Lopez, N.; Janssens, T.V.W.; Clausen, B.S.; Xu, Y.; Mavrikakis, M.; Bligaard, T.; Norskov, J.K. On the origin of the catalytic activity of gold nanoparticles for low-temperature CO oxidation. J. *Catal.* **2004**, *223*, 232–235.
98. Alshammari, A.; Kalevaru, V.N.; Martin, A. Bimetallic catalysts containing gold and palladium for environmentally important reactions. *Catalysts* **2016**, *6(7)*, 97.
99. Sokolovskii, V.D. Principles of oxidative catalysis on solid oxides. *Catal. Rev. Sci. Eng.* **1990**, *32*, 1–49.
100. Bell, G.H. Solubilities of normal aliphatic acids, alcohols and alkanes in water. *Chem. Phys. Lipids*. **1973**, *10*, 1-10.
101. Johansson, A. By-product recovery and valorisation in the kraft industry: A review of current trends in the recovery and use of turpentine and tall oil derivatives. *Biomass* **1982**, *2*, 103–113.
102. Marqués, G.; Río, J.C.; Gutiérrez, A. Lipophilic extractives from several nonwoody lignocellulosic crops (flax, hemp, sisal, abaca) and their fate during alkaline pulping and TCF/ECF bleaching. *Bioresour. Technol.* **2010**, *101*, 260– 267.
103. Nielsen, J.; Raschke, T.; Riedel, H. Cosmetical and dermatological preparations in the form of o/ω-emulsions containing sterols and/or C12-C40 fatty alcohols. US Patent 0037036A1, **2005**.
104. Coupland, K.; Smith, P.J. Humectants. EU Patent EP0327379, **1989**.
105. Nuwayser, E. High drug loaded injectable microparticle compositions and methods of treating opioid drug dependence. US Patent 7041320 B1, **2006**.

106. Loh, J.; Almendarez, M.; Hanse, T.; Herbst, L.; Gaonkar, A. US Patent 0101601, 2004
107. Beare-Rogers, J.; Dieffenbacher, A.; Holm, J.V. *Lexicon of lipid nutrition (IUPAC Technical Report). Pure Appl. Chem.* **2001**, *73*, 685–744.
108. Dijksman, A.I.; Arends, W.C.E.; Sheldon, R.A. Efficient ruthenium–TEMPO-catalysed aerobic oxidation of aliphatic alcohols into aldehydes and ketones. *Chem. Commun.* **1999**, 1591–1592.
109. Yamaguchi, K.; Mizuno, N. Supported Ruthenium Catalyst for the Heterogeneous Oxidation of Alcohols with Molecular Oxygen. *Angew. Chem. Int. Ed.* **2002**, 41, 4538–4542.
110. Ji, H.; Mizugaki, T.; Ebitani, K.; Kaneda, K. Highly Efficient Oxidation of Alcohols to Carbonyl Compounds in the Presence of Molecular Oxygen Using a Novel Heterogeneous Ruthenium Catalyst. *Tetrahedron Lett.* **2002**, *43*, 7179–7183.
111. Anderson, R.; Griffin, K.; Johnston, P.; Alsters, P.L. Selective oxidation of alcohols to carbonyl compounds and carboxylic acids with platinum group metal catalysts. *Adv. Synth. Catal.* **2003**, *45*, 517–523.
112. Dimitratos, N.; Villa, A.; Wang, D.; Porta, F.; Su, D.S.; Prati, L. Pd and Pt catalysts modified by alloying with Au in the selective oxidation of alcohols. *J. Catal.* **2006**, *244*, 113–121.
113. Uozomi, Y.; Yamada, Y.M.A. Development of an amphiphilic resin-dispersion of nanopalladium and nanoplatinum catalysts: Design, preparation, and their use in green organic transformations. *Chem. Rec.* **2009**, *9*, 51–65.
114. Jenzer, G.; Schneider, M.S.; Wandeler, R.; Mallat, T.; Baiker, A. Palladium-catalyzed oxidation of octyl alcohols in "Supercritical" Carbon dioxide. *J. Catal.* **2001**, *199*, 141–148.
115. Villa, A.; Janjic, N.; Spontoni, P.; Wang, D.; Su, D.S.; Prati, L. Au–Pd/AC as catalysts for alcohol oxidation: Effect of reaction parameters on catalytic activity and selectivity. *Appl. Catal. A: Gen.* **2009**, *364*, 221–228.
116. Shi, Y.; Yang, X.; Zhao, X.; Cao, T.; Chen, J.; Zhu, W.; Yu, Y.; Hou, Z. Au–Pd nanoparticles on layered double hydroxide: Highly active catalyst for aerobic oxidation of alcohols in aqueous phase. *Catal. Commun.* **2012**, *18*, 142–146.
117. Enache, D.I.; Knight, D.W.; Hutchings, G.J. Solvent-free oxidation of primary alcohols to aldehydes using supported gold catalysts. *Catal. Lett.* **2005**, *103*, 43-52.
118. Kolobova; E.; Kotolevich; Y.; Pakrieva; E.; Mamontov, G.; Farias, M.H.; Cortés Corberán, V; Bogdanchikova, N.; Hemming, J.; Smeds, A.; Mäki-Arvela, P.; *et al.* Modified Ag/TiO_2 systems: Promising catalysts for liquid-phase oxidation of alcohols. *Fuel* **2018**, *234*, 110-119.
119. Beier, M.J.; Hansen, T.W.; Grunwaldt, J.-D. Selective liquid-phase oxidation of alcohols catalyzed by a silver-based catalyst promoted by the presence of ceria. *J. Catal.* **2009**, *266*, 320–330.
120. Ben-Daniel, R.; Alster, P.; Neumann, R. Selective aerobic oxidation of alcohols with a combination of a polyoxometalate and nitroxyl radical as catalysts. *J. Org. Chem.* **2001**, *66*, 8650-8653.

121. Pagliaro, M.; Ciriminna, R. New recyclable catalysts for aerobic alcohols oxidation: Sol gel ormosils doped with TPAP/M. *Tetrahedron Lett*. **2001**, *42*, 4511–4514.
122. Iwahama, T.S.; Nishiyama, Y.; Ishii, Y. Aerobic oxidation of alcohols to carbonyl compounds catalyzed by *n*-hydroxyphthalimide (NHPI) combined with $Co(acac)_3$. *Tetrahedron Lett.* **1995**, *36*, 6923–6926.
123. Rajabi, F.; Karimi, B. Efficient aerobic oxidation of alcohols using a novel combination *N*-hydroxy phthalimide (NHPI) and a recyclable heterogeneous cobalt complex. *J. Mol. Catal. A: Chem.* **2005**, 232, 95–99.
124. Kumar, R.T.; Selvam, N.C.S.; Adinaveen, T.; Kennedy, L.J.; Vidaya, J.J. Strontium(II)-added $CoAl_2O_4$ nanocatalysts for the selective oxidation of alcohols. *React. Kinet. Mech. Catal.* **2012**, *106*, 379–394.
125. Krohn, K.; Vinke, I.; Adam, H. Transition-metal catalyzed oxidations. 7. Zirconium-catalyzed oxidation of primary and secondary alcohols with hydroperoxides. *J. Org. Chem.* **1996**, *61*, 1467–1472.
126. Zhou, Y.; Dong, F.; Kunimasa, A.; Zhang, Y.; Cheng, S.; Lu, J.; Zhang, L.; Murata, A.; Mayer, F. "Occurrence of glycosidically conjugated 1-phenylethanol and its hydrolase β-primeverosidase in tea (Camellia sinensis) flowers". *J Agric. Food Chem.* **2014**, *62 (32)*, 8042–8050.
127. Burdock, G.A. *Fenaroli's Handbook of Flavor Ingredients.* Fifth Edition. CRC Press. 2005.
128. Anbu, S.; Alegria, E.C.B.A.; Pombeiro, A.J.L. Catalytic activity of a benzoyl hydrazone based dimeric dicopper (II) complex in catechol and alcohol oxidation reactions. *Inorg. Chim. Acta* **2015**, *431*, 139–144.
129. Nesterova, O.V.; Nesterov, D.S.; Krogul-Sobczak, A.; Guedes da Silva, M.C.; Pombeiro, A.J.L. Synthesis, crystal structures and catalytic activity of Cu (II) and Mn (III) Schiff base complexes: Influence of additives on the oxidation catalysis of cyclohexane and 1-phenylehanol. *J. Mol. Catal. A: Chem*. **2017**, *426*, 506–515.
130. Sutradhar, M.; Alegria, E.C.B.A.; Roy Barman, T.; Scorcelletti, F.; Guedes da Silva, M.C.; Pombeiro, A.J.L. Microwave-assisted peroxidative oxidation of toluene and 1-phenylethanol with monomeric keto and polymeric enolaroylhydrazone Cu (II) complexes. *Mol. Catal.* **2017**, *439*, 224–232.
131. Ribeiro, A.P.C.; Fontolan, E.; Alegria, E.C.B.A.; Kopylovich, M.N.; Bertani, R.; Pombeiro, A.J.L. The influence of multiwalled carbon nanotubes and graphene oxide additives on the catalytic activity of 3d metal catalysts towards 1-phenylethanol oxidation. *J. Mol. Catal. A: Chem.* **2017**, *426*, 557–563.
132. Karmakar, A.; Martins, L.M.D.R.S.; Guedes da Silva, M.F.C.; Hazra, S.; Pombeiro, A.J.L. Solvent-free microwave-assisted peroxidative oxidation of alcohols catalyzed by iron (III)-TEMPO catalytic systems. *Catal. Lett.* **2015**, *145*, 2066–2076.
133. Cozzi, I.S.; Crotti, C.; Farnetti, E. Microwave-assisted green oxidation of alcohols with hydrogen peroxide catalyzed by iron complexes with nitrogen ligands. *J. Organomet. Chem.* **2018**, *878*, 38–47.

134. Du, Z.; Ma, J.; Ma, H.; Gao, J.; Xu, J. Synergistic effect of vanadium–phosphorus promoted oxidation of benzylic alcohols with molecular oxygen in water. *Green Chem.* **2010**, *12*, 590–592.
135. Sasaki, T.; Ichikuni, N.; Hara, T.; Shimazu, S. Study on the promoting effect of nickel silicate for 1-phenylethanol oxidation on supported NiO nanocluster catalysts. *Catal. Today* **2018**, *307*, 29–34.
136. Bhaumik, C.; Stein, D.; Vincendeau, S.; Poli, R.; Manoury, E. Oxidation of alcohols by TBHP in the presence of sub-stoichiometric amounts of MnO_2. *C. R. Chim.* **2016**, *19*, 566–570.
137. Reis, M.C.; Barros, S.D.T.; Lachter, E.R.; San Gil, R.A.S.; Floresc, J.H.; Pais da Silva, M.I.; Onfroyd, T. Synthesis, characterization and catalytic activity of meso-niobium phosphate in the oxidation of benzyl alcohols. *Catal. Today* **2012**, *192*, 117–122.
138. Burange, A.S.; Jayaram, R.V.; Shukla, R.; Tyagi, A.K. Oxidation of benzylic alcohols to carbonyls using *tert*-butyl hydroperoxide over pure phase nanocrystalline $CeCrO_3$. *Catal. Commun.* **2013**, *40*, 27–31.
139. Yadav, G.D.; Yadav, A.R. Selective liquid phase oxidation of secondary alcohols into ketones by *tert*-butyl hydroperoxide on nano-fibrous Ag-OMS-2 catalyst. *J. Mol. Catal. A: Chem.* **2013**, *380*, 70–77.
140. Antonetti, C.; Toniolo, L.; Cavinato, G.; Forte, C.; Ghignoli, C.; Ishake, R.; Cavani, F.; RaspolliGalletti, A.M. A hybrid polyketone–SiO_2 support for palladium catalysts and their applications in cinnamaldehyde hydrogenation and in 1-phenylethanol oxidation. *Appl. Catal. A: Gen.* **2015**, *496*, 40–50.
141. Yasueda, T.; Seike, R.; Ikenaga, N.; Miyake, T.; Suzuki, T. Palladium-loaded oxidized diamond catalysis for the selective oxidation of alcohols. *J. Mol. Catal. A: Chem.* **2009**, *306*, 136–142.
142. Kantam, M.L.; Reddy, R.S.; Pal, U.; Sudhakar, M.; Venugopal, A.; JeevaRatnam, K.; Figueras, F.; Reddy Chintareddy, V.; Nishinad, Y. Ruthenium/magnesium–lanthanum mixed oxide: An efficient reusable catalyst for oxidation of alcohols by using molecular oxygen. *J. Mol. Catal. A: Chem.* **2012**, *359*, 1–7.
143. Hosseini-Monfared, H.; Meyer, H.; Janiak, C. Dioxygen oxidation of 1-phenylethanol with gold nanoparticles and *N*-hydroxyphthalimide in ionic liquid. *J. Mol. Catal. A: Chem.* **2013**, *372*, 72–78.
144. Restrepo, J.; Lozano, P.; Burguete, M.I.; García-Verdugo, E.; Luis, S.V. Gold nanoparticles immobilized onto supported ionic liquid-like phases for microwave phenylethanol oxidation in water. *Catal. Today* **2015**, *255*, 97–101.
145. Abad, A.; Concepcion, P.; Corma, A.; Garcia, H. A collaborative effect between gold and a support induces the selective oxidation of alcohols. *Angew. Chem. Int. Ed.* **2005**, *44*, 4066–4069.
146. Daliran, S.; Santiago-Portillo, A.; Navalón, S.; Oveisi, A.; Álvaro, M.; Ghorbani-Vaghei, R.; Azarifar, D.; García, H. Cu(II)-Schiff base covalently anchored to MIL-125(Ti)-NH_2 as heterogeneous catalyst for oxidation reactions. *J. Coll. Interface Sci.* **2018**, *532*, 700–710.

147. Wu, J.; Liu, Y.; Ma, X.; Liu, P.; Gu, C.; Dai, B. Metal-free oxidation of secondary benzylic alcohols using aqueous TBHP. *Synth. Commun.* **2006**, *46*, 1747–1758.
148. Zanella, R.; Giorgio, S.; Henry, C.R.; Louis, C. Alternative methods for the preparation of gold nanoparticles supported on TiO_2. *J. Phys. Chem. B.* **2002**, *106*, 7634–7642.
149. Zanella, R.; Louis, C. Influence of the conditions of thermal treatments and of storage on the size of the gold particles in Au/TiO_2 samples. *Catal. Today* **2005**, *107*, 768–777.
150. Perdew, J.P.; Burke, K.; Ernzerhof, M. Generalized Gradient Approximation Made Simple. *Phys. Rev. Lett.* **1996**, 77, 3865–3868.
151. Xiao, L.; Tollberg, B.; Hu, X.; Wang, L. Structural study of gold clusters. *J. Chem. Phys.* **2006**, *124*, 114309.
152. Mukhamedzyanova, D.F.; Ratmanova, N.K.; Pichugina, D.A.; Kuzmenko, E.N. A structural and stability evaluation of Au12 from an isolated cluster to the deposited material. *J. Phys. Chem. C.* **2012**, *116*, 11507–11518.
153. Beletskaya, A.V.; Pichugina, D.A.; Shestakov, A.F.; Kuz'menko N.E. Formation of H_2O_2 on Au_{20} and $Au_{19}Pd$ Clusters: Understanding the Structure Effect on the Atomic Level. *J. Phys. Chem. A.* **2013**, *117*, 6817–6826.
154. Laikov, D.N.; Ustynyuk, Y.A. PRIRODA-04: A Quantum-Chemical Program Suite. New Possibilities in the Study of Molecular Systems with the Application of Parallel Computing. *Russ. Chem. Bull.* **2005,** *54*, 820–826.
155. Sadovnichy, V.; Tikhonravov, A.; Voevodin, V.; Opanasenko, V. *Contemporary High Performance Computing: From Petascale toward Exascale;* CRC Press: Boca Raton, FL, USA, 2013.
156. Kolobova, E.; Pakrieva, E.; Pascual, L.; Cortés Corberán, V.; Bogdanchikova, N.; Farias, M.; Pestryakov, A. Selective oxidation of n-octanol on unmodified and La-modified nanogold catalysts: Effect of metal content. *Catal. Today* **2019**, *333C*, 127–132.
157. Pakrieva, E.; Kolobova, E.; Mamontov, G.; Bogdanchikova, N.; Farias, M.H.; Pascual, L.; Cortés Corberán, V.; Martinez Gonzalez, S.; Carabineiro, S.A.C.; Pestryakov, A. Green oxidation of n-octanol on supported nanogold catalysts: Formation of gold active sites under combined effect of gold content, additive nature and redox pretreatment. *ChemCatChem* **2019**, *11*, 1615–1624.
158. Pakrieva, E.; Kolobova, E.; Kotolevich, Y.; Pascual, L.; Carabineiro, S.A.C.; Kharlanov, A.N.; Pichugina, D.; Nikitina, N.; German, D.; Zepeda Partida, T.A.; et al. Effect of gold electronic state on the catalytic performance of nano gold catalysts in n-octanol oxidation. *Nanomaterials* **2020**, *10*, 880.
159. Pakrieva, E.; Ribeiro, A.P.C.; Kolobova, E.; Martins, L.M.D.R.S.; Carabineiro, S.A.C.; German, D.; Pichugina, D.; Jiang, C.; Pombeiro, A.J.L.; Bogdanchikova, N.; et al. Supported gold nanoparticles as catalysts in peroxidative and aerobic oxidation of 1-phenylethanol under mild conditions. *Nanomaterials* **2020**, *10*, 151.

160. Kolobova, E.; Kotolevich, Y.; Pakrieva, E.G.; Mamontov, G.; Farias, M.H.; Bogdanchikova, N.; Pestryakov, A. Causes of activation and deactivation of modified nanogold catalysts during prolonged storage and redox treatments. *Molecules* **2016**, *21*, 486.
161. Ishida, T.; Ogihara, Y.; Ohashi, H.; Akita, T.; Honma, T.; Oji, H.; Haruta, M. Base-free direct oxidation of 1-octanol to octanoic acid and its octyl ester over supported gold catalysts. *ChemSusChem* **2012**, *5*, 2243–2248.
162. Carabineiro, S.A.C.; Bogdanchikova, N.; Avalos-Borja, M.; Pestryakov, A.; Tavares, P.B.; Figueiredo, J.L. Gold supported on metal oxides for carbon monoxide oxidation. *Nano Res.* **2011**, *4*, 180–193.
163. Khan, S.A.; Ali, S.; Sohail, M.; Morsy, M.A.; Yamani, Z.H. Fabrication of TiO_2/Ag/Ag_2O Nanoparticles to Enhance the Photocatalytic Activity of Degussa P25 Titania. *Aust. J. Chem.* **2016**, *69 (1)*, 41–46.
164. Teng, W.; Li, X.; Zhao, Q.; Chen, G. A Fabrication of Ag/Ag_3PO_4/TiO_2 heterostructure photoelectrodes for efficient decomposition of 2-chlorophenol under visible light irradiation. *J. Mater. Chem.* **2013**, *1*, 9060–9068.
165. Martínez-González, S.; Gómez-Avilés, A.; Martynyuk, O.; Pestryakov, A.; Bogdanchikova, N.; Corberán, V.C. Selective oxidation of 1-octanol over gold supported on mesoporous metal-modified HMS: The effect of the support. *Catal. Today* **2014**, *227*, 65–70.
166. Zhu, H.; Qin, Z.; Shan, W.; Shen, W.; Wang. J. Pd/CeO_2–TiO_2 catalyst for CO oxidation at low temperature: a TPR study with H_2 and CO as reducing agents. *J. Catal.* **2004**, *225*, 267–277.
167. Mamontov, G.V.; Grabchenko, M.V.; Sobolev, V.I.; Zaikovskii, V.I.; Vodyankina, O.V. Ethanol dehydrogenation over Ag-CeO_2/SiO_2 catalyst: Role of Ag-CeO_2 interface. *Appl. Catal. A: Gen.* **2016**, *528*, 161–167.
168. Carabineiro, S.A.C.; Silva, A.M.T.; Drazic, G.; Tavares, P.B.; Figueiredo, J.L. Gold nanoparticles on ceria supports for the oxidation of carbon monoxide. *Catal. Today* **2010**, *154*, 21–30.
169. Zhu, J.; Carabineiro, S.A.C.; Shan, D.; Faria, J.L.; Zhu, Y.; Figueiredo, J.L. Oxygen activation sites in gold and iron catalysts supported on carbon nitride and activated carbon. *J. Catal.* **2010**, *274*, 207–214.
170. Ibrahim, A.A.; Al-Fatesh, A.S.; Khan, W.U.; Soliman, M.A.; AL Otaibi, R.L.; Fakeeha, A.H. Influence of Support Type and Metal Loading in Methane Decomposition over Iron Catalyst for Hydrogen Production. *J. Chin. Chem. Soc.* **2015**, *62(7)*, 592–599.
171. Biabani-Ravandi, A.; Rezaei, M.; Fattah, Z. Catalytic Performance of Ag/Fe_2O_3 for the low temperature oxidation of carbon monoxide. *Chem. Eng. J.* **2013**, *219*, 124–130.
172. Wang, Y.; Liang, S.; Cao, A.; Thompson, R.L.; Vesera, G. Au-mixed lanthanum/cerium oxide catalysts for water gas shift. *Appl. Catal. B: Environ.* **2010**, *99*, 89–95.

173. Parmaliana, A.; Arena, F.; Frusteri F, Giordano N: Temperature-programmed reduction study of NiO-MgO interactions in magnesia-supported Ni catalysts and NiO-MgO physical mixture. *J. Chem. Soc. Faraday Trans*. **1990**, 86, 2663.
174. Guzman, J.; Gates, BC. Oxidation states of gold in MgO-supported complexes and clusters: Characterization by X-ray absorption spectroscopy and temperature-programmed oxidation and reduction. *J. Phys. Chem. B* **2003**, *107*, 2242-2248.
175. Carabineiro, S.A.C.; Bogdanchikova, N.; Pestryakov, A.; Tavares, P.B.; Fernandes, L.S.G.; Figueiredo, J.L. Gold nanoparticles supported on magnesium oxide for CO oxidation. *Nanoscale Res. Lett*. **2011**, *6*, 435.
176. Grabchenko, M.V.; Mamontov, G.V.; Zaikovskii, V.I.; Vodyankina, O.V. Effect of the metal–support interaction in Ag/CeO_2 catalysts on their activity in ethanol oxidation. *Kinet. Catal.* **2017**, *58*, 642–648.
177. Liu, Y.; Liu, B.; Wang, Q.; Liu, Y.; Li, C.; Hu, W.; Jing, P.; Zhao, W.; Zhang, J. Three dimensionally ordered macroporous Au/CeO_2 catalysts synthesized *via* different methods for enhanced CO preferential oxidation in H_2-rich gases. *RSC Adv.* **2014**, *4*, 5975–5985.
178. Moulder, J.F.; Stickle, W.F.; Sobol, P.E.; Bomben, K.D. Handbook of X-Ray Photoelectron Spectroscopy; Chastain, J., Ed.; Perkin-Elmer Corp., Eden Prairie, MN, USA, 1992.
179. Casaletto, M.P.; Longo, A.; Martorana, A.; Prestianni, A.; Venezia, A.M. XPS study of supported gold catalysts: The role of Au^0 and $Au^{+\delta}$ species as active sites. *Surf. Interface Anal.* **2006**, *38*, 215–218.
180. Costa, V.V.; Estrada, M.; Demidova, Y.; Prosvirin, I.; Kriventsov, V.; Cotta, R.F.; Fuentes, S.; Simakov, A.; Gusevskaya, E. Gold nanoparticles supported on magnesium oxide as catalysts for the aerobic oxidation of alcohols under alkali-free conditions. *J. Catal.* **2012**, *292*, 148–156.
181. Feng, R.; Li, M.; Liu, J. Synthesis of core–shell Au@Pt nanoparticles supported on Vulcan XC-72 carbon and their electrocatalytic activities for methanol oxidation. *Colloids Surf. A* **2012**, *406*, 6–12.
182. Zhang, Y.L.; Xiao, Q.; Bao, Y.S.; Zhang, Y.J.; Bottle, S.; Sarina, S.; Zhaorigetu, B.; Zhu, H.Y. Direct photocatalytic conversion of aldehydes to esters using supported gold nanoparticles under visible light irradiation at room temperature. *J. Phys. Chem. C* **2014**, *118*, 19062–19069.
183. Pojanavaraphan, C.; Satitthai, U.; Luengnaruemitchai, A.; Gulari, E. Activity and stability of Au/CeO_2-Fe_2O_3 catalysts for the hydrogen production via oxidative steam reforming of methanol. *J Ind. Eng. Chem.* **2015**, *22*, 41–52.
184. Epling, W.S.; Hoflund, G.B.; Weaver, J.F.; Tsubota, S.; Haruta, M. Surface characterization study of Au/α-Fe_2O_3 and Au/Co_3O_4 low-temperature CO oxidation catalysts. *J. Phys. Chem.* **1996**, *100*, 9929–9934.
185. Luengnaruemitchai, A.; Srihamat, K.; Pojanavaraphan, C.; Wanchanthuek, R. Activity of Au/Fe_2O_3 -TiO_2 catalyst for preferential CO oxidation. *Int. J. Hydrogen Energy* **2015**, *40*, 13443–13455.

186. Penkova, A.; Chakarova, K.; Laguna, O.H.; Hadjiivanov, K.; Romero Saria, F.; Centeno, M.A.; Odriozola, J.A. Redox chemistry of gold in a $Au/FeO_x/CeO_2$ CO oxidation catalyst. *Catal. Commun.* **2009**, *10*, 1196–1202.
187. Pestryakov, A.N.; Davydov, A.A. Active electronic states of silver catalysts for methanol selective oxidation. *Appl. Catal. A: Gen.* **1994**, *120*, 7–15.
188. Simakov, A.; Tuzovskaya, I.; Pestryakov, A.; Bogdanchikova, N.; Gurin, V.; Avalos, M.; Farías, M.H. On the nature of active gold species in zeolites in CO oxidation. *Appl. Catal. A: Gen.* **2007**, *331*, 121–128.
189. Minico, S.; Scire, S.; Crisafalli, C.; Visco, A.M.; Galvagno, S. FT-IR study of Au/Fe_2O_3 catalysts for CO oxidation at low temperature. *Catal. Lett.* **1997**, *47*, 273–276.
190. Hadjiivanov, K.I.; Vayssilov, G.N. Characterization of oxide surfaces and zeolites by carbon monoxide as an IR probe molecule. *Adv. Catal.* **2002**, *47*, 307–511.
191. Qiu, S.; Ohnishi, R.; Ichikawa, M. Novel preparation of gold(I) carbonyls and nitrosyls in NaY zeolite and their catalytic activity for NO reduction with CO. *J. Chem. Soc. Chem. Commun.* **1992**, 1425–1427.
192. Mihaylov, M.; Knoezinger, H.; Hadjiivanov, K.; Gates, B.C. Characterization of the oxidation states of supported gold species by IR spectroscopy of adsorbed CO. *Chem. Ing. Tech.* **2007**, *79*, 795–806.
193. Chen, Y.-W.; Chen, H.-J.; Lee, D.-S. Au/Co_3O_4 -TiO_2 catalysts for preferential oxidation of CO in H_2 stream. *J. Mol. Catal. A: Chem.* **2012**, 363–364, 470–480.
194. Eblagon, K.M.; Pastrana-Martinez, L.M.; Pereira, M.F.R.; Figueiredo, J.L. Cascade conversion of cellobiose to gluconic acid: The large impact of the small modification of electronic interaction on the performance of Au/TiO_2 bifunctional catalysts. *Energy Technol.* **2018**, *6*, 1675–1686.
195. Ganduglia-Pirovano, M.V.; Hofmann, A.; Sauer, J. Oxygen vacancies in transition metal and rare earth oxides: Current state of understanding and remaining challenges. *Surf. Sci. Rep.* **2007**, *62*, 219–270.
196. Ariyanti, D.; Mills, L.; Dong, J.; Yao, Y.; Gao, W. $NaBH_4$ modified TiO_2: Defect site enhancement related to its photocatalytic activity. *Mater. Chem. Phys.* **2017**, *199*, 571–576.
197. Liu, H.; Ma, H.T.; Li, X.Z.; Li, W.Z.; Wu, M.; Bao, X.H. The enhancement of TiO_2 photocatalytic activity by hydrogen thermal treatment. *Chemosphere* **2003**, *50*, 39–46.
198. Kolobova, E.N.; Pakrieva, E.G.; Carabineiro, S.; Bogdanchikova, N.; Kharlanov, A.; Kazantsev, S.O.; Hemming, J.; Mäki-Arvela, P.; Pestryakov, A.N.; Murzin, D. Oxidation of a wood extractive betulin to biologically active oxo-derivatives using supported gold catalysts. *Green Chem.* **2019**, *21*, 3370–3382.
199. Nayak, S.V.; Chodhary, R.V. Acid strength distribution and catalytic properties of H-ZSM-5: Effect of deammoniation conditions of NH_4-ZSM-5. *J. Catal.* **1983**, *81(1)*, 26–45.
200. Olson, H.D.; Kokotailo, T.G.; Lawton, L.S.; Meier, M.W. Crystal structure and structure-related properties of ZSM-5. *J. Phys. Chem.* **1981**, *85(15)*, 2238–2243.

201. Zhu, L.; Zeng, Y.; Zhang, Sh.; Deng, J.; Zhong, Q. Effects of synthesis methods on catalytic activities of CoO_x–TiO_2 for low-temperature NH_3-SCR of NO. *J. Environ. Sci*. **2017**, *54*, 277–287.
202. Amaniampong, P.N.; Li, K.; Jia, X.; Wang, B.; Borgna, A.; Yang, Y. Titania-supported gold nanoparticles as efficient catalysts for the oxidation of cellobiose to organic acids in aqueous medium. *ChemCatChem* **2014**, *6*, 2105–2114.
203. Thanh, D.N.; Kikhtyanin, O.; Ramos, R.; Kothari, M.; Ulbrich, P.; Munshi, T. Kubicka, D. Nanosized TiO_2—A promising catalyst for the aldol condensation of furfural with acetone in biomass upgrading. *Catal. Today* **2016**, *277*, 97–107.
204. Cosimo, J.I. Di.; Dıez, V.K.; Xu, M.; Iglesia, E.; Apesteguıa, C.R. Structure and surface and catalytic properties of Mg-Al basic oxides. *J. Catal.* **1998**, *178*, 499–510.
205. Serio, M. Di.; Ledda, M.; Cozzolino, M.; Minutillo, G.; Tesser, R.; Santacesaria, E. Transesterification of soybean oil to biodiesel by using heterogeneous basic catalysts. *Ind. Eng. Chem. Res*, **2006**, *45*, 3009–3014.
206. Veloso, C.O.; Pérez, C.N.; Souza, de B.M.; Lima, E.C.; Dias, A.G.; Monteiro, J.L.F.; Henriques, C.A. Condensation of glyceraldehyde acetonide with ethyl acetoacetate over Mg, Al-mixed oxides derived from hydrotalcites. *Microp. Mesop. Mater.* **2008**, *107*, 23–30.
207. Kubicka, D.; Kumar, N.; Mäki-Arvela, P.; Tiitta, M.; Niemi, V.; Karhu, H.; Salmi, T.; Murzin, D. Yu. Ring opening of decalin over zeolites: II. Activity and selectivity of platinum-modified zeolites. *J. Catal.* **2004**, *227*, 313–327.
208. Kubicka, D.; Kumar, N.; Venäläinen, T.; Karhu, H.; Kubickova, I.; Österholm, H.; Murzin, D. Yu. Metal−support interactions in zeolite-supported noble metals: Influence of metal crystallites on the support acidity. *J. Phys. Chem. B* **2006**, *110*, 4937–4946.
209. Villegas, J.I.; Kubicka, D.; Karhu, H.; Österholm, H.; Kumar, N.; Salmi, T. Murzin, D. Yu. On the mutual interactions between noble metal crystallites and zeolitic supports and their impacts on catalysis. *J. Mol. Catal. A: Chem*. **2007**, *264*, 192–201.
210. Iheva, L.I.; Andreeva, D.H.; Andreev, A.A. TPR and TPD investigation of Au/α~-Fe_2O_3. *Thermochimica Acta* **1997**, *292*, 169–174.
211. Glazneva, T.S.; Kotsarenko, N.S.; Paukshtis, E.A. Surface acidity and basicity of oxide catalysts: From aqueous suspensions to in situ measurements. *Kinet. Catal.* **2008**, *49*, 859–867.
212. Mihaylov, M.; Ivanova, E.; Hao, Y.; Hadjiivanov, K.; Gates, B.C.; Knozinger, H. Oxidation by CO_2 of Au0 species on La_2O_3 -supported gold clusters. *Chem. Commun.* **2008**, 175–177.
213. Mihaylov, M.; Ivanova, E.; Hao, Y.; Hadjiivanov, K.; Knozinger, H.; Gates, B.C. Gold supported on La_2O_3: Structure and reactivity with CO_2 and implications for CO oxidation catalysis. *J. Phys. Chem. C* **2008**, *112*, 18973–18983.
214. Kruse, N.; Chenakin, S. XPS characterization of Au/TiO_2 catalysts: binding energy assessment and irradiation effects. *Applied Catalysis A: Gen.* **2011**, *391*, 367–376.

215. Barrère, F.; Lebugle, A.; van Blitterswijk, C.A.; de Groot, K.; Layrolle, P.; Rey, C. Calcium phosphate interactions with titanium oxide and alumina substrates: an XPS study. *J Mater. Sci.: Mater. Med.* **2003**, *14*, 419–425.
216. Liu, H.; Yang, W.; Ma, Y.; Cao, Y.; Yao, J.; Zhang, J.; Hu, T. Synthesis and characterization of titania prepared by using a photoassisted sol− gel method. *Langmuir* **2003**, *19*, 3001–3005.
217. Bharti, B.; Kumar, S.; Lee, H.N.; Kumar, R. Formation of oxygen vacancies and Ti^{3+} state in TiO_2 thin film and enhanced optical properties by air plasma treatment. *Sci. Reports* **2016**, *6*, 32355.
218. Sanjinés, R.; Tang, H.; Berger, H.; Gozzo, F.; Margaritondo, G.; Lévy, F. Electronic structure of anatase TiO_2 oxide. *J. Appl. Phys.* **1994**, *75*, 2945–2951.
219. McCafferty, E.; Wightman, J.P. Determination of the concentration of surface hydroxyl groups on metal oxide films by a quantitative XPS method. *Surf. Interface Anal.* **1998**, *26*, 549–564.
220. Husnain, N.; Wang, E.; Fareed, S.; Tuoqeer Anwar, M. Comparision on the Low-Temperature NH_3-SCR Performance of γ-Fe_2O_3 Catalysts Prepared by Two Different Methods. *Catalysts* **2019**, *9*(12), 1018.
221. Roberts, M.W.; Wood, P.R. The mechanism of the oxidation and passivation of iron by water vapour: an electron spectroscopic study. *J. Electron Spectrosc. Relat. Phenom.* **1977**, *11*, 431–437.
222. Yu, J.; Wu, G.; Mao, D. Effect of La_2O_3 on catalytic performance of Au/TiO_2 for CO oxidation. *Acta Phys.-Chim. Sin.* **2008**, *24*, 1751–1755.
223. Lee, K.J.; Kumar, P.A.; Maqbool, M.S.; Rao, K.N.; Song, K.H.; Ha, H.P. Ceria added Sb-V_2O_5/TiO_2 catalysts for low temperature NH_3 SCR: Physico-chemical properties and catalytic activity. *Appl. Catal. B: Environ.* **2013**, *142*, 705–717.
224. Carja, G.; Kameshima, Y.; Okada, K.; Madhusoodana, C.D. Mn–Ce/ZSM5 as a new superior catalyst for NO reduction with NH_3. *Appl. Catal. B: Environ.* **2007**, 73, 60–64.
225. Kang, M.; Park, E.D.; Kim, J.M.; Yie, J.E. Manganese oxide catalysts for NOx reduction with NH_3 at low temperatures. *Appl. Catal. A: Gen.* **2007**, *327*, 261–269.